

Universidade de Lisboa

Faculdade de Farmácia



**WATER-IN-OIL-IN-WATER EMULSIONS OF BIOPHARMACEUTICALS FOR  
ADMINISTRATION BY INJECTION**

Carolina Esteves Buracas

Dissertation supervised by Professor Doctor João Almeida Lopes and co-supervised  
by Doctor Cláudia Consuelo Vieira Reis Leite Moura

Master of Science Degree in Pharmaceutical Engineering

2021



## Acknowledgements

First of all, I would like to express my deep gratitude to Hovione Farmaciencia, SA for the opportunity to do an internship and the thesis work in such great company.

I would like to express my deeply grateful to my Hovione supervisor, Doctor Cláudia Moura, for all the friendly words, advice and guidance, help, patience and motivation at the end of the journey. I would also like to express my gratitude to my university supervisor, Professor João Almeida Lopes, for all the patience, support advice and contribution during the development of this work.

I wish to give a special thanks to DPD, with a special mention to João Sá, Maria, Nuno, Paulo Francisco, Beatriz, Paulo and Clara. I would also like to extend my special thanks to the DPD technicians of the laboratory, Miguel, Calixto, Pedro, Ricardo, André, Norberto and Eloy for the support and all the help.

A special thanks go to Teresa Marta not only for all the help with the analytical characterization but also for all the friendly words, motivation and laugh. I would also like to extend my thanks to Graça and Mila for providing all the material needed for my work.

I want to thanks to Patricia Nunes, Patricia Henriques, Filipa, Susana and António for all the lunches, advises and moments well spent.

A huge thanks to my Becas for the friendship, the laugh, all the help and guidance in the difficult times during this master's degree. Without you, this journey will not be the same.

A special thanks to Mira, Miguel, Marta, Barbara, Mariana, Turbi, Catarina and José for their friendship, love, good memories and support in the last years.

And lastly, I want to express my deep gratitude to my parents for all the support, encouragement throughout this process. Without you, it would never be possible. I do not have enough words to express my gratitude. I also want to thanks to my family for being there for me.

I would like to thanks to Tomás for all his love, support and encouragement in the past few years.



## Abstract

The growth of the biopharmaceuticals market and the interest of controlled-release (CR) formulations combined with the production of microparticles based on biodegradable polymers such as Poly(lactic-co-glycolic acid) (PLGA) have been widely studied for encapsulation of biomolecules. In this work, two different formulations for Lysozyme encapsulations in PLGA microspheres have been developed and optimized as well as the production process based on the double emulsion water-in-oil-in-water (W/O/W) solvent evaporation technique. During the process development, morphology, encapsulation efficiency (EE), protein activity and release of the microspheres were assessed.

The production of the W/O/W consist of the emulsification of the first aqueous phase, that contains dissolved lysozyme, with the oil phase, PLGA solution, and then with the second aqueous phase. The production technology used was the high shear mixer and the lyophilization. The combination of PVA and NaCl in the external aqueous phase ( $W_2$ ) proved to be the best choice in terms of surfactants. The microspheres obtained were spheric, rigid, the EE was close to 100% and the protein activity was maintained. During the production stages, the washing step was optimized until the last stage (stage 4) where the desired condition was achieved - a clean surface. The tempering process, time required for solvent evaporation, is critical for the solidification of the microspheres. Without proper time adjustment in this step, microspheres are not obtained in the subsequent washing step

The development of a new formulation for control delivery requires months of research and in vitro release (IVR) studies to target the desired drug release profile. A way to shorten this time is to predict data with minimal experimental load using empirical or mathematical models. The Weibull Equation can predict the drug release profile controlled by polymer erosion linked with minimal initial burst release and minimal diffusive release but real-time and accelerated IVR data are needed. The selected mathematical model and analytical framework, for the prediction of CR from bulk biodegrading polymer microspheres is based on raw-materials and microspheres material attributes. The implementation of this model however require further research in order to increase its predictions robustness.

**Keywords:** Biopharmaceuticals; Controlled Release; Double Emulsion Water-in-Oil-in-Water (W/O/W); Protein activity; Accelerated in Vitro release.



## Resumo

O crescimento do mercado biofarmacêutico, o interesse em formulações de liberação controlada (CR) combinado com a produção de micropartículas à base de polímero biodegradável, como o *Poly(lactic-co-glycolic acid)* (PLGA) têm sido amplamente estudado para o encapsulamento de biomoléculas. Neste trabalho, duas formulações para o encapsulamento da lisozima em microesferas PLGA foram desenvolvidas e otimizadas, bem como o processo de produção baseado na técnica dupla emulsão evaporação de solvente, água-em-óleo-em-água (W/O/W). Durante o desenvolvimento do processo, foi avaliado a morfologia, a eficiência de encapsulamento (EE), a atividade proteica e a liberação da proteína das microesferas.

A produção da W/O/W consiste na emulsificação da primeira fase aquosa, que contém lisozima dissolvida, com a fase oleosa, solução de PLGA, e de seguida com a segunda fase aquosa. A tecnologia de produção utilizada foi um misturador de alto cisalhamento e um liofilizador. A combinação de PVA e NaCl na fase aquosa externa ( $W_2$ ) mostrou-se a melhor escolha como estabilizante da emulsão. As microesferas obtidas apresentam uma forma esférica, rígidas, o EE foi de ~ 100% e a atividade da proteína foi mantida. Durante as etapas de produção, a etapa de lavagem foi otimizada até a última etapa (stage 4) onde uma superfície limpa foi alcançada. A etapa de *tempering*, tempo necessário para a evaporação do solvente, é uma etapa crítica para a solidificação das microesferas, sem um tempo adequado nesta etapa as microesferas iram desfazer-se quando a etapa de lavagem fosse realizada.

O desenvolvimento de uma nova formulação de liberação controlada requer meses de pesquisa e estudos de liberação *in vitro* (IVR) para atingir o perfil de liberação desejado do medicamento. Uma maneira de reduzir esse tempo é tentar prever esses dados com o mínimo de tempo experimental usando modelos empíricos ou matemáticos. A equação de *Weibull*, modelo empírico, consegue prever o perfil de liberação do medicamento que é controlado pela erosão do polímero juntamente com uma explosão inicial de liberação mínima e uma liberação difusiva mínima, mas dados de IVR em tempo real e acelerados são necessários. O modelo matemático selecionado, uma *framework* analítica, para a previsão da liberação da substância ativa de microesferas de liberação controlada baseado em valores de parâmetros da matéria-prima e do produto final (microesferas). Com base em um artigo que descreve este modelo, a implementação foi tentada sem sucesso. Apesar deste modelo se encontrar amplamente estudado mais pesquisa é necessária para ajudar a construir um modelo robusto.

**Palavras chave:** Biofarmacêuticos, Liberação Controlada, Dupla emulsão Água-em-Óleo-em-Água (W/O/W), Atividade Proteica, Liberação acelerada *In Vitro*.





# Contents

<b>Acknowledgements</b> .....	<b>i</b>
<b>Abstract</b> .....	<b>iii</b>
<b>Resumo</b> .....	<b>v</b>
<b>List of Figures</b> .....	<b>xi</b>
<b>List of Tables</b> .....	<b>xv</b>
<b>Acronyms</b> .....	<b>xvii</b>
<b>List of Symbols</b> .....	<b>xix</b>
<b>1 INTRODUCTION</b> .....	<b>1</b>
1.1 Thesis Outline.....	1
1.2 Biopharmaceuticals.....	2
1.3 Controlled Release.....	4
1.3.1 Burst Release.....	5
1.3.2 Mitigation of Burst Release.....	5
1.4 Polymeric Matrices.....	6
1.4.1 PLGA.....	6
1.4.1.1 Mechanism of Degradation.....	8
1.4.1.2 Mechanism of Release.....	9
1.5 Microparticles manufacturing techniques for Controlled Release.....	10
1.6 <i>Double Emulsion</i> .....	16
1.7 Protein Encapsulation.....	20
1.7.1 Strategies for protein stabilization.....	21
1.7.1.1 Effect of the surfactant.....	21
1.7.1.2 Effect of the polymer.....	22
1.7.1.3 Effect of the organic solvent.....	22
1.7.1.4 pH.....	22
1.7.1.5 Inner aqueous phase constitution.....	23
1.8 Quality by Design approach.....	24
1.9 <i>In Vitro Release</i> – state of the art.....	25
1.9.1 Accelerated <i>In Vitro</i> Release.....	25
1.9.2 Impact of IVR Conditions.....	25

1.10	Controlled Release Models .....	27
1.11	Sustained Release Models .....	29
1.11.1	Models .....	30
1.11.1.1	Empirical .....	30
1.11.1.2	Mechanistic.....	30
<b>2</b>	<b>MATERIALS AND METHODS.....</b>	<b>33</b>
2.1	Materials.....	33
2.2	Methods.....	33
2.2.1	Design of Experiments .....	33
2.2.1.1	Stage 1 – Screening .....	33
2.2.1.2	Stage 2 – Optimization .....	34
2.2.1.3	Test 1 – Impact of the mixing speed.....	35
2.2.1.4	Stage 3 – Optimization .....	35
2.2.1.5	Test 2 - Impact of tempering time .....	38
2.2.1.6	Stage 4 – Optimization .....	38
2.2.2	Solution preparation .....	39
2.2.3	High Shear Mixer .....	40
2.2.4	Washing.....	40
2.2.5	Freeze Drying .....	40
2.2.6	Lysozyme loading and encapsulation efficiency .....	41
2.2.7	Morphology .....	41
2.2.8	Scanning Electron Microscopy .....	41
2.2.9	Laser diffraction .....	41
2.2.10	Differential Scanning Calorimetry .....	41
2.2.11	Thermal Gravimetric Analysis.....	42
2.2.12	Lysozyme activity kit .....	42
2.2.13	In Vitro Release .....	42
2.2.14	Implementation of the Weibull equation .....	43
2.2.15	Implementation of the mechanistic model (54,55).....	43
<b>3</b>	<b>RESULTS AND DISCUSSION.....</b>	<b>45</b>
3.1	Double emulsion .....	45
3.1.1	Optical conditions tests.....	52

3.2	Sustain Release Models .....	55
3.2.1	Weibull equation .....	56
3.2.2	Mechanistic model .....	60
<b>4</b>	<b>CONCLUSIONS .....</b>	<b>63</b>
	<b>REFERENCES .....</b>	<b>65</b>



## List of Figures

Figure 1.1: Schematic comparison between the plasma drug level from conventional release systems, a combination of multiple oral tablets or injection dosing (blue dashed curve), and CR systems (red continuous curve) (Adapted from (15)).	4
Figure 1.2: Schematic showing the burst effect in a zero-order drug delivery system (Adapted from (8)).	5
Figure 1.3: Chemical structure of poly (lactic-co-glycolic acid). x corresponds to the number of units of lactic acid and y to the number of units of glycolic acid. z corresponds to the end group that can be acid (-OH) or ester (-H) (Adapted from (7)).	6
Figure 1.4: Schematic illustration of drug release and polymer erosion, surface erosion and bulk erosion processes, from polymeric microspheres.(25)	9
Figure 1.5: Schematic representation of the release mechanism: (1a) diffusion through water-filled pores; (1b) osmotic pumping; (2) transport through the polymer; (3) erosion (Adapted from (27)).	10
Figure 1.6: Schematic representation of the properties of the material and process parameters that can affect the release mechanism (adapted from (14)).	10
Figure 1.7: Schematic illustration of the different microparticle structures: (a) mononuclear/single core/core-shell, (b) multi-wall, (c) polynuclear/multiple core, (d) matrix, (e) coated polynuclear core, (f) coated matrix particle, (g) patchy microparticle, (h) dual-compartment microcapsule (Adapted from (29)).	11
Figure 1.8: Scheme of microparticles preparation by the double emulsion solvent evaporation method.(28)	17
Figure 1.9: Examples of vessels for microparticle release testing: centrifuge tube (a), glass tube (b), glass flask (c) and glass jar (d).(51)	26
Figure 1.10: Schematic representation of the four-phase release considered in the model. a) Cross-section diagram of the four-phase release for double emulsion microparticles with an encapsulated agent in its occlusions. b) Release profile for a macromolecular drug in a PLGA matrix with four-phase release. The number in the cross-section diagram is associated with the phase of release. These phases are 1) the initial burst, 2) the lag phase, 3) the secondary burst, and 4) the final release. (Retired from (54,55))	31
Figure 2.1: Scheme of production of the microspheres in stage 1 by double emulsion.	34
Figure 2.2: Optimized scheme of microsphere production based on stage 1 (the alterations in the scheme are in light blue).	35
Figure 2.3: Scheme of production of the first emulsion, $W_1/O$ , with two mixing steps.	35
Figure 2.4: Optimized scheme of microsphere production based on stage 2 and test 1 (the alterations in the scheme are in light blue).	36
Figure 2.5: Design of experience.	37
Figure 2.6: Scheme of the test for solvents evaporation, DCM, in water.	38
Figure 2.7: Optimized scheme of microsphere production based on stage 3 and test 2 (the alterations in the scheme are in light blue).	39

Figure 2.8: Work head of the L4RT-A used for forming the microspheres. (taken from the equipment manual (61)) .....	40
Figure 3.1: SEM images of microspheres obtained in the different batches. Batch A magnification of 265 times, batch B magnification 480 times, batch C magnification of 510 times, batch D magnification of 255 times, batch E magnification of 660 times, batch F magnification of 840 times, batch G magnification of 410 times, batch H magnification of 330 times, batch I magnification of 255 times, batch J magnification of 1250 times, batch K magnification of 560 times and batch L magnification of 290 times. ....	48
Figure 3.2: Morphologi images of the sample taken at the end of each batch starting in stage 3. Batch F scale bar of 50 $\mu\text{m}$ , batch G scale bar of 100 $\mu\text{m}$ , batches H and I scale bar of 20 $\mu\text{m}$ , batches J and K scale bar of 20 $\mu\text{m}$ , batch L scale bar of 200 $\mu\text{m}$ and batch M scale bar of 20 $\mu\text{m}$ . ....	49
Figure 3.3: Morphologi images of the sample taken after mixing at 8 900 rpm: A) moments after the sample was taken and B) a few minutes after the first image was taken. ....	50
Figure 3.4: White mass formed during the tempering step for batches L and M. ....	52
Figure 3.5: Particle size distribution for the batch J, n=1 (green) and n=2 (blue). ....	52
Figure 3.6: IVR data for batch J, A is n=1 (blue) and B is n=2 (orange). ....	53
Figure 3.7: Activity data of the Lysozyme for batch J, A is n=1 (blue) and B is n=2 (orange). ....	54
Figure 3.8: Representation of four different formulations. A and B lysozyme, C) vivitrol® and D) Risperdal. The different colors in the graphic representation indicates the different parts of the IVR curve. ....	56
Figure 3.9: IVR data and values of API release obtain by Weibull Equation for diclofenac: (A) IVR experimental data of real-time release and Weibull values for real-time; (B) IVR experimental data of accelerated time release and Weibull values for accelerated time; (C) Correlation between predicted real and accelerated time data; (D) IVR data of real-time and predicted data with the equation: $y = 0.0008e^{0.0942x}$ . ....	57
Figure 3.10: IVR data and values of API release obtain by Weibull Equation for risperdal: (A) IVR experimental data of real-time release and Weibull values for real-time; (B) IVR experimental data of accelerated time release and Weibull values for accelerated time; (C) Correlation between predicted real and accelerated time data; (D) IVR data of real-time and predicted data with the equation: $y = 4E-05x^3 - 0.0059x^2 + 0.5318x + 9.5182$ . ....	58
Figure 3.11: IVR data and values of API release obtain by Weibull Equation for naltrexone: (A) IVR experimental data of real-time release and Weibull values for real-time; (B) IVR experimental data of accelerated time release and Weibull values for accelerated time; (C) Correlation between predicted real and accelerated time data; (D) IVR data of real-time and predicted data with the equation: $y = 2E-05x^3 - 0.0033x^2 + 0.3255x + 3.666$ . ....	59
Figure 3.12: IVR data and values of API release obtain by Weibull Equation for vivitrol®: (A) IVR experimental data of real-time release and Weibull values for real-time; (B) IVR experimental data of accelerated time release and Weibull values for accelerated time; (C) Correlation between predicted real and accelerated time data; (D) IVR data of real-time and predicted data with the equation: $y = 4E-07x^4 - 4E-05x^3 + 0.0012x^2 + 0.2002x + 1.7976$ . ....	60

Figure 3.13: Release profile of a peptide, melittin  $MWA = 2.86 \text{ kDa}$ , from poly lactic-co-glycolic acid (PLGA) microspheres, PLGA 75:25  $MW0 = 9.3 \text{ kDa}$ . The  $MWr = 4.68 \text{ kDa}$ ,  $D=6.34 \times 10^{-18}$ ,  $Rp=4.5 \mu\text{m}$  and  $Rocc=0.54 \mu\text{m}$ . (Adapted from (54))...... 61

Figure 3.14: Melittin release profile obtained in the simulation in Matlab, using the same parameters values of Figure 3.13. .... 61





## List of Tables

Table 1.1: List of licensed biological products by FDA. (5) .....	2
Table 1.2: Examples of different grades of PLGA commercialized by Evonik.(21).....	7
Table 1.3: Examples of marketed extended release formulations produced with PLGA.(22) .....	8
Table 1.4: Methods for producing biodegradable polymer-based microparticles for sustained CR formulations: advantages and disadvantages. ....	12
Table 1.5: Description of different experimental conditions based on the literature review about W/O/W technique. ....	18
Table 1.6: Applications of Quality by Design in double emulsion process. (11,49) .....	24
Table 1.7: List of some relevant empirical/semi-empirical models to simulate drug controlled release. ....	28
Table 1.8: List of some important mechanistic mathematical models for simulating drug controlled release. ....	28
Table 2.1: Proposal for the experiences and formulations. ....	37
Table 3.1: Experimental conditions, process parameters and analytical results of the different batch of lysozyme polymeric microparticles. ....	46



## Acronyms

<b>API</b>	Active pharmaceutical ingredient
<b>aIVR</b>	Accelerated <i>in vitro</i> release
<b>CES</b>	Coaxial Electrospray
<b>CMAs</b>	Critical material attributes
<b>CPPs</b>	Critical process parameters
<b>CQAs</b>	Critical quality attributes
<b>CR</b>	Controlled release
<b>CV</b>	Coefficient of variation of particle size
<b>DCM</b>	Dichloromethane
<b>DDS</b>	Drug delivery system
<b>DL</b>	Drug Loading
<b>DoE</b>	Design of Experiments
<b>DSC</b>	Differential scanning calorimetry
<b>FDA</b>	Food and Drug Administration
<b>ICH</b>	International Council for Harmonization
<b>IVIVC</b>	<i>In-vitro-in-vivo</i> correlation
<b>IVR</b>	<i>In vitro</i> release
<b>EA</b>	Ethyl Acetate
<b>EE</b>	Encapsulation Efficiency
<b>EMA</b>	European Medicines Agency
<b>Mw</b>	Molecular weight
<b>PBS</b>	Phosphate-buffered saline
<b>PEG</b>	Polyethylene glycol
<b>PGA</b>	Polyglycolic acid
<b>pI</b>	Isoelectric point
<b>PLA</b>	Poly lactide acid
<b>PLGA</b>	Poly(lactic-co-glycolic acid)
<b>PSD</b>	Particle size distribution
<b>PVA</b>	Poly(vinyl alcohol)
<b>QbD</b>	Quality-by-Design
<b>QTPP</b>	Quality target product profile
<b>SDS</b>	Sulphate dodecyl sodium
<b>SEM</b>	Scanning electron microscopy

**TGA** Thermal gravimetric analysis  
**RT-IVR** Real-time *in vitro* release

## List of Symbols

$A_{450}$	Absorbance at 450 nm
<b>Activity</b>	Bioactivity of the Lysozyme in Units/mg of protein
$D$	Diffusivity
$kC_W$	Polymer degradation rate constant
$M_I$	Initial mass of lysozyme
$\%M_I$	Percentage of lysozyme in the formulation
$M_F$	Mass of lysozyme
$\%M_F$	Percentage of lysozyme in the microspheres
$m_t$	Total magnitude of the agent at any instant of time
$m_{t_1}$	Magnitude of the available agent at any instant of time during the initial burst
$m_{t_2}$	Magnitude of the available agent at any instant of time during the secondary burst phase
$MW_A$	Molecular weight of the releasing agent
$MW_0$	Initial molecular weight of the polymer
$m_\infty$	Total magnitude of the agent
$m_{\infty 1}$	Magnitude of the available agent during the initial burst phase
$m_{\infty 2}$	Magnitude of the available agent during the secondary burst
$Na_2HPO_4$	Di-sodium phosphate
$NaOH$	Sodium hydroxide
$O/W$	Oil-in-Water
<b>PLA:PGA</b>	Ratio of lactic acid to glycolic acid
<b>Protein:PLGA</b>	Ratio of Protein PLGA
$R^2$	Goodness of fit
$R_{occ}$	Occlusion radius
$R_p$	Microsphere radius
$S/O/W$	Solid-in-Oil-in-Water
$t$	Time
$T_g$	Glass transition temperature
$U$	Decrease in the $A_{450}$ per the Unit definition
$w$	Weight fraction
$W_1$	Internal aqueous phase
$W_2$	External aqueous phase
$W_1/O$	First emulsion
$W/O/W$	Water-in-Oil-in-Water

$W_1/O/W_2$	Double emulsion
$w/v$	Weight/volume
$X$	Percentage of drug released at time
$X_{Inf}$	Percentage of drug release
$\alpha$	Scale factor corresponding to the apparent rate constant
$\beta$	Shape factor
$\Delta A_{450}/min\ Blank$	Linear rate in which the absorbance of decreases per minute in the blank
$\Delta A_{450}/min\ Test$	Linear rate in which the absorbance of decreases per minute in the sample
$\rho$	Density
$\bar{\sigma}$	Average standard deviation
$\delta^2$	Variance of time required form pores
$\tau$	Time for pore formation
$\bar{\tau}$	Meantime for pore formation
$\varphi$	Ratio of the first layer of matrix volume to the total volume of the matrix

# 1 INTRODUCTION

---

## 1.1 Thesis Outline

The main goal of this thesis was to design and optimize a formulation to produce stable double emulsions for controlled-release (CR) of biopharmaceuticals. With this goal, a protein was used as a model drug for the case study. PLGA-lysozyme loaded particles were produced using the Water-in-Oil-in-water (W/O/W) approach. The material was characterized and the CR was assessed.

The commercial growth rate of biopharmaceuticals is exceeding the commercial growth of small molecules. However, classical oral formulation is inadequate for proteins and antibodies due to degradation in the digestive tract. Thus, most of the biopharmaceuticals are administered by injection at the target site of action. Injection usually causes a burst release of the drug that undermines its clinical safety and dose regimen. Consequently, drug-delivery forms that allow controlled-release (CR) are highly desirable since enables reduction of the injection frequency, increasing thus patient compliance and adherence to the treatment. For this purpose, microspheres were prepared by double emulsion solvent evaporation technique (W/O/W) using a high shear mixer and later dried in a freeze-dryer.

Lysozyme was used as a model protein because it has well-known characteristics and due to its biostability. Poly(lactic-co-glycolic acid) (PLGA) was used as a protein carrier system due to its excellent biodegradability and biocompatibility and is recognized as safe by international regulatory agencies including the Food and Drug Administration (FDA). During the process development, the morphology, encapsulation efficiency (EE) and the protein activity of the microspheres were assessed. Real-time *in vitro* release (RT-IVR) was assessed for the optimized formulation.

The complete API release of CR formulations may take a week, 1 month or 6 months depending on several factors. In order to accelerate the testing time of these formulations, accelerated *in vitro* release (aIVR) tests are performed which can be correlated to the RT-IVR data. Several approaches can be used to predict the RT-IVR from a formulation: Using statistical models from a CR formulation database, applying the Weibull equation to describe the release profile. The purpose was to assess which model could better describe and predict the formulation of *in vitro* release (IVR) performance.

The thesis was divided in four chapters: The first chapter comprised the introduction to the topic with a detailed description of the W/O/W emulsions and different models were assessed to predict IVR data, the second chapter includes the materials and methods; in chapter 3, results/discussion were presented and in chapter 4 the main conclusions were presented.

## 1.2 Biopharmaceuticals

A biopharmaceutical is a medicine that the active agent derives from biologic sources. This treatment is an important and growing component of the modern healthcare system, with emerging treatments composed of more complex biomolecules that offer solutions to chronic and debilitating disorders (1).

From 2010 to 2017, FDA approved 101 new substances, the majority being orphan drugs - drugs to treat a condition on a small patient population. The numbers provided by Deloitte, indicate that the biotech drug sales were ~ US\$162 billion in 2018 and are projected to grow to US\$178 billion by 2024. Also, biotech's share of worldwide prescription drug sales is expected to reach US\$1.18 trillion in 2024 (2–4).

In the following table, it is possible to see the most recent licensed biological products (Table 1.1). Some of the products listed below are also approved by the European Medicines Agency (EMA) such as Sarclisa, Ajovy and Darzalex Faspro.

*Table 1.1: List of licensed biological products by FDA (5).*

Brand Name	API	Company	Approval Year
<b>Darzalex Faspro</b>	Daratumumab and Hyaluronidase	Janssen Biotech, Inc.	2020
<b>Lyumjev</b>	Insulin lispro	Eli Lilly and Company	2020
<b>Ajovy</b>	Fremanezumab	Teva Pharmaceuticals USA, Inc.	2020
<b>Pulmotech MAA</b>	Kit for the preparation of technetium Tc-99m albumin aggregated	Cis Bio International	2020
<b>Sarclisa</b>	Isatuximab	sanofi-aventis U.S. LLC	2020
<b>Semglee</b>	Insulin glargine	Mylan Pharmaceuticals Inc.	2020
<b>Tepezza</b>	Teprotumumab	Horizon Therapeutics Ireland DAC	2020
<b>Trodelvy</b>	Sacituzumab govitecan	Immunomedics, Inc.	2020
<b>Uplizna</b>	Inebilizumab	Viela Bio	2020

The acquisition of a working technology for biopharmaceuticals would mean a strong move into the growing and financially interesting market of biologics.

Biopharmaceuticals offer a highly specific set of functions and efficacy, low immunogenicity, the potential to replace gene therapy, faster clinical development and approval time as well as better patent protection. These are the main advantages of biopharmaceuticals over conventional drugs (6).

Drug delivery of biopharmaceuticals may require parenteral formulations to avoid degradation in the digestive tract and first-pass metabolism. This route of administration can present some drawbacks



for the patient due to initial burst release of the drug that undermines its clinical safety and dose regimen (7–11).

Using CR formulations as a technique to reduce biopharmaceuticals injection dosing frequency of biopharmaceutical has other advantages. These advantages include better therapeutic control, patients comfort, and, consequently, the increase of the adherence to therapy by patients (12).

### 1.3 Controlled Release

In the last few years, the interest in CR of chemical and biologic agents in polymeric systems has been growing. The goal of CR formulations is to maintain the concentration of the active pharmaceutical ingredient (API) inside the therapeutic window with minimal fluctuation in the blood levels over a prolonged period at the desired site of action. In contrast, immediate release formulations release the drug immediately after the administration (Figure 1.1). The fluctuation of the drug levels in the blood can lead to a toxicity and efficacy concern (8,12–14).

CR systems have several benefits in drug delivery (8,14):

- eliminate the need for repetitive dosing to maintain the therapeutical effect;
- provide better control of the therapy;
- improve patient comfort and compliance;
- reduce the drug levels fluctuation in the blood and
- increase the use of injectable drugs (e.g. biopharmaceutical).

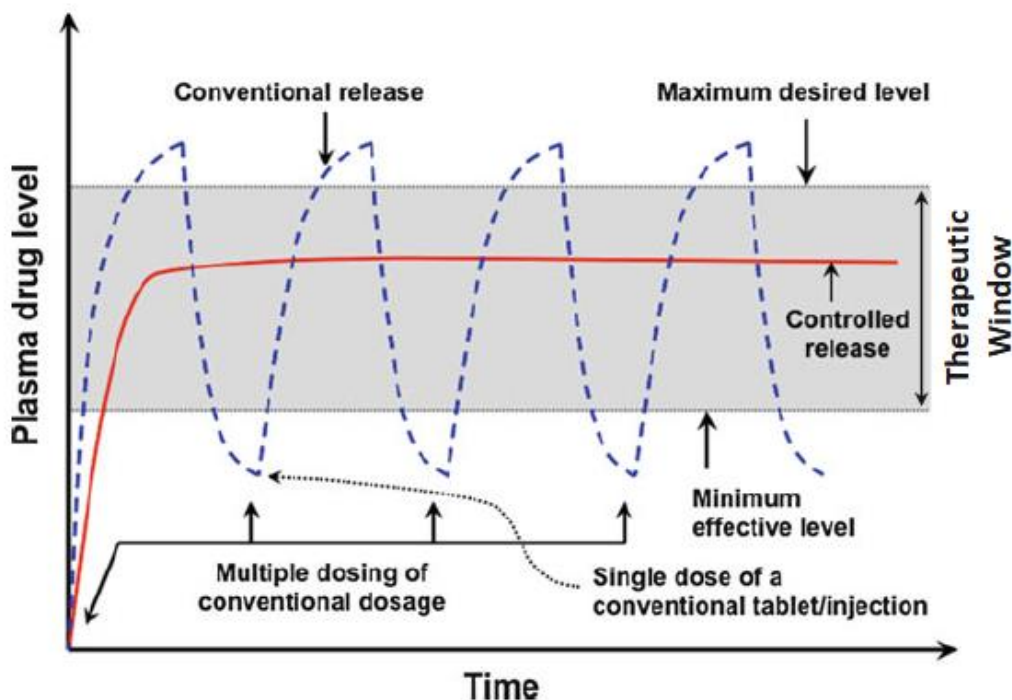


Figure 1.1: Schematic comparison between the plasma drug level from conventional release systems, a combination of multiple oral tablets or injection dosing (blue dashed curve), and CR systems (red continuous curve) (Adapted from (15)).

With this approach it is possible to have several routes of administration (e.g., oral, injectable, transdermal) and carrier systems (e.g., microparticles, pellets, films). To avoid the inconvenient surgical insertion of large implants, injectable biodegradable and biocompatible PLGA particles (e.g., microspheres, microcapsules, nanocapsules, nanospheres) could be employed for CR dosage forms. The injectable microparticles are the most common delivery system of the CR systems (7,14).

### 1.3.1 Burst Release

In many CR formulations, after the particles enter in contact with the release medium, an initial large concentration of API release can occur. This phenomenon, the so-called burst release, leads to high levels of initial drug delivery that can reach a toxic concentration in the blood and also reduces the effective lifetime of the drug (Figure 1.2) (8).

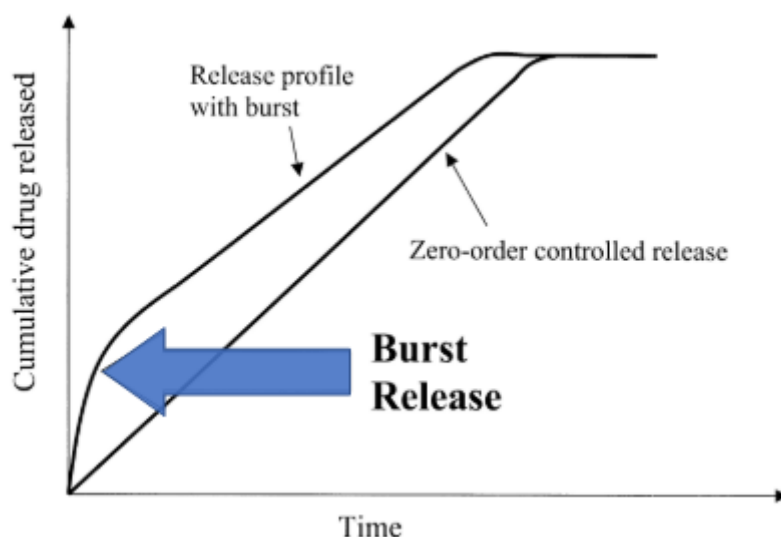


Figure 1.2: Schematic showing the burst effect in a zero-order drug delivery system (Adapted from (8)).

This effect is attributed to the release of API present at the surface of the particles which is easily detached upon placement of the particle in the release medium. This initial burst is more pronounced in the case of the small particles (e.g., nanoparticles, microparticles) where the large surface area facilitates the release of the API. After the burst release, the release is mainly controlled by polymer degradation (8,16).

The burst release can be seen from two perspectives: a negative consequence or as desirable in situations where a rapid delivery release is needed. In CR formulation, a zero-order release should be achieved and the burst release must be avoided (8).

### 1.3.2 Mitigation of Burst Release

In most cases, burst release is considered a negative effect on polymer/drug delivery systems. There are several publications focused on developing methods to prevent or minimize the burst effect in systems for CR because ideally the release process should follow in a single step (8).

The methods to avoid burst release can be 1) surface extraction and 2) coated surface (8).

The surface extraction consists of washing the particles to eliminate the presence of API on the surface. This technique is effective but has a drawback the fraction of API removed by extraction can be a significant portion of the total API (8).

The coated surface method is a surface modification technique. In this case, the burst release is avoided by an additional coating of the surface of the drug delivery system. This coating step not only prevents the release of the API on the surface layer but also prevents the release of the API through the pores present on the polymer surface by diffusion (8).

## 1.4 Polymeric Matrices

Biodegradable polymers carrier systems have gained considerable interest in the last years because they can be degraded in vivo to produce biocompatible and toxicologically safe by-products that are further eliminated by the normal metabolic pathway. These carrier systems can be used for encapsulation, protection, and CR of the active agents. The biodegradable polymers can be natural or synthetic. The synthetic biodegradable polymers most used are the aliphatic polyesters, such as poly (lactide acid) (PLA), poly (glycolic acid) (PGA) and their copolymer poly (lactic-co-glycolic acid) (PLGA). These polymers belong to the family of FDA-approved biodegradable polymers and have been extensively studied and are well known for their biodegradability, biocompatibility and non-toxic properties which make them suitable as carrier systems for CR. Natural derived polymers include polysaccharides (e.g. starch, and chitosan) and proteins (e.g. albumin, collagen and gelatin) (7,12,16,17).

The use of synthetic polymers instead of naturals provides several advantages such as: 1) lower batch-to-batch variability; 2) have an unlimited availability; 3) can be produced with modified properties depending on the application (e.g., physical, chemical and mechanical) (17).

### 1.4.1 PLGA

The poly lactic-co-glycolic acid (PLGA) has been among the most attractive biomaterials for drug encapsulation and parental sustained release of therapeutic drugs, proteins and various other macromolecules such as DNA, RNA and peptides (7,18).

PLGA is the most popular biodegradable polymer because of the long clinical experience, low cytotoxicity, high biocompatibility and biodegradation rate with the release of non-toxic by-products and processability into almost any shape and size (7,18,19).

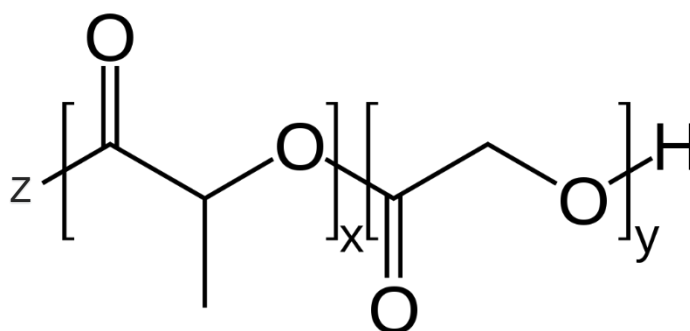


Figure 1.3: Chemical structure of poly (lactic-co-glycolic acid). x corresponds to the number of units of lactic acid and y to the number of units of glycolic acid. z corresponds to the end group that can be acid (-OH) or ester (-H) (Adapted from (7)).

In contact with water, PLGA biodegrades into its monomers, lactic and glycolic acid, by hydrolysis of its ester linkages. It is possible to modify the API release of this polymer-drug matrix by controlling the relevant parameters such as: 1) polymer molecular weight; 2) ratio of lactic to glycolic acid; 3) the polymer end group (ester or acid); 4) drug concentration to achieve the desired dosage and release interval among other factors. Also, when PLGA is richer in PLA than PGA, is less hydrophilic, absorb less water and then degrades more slowly (7,18).

There are several grades of PLGA with different ratios of lactic to glycolic acid (PLA:PGA) and end group, consequently different molecular weight, viscosity, degradation time and glass transition temperature (T<sub>g</sub>) (Table 1.2:). The molecular weight of PLGA influences the degradation rate. A low molecular weight leads to faster degradation and as a result, it causes a faster drug release and initial burst. PLGA viscosity is directly related to molecular weight. The higher the molecular weight, The higher the viscosity (7,11,12).

Different end group means different degradation time in water. PLGA with an acid end group has a free carboxyl group, which is more hydrophilic and causes faster degradation in water than a PLGA with an ester end group (10,11).

The T<sub>g</sub> of the PLGA is reported to be above 37°C, so is glassy in nature, exhibiting a rigid chain structure. It has been reported that T<sub>g</sub> decreases with a decrease of lactide content in the copolymer compositions and with an increase in molecular weight. The crystalline PGA when co-polymerized with PLA, reduces the degree of crystallinity of PLGA (7,20).

*Table 1.2: Examples of different grades of PLGA commercialized by Evonik (21).*

<b>Composition Poly (D,L-lactic-co-glycolic)</b>	<b>Inherent viscosity (dl/g)</b>	<b>Degradation timeframe</b>	<b>End group</b>
<b>45:55</b>	0.08 – 0.16	< 3 months	Acid
<b>50:50</b>	0.16 – 0.24	< 3 months	Ester/Acid
<b>50:50</b>	0.32 – 0.44	< 3 months	Ester/Acid
<b>50:50</b>	0.45 – 0.60	< 3 months	Ester/Acid
<b>50:50</b>	0.61 – 0.74	< 3 months	Ester
<b>65:35</b>	0.32 – 0.44	< 3 months	Acid
<b>75:25</b>	0.8 – 1.2	< 6 months	Ester
<b>75:25</b>	0.14 – 0.22	< 6 months	Acid
<b>75:25</b>	0.16 – 0.24	< 6 months	Ester
<b>75:25</b>	0.32 – 0.44	< 6 months	Ester/Acid
<b>75:25</b>	0.50 – 0.70	< 6 months	Ester
<b>75:25</b>	0.71 – 1.0	< 6 months	Ester
<b>75:25</b>	0.9 – 1.3	< 6 months	Ester
<b>85:15</b>	1.3 – 1.7	< 9 months	Ester

There are several CR formulations in the market where the API is encapsulated within PLGA microparticles (Table 1.3). In the table below, it is important to note that some of the API are small molecules (e.g., naltrexone and risperidone) and some are biopharmaceuticals (e.g., leuprolide acetate and exenatide) (22).

Table 1.3: Examples of marketed extended release formulations produced with PLGA (22).

<b>Brand Name</b>	<b>API</b>	<b>Indication</b>	<b>Company</b>
<b>Vivitrol</b>	Naltrexone	Alcohol dependence	Alkermes
<b>Zoladex</b>	Goserelin acetate	Prostate/Breast Cancer	AstraZeneca
<b>Lupron Depot</b>	Leuprolide acetate	Prostate cancer	TAP Pharmaceuticals
<b>Sandostatin LAR</b>	Octreotide	Acromegaly	Novartis
<b>Trelstar</b>	Triptorelin pamoate	Prostate cancer	Pfizer
<b>Arestin</b>	Minocycline HCl	Periodontitis	Orapharma
<b>Eligard</b>	Leuprolide acetate	Prostate cancer	Astellas
<b>Risperdal Consta</b>	Risperidone	Schizophrenia	Janssen / Alkermes
<b>Ozurdex</b>	Dexamethasone	Macular Edema	Allergan
<b>Bydureon</b>	Exenatide	Diabetes Type 2	AstraZeneca
<b>Lupaneta Pack</b>	Leuprolide acetate; Norethindrone acetate	Endometriosis	AbbVie
<b>Signifor LAR</b>	Pasireotide pamoate	Acromegaly	Novartis

#### 1.4.1.1 Mechanism of Degradation

PLGA has been reported to degrade by hydrolysis of its ester bonds. In other words, the polymer chain is cleaved into monomers. The role of enzymes in PLGA degradation is still unclear. However, some authors suggested an enzymatic role in PLGA degradation based on some differences between *in vitro* and *in vivo* degradation rates (7,20,23).

The hydrolytic degradation process can be through bulk erosion or surface erosion in aqueous environments (Figure 1.3). Bulk erosion is characterized by a homogeneous degradation of the entire matrix of the microparticle. In this process, the rate of water penetration into the matrix is higher than the rate of polymer degradation and the size of the microparticle will remain unchanged until the last stages of degradation. In contrast, surface erosion is characterized by a degradation throughout the exterior surface of the microparticle. Consequently, the size of the microparticle will decrease over time and the interior is essentially unaffected (23,24).

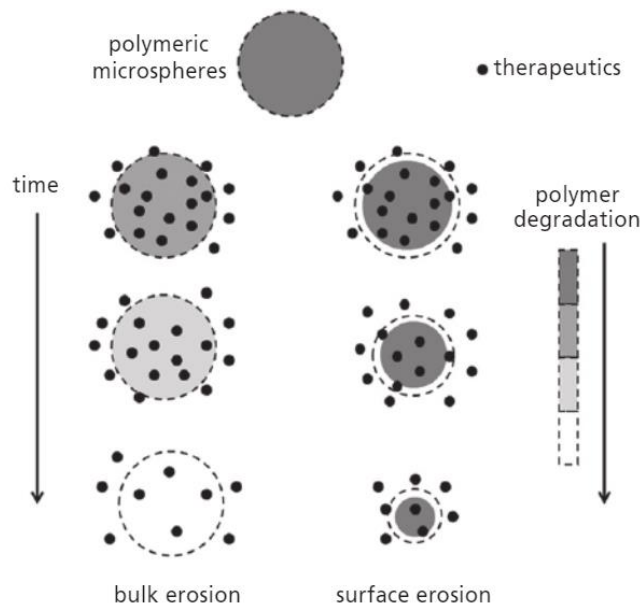


Figure 1.4: Schematic illustration of drug release and polymer erosion, surface erosion and bulk erosion processes, from polymeric microspheres (25).

The PLGA degradation process by hydrolysis can be described in four steps based on bulk erosion. The steps are: 1) water diffusion, hydration of the microparticles; 2) degradation begins, the covalent bonds are cleaved and a decrease in the molecular weight occurs; 3) insoluble oligomers with carboxylic end groups autocatalyze the degradation process, and polymer's molecular weight loss begins; 4) the soluble oligomers form are widespread in the aqueous environment. In the last step, the polymeric matrix becomes highly porous and the degradation process continuously slow down (20,26).

#### 1.4.1.2 Mechanism of Release

The drug release from a PLGA-based drug delivery system (DDS) can occur in three possible ways: 1) transport through water-filled pores; 2) transport through the polymer and 3) dissolution of the encapsulating polymer, which does not require drug transport (Figure 1.5 - 3). The most common way to release the API is transport through water-filled pores (Figure 1.5 - 1a) especially for biopharmaceuticals, such as proteins or peptides because they are too large and hydrophilic to be transported through the polymer (Figure 1.5 - 2) (27).

Transport through water-filled pores can occur in two ways: diffusion or convection. Diffusion is the most common and is characterized by random movements of the molecules forced by the concentration gradient. Convection can be described as a driven force such as osmotic pressure; this force is called osmotic pumping. The osmotic pressure may create an influx of water into a non-swelling system. The osmotic pumping release is more common in a polymer such as an ethylcellulose because PLGA absorbs a large amount of water and is susceptible to swell (27).

Transport through the polymer phase can occur for small and hydrophobic drug molecules. In this case, the drug molecule can enter the water by the surface or the pores of the polymeric carrier system (27).

The dissolution of the encapsulated drug can occur by erosion because erosion creates pores in the polymeric matrix. So, increase the diffusion of the drug molecules without any drug transport (27).

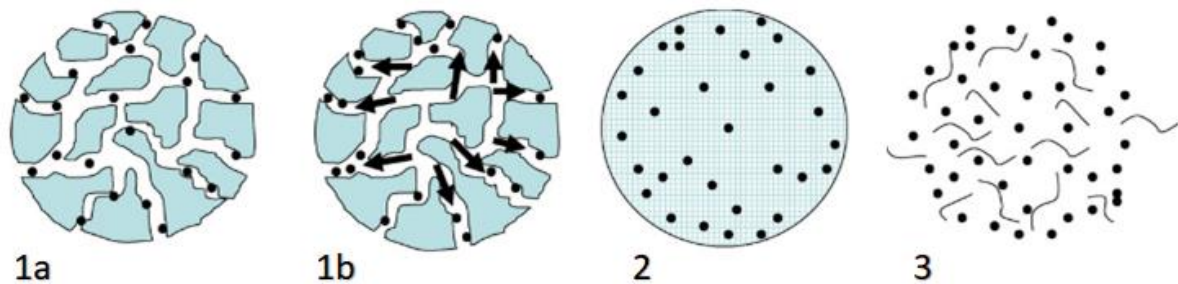


Figure 1.5: Schematic representation of the release mechanism: (1a) diffusion through water-filled pores; (1b) osmotic pumping; (2) transport through the polymer; (3) erosion (Adapted from (27)).

It is important to notice that due to the complexity of the system It is not always clear which of the releases mechanism of the process are dominating (27). The physicochemical properties of the drug, such as molecular size, hydrophilicity, and charge can influence the drug release rate. For example, a hydrophobic drug can obstruct water diffusion into microparticulate systems and reduce the rate of polymer degradation (18). The properties of the carrier system may also contribute to the release mechanism, such as 1) water penetration and solubilization when the polymeric particles enter in contact with the medium solution and 2) rate of degradation of the PLGA (14,27).

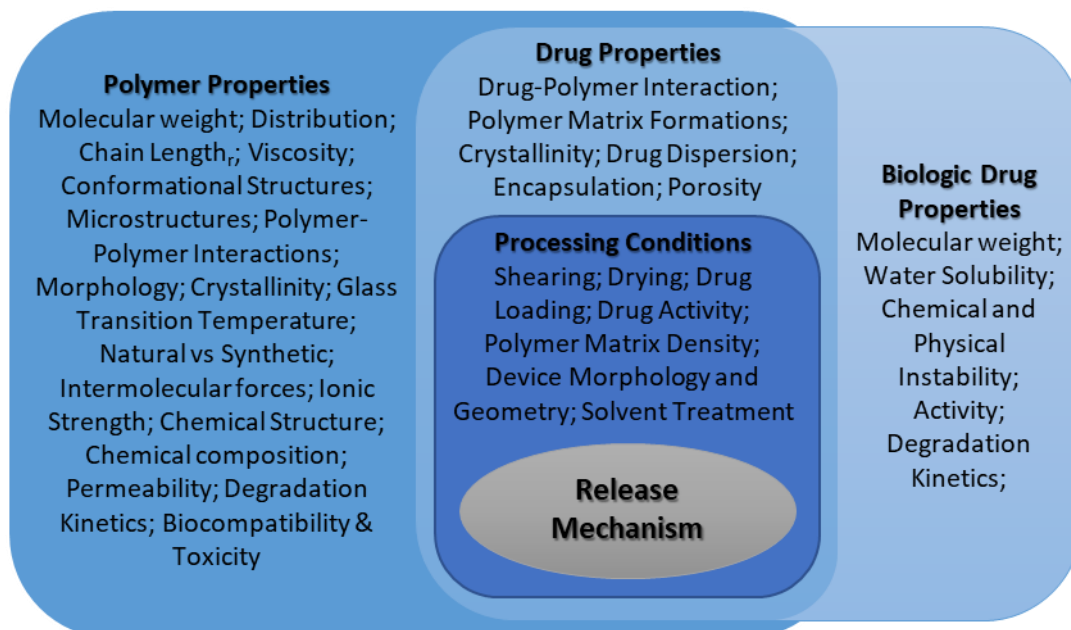


Figure 1.6: Schematic representation of the properties of the material and process parameters that can affect the release mechanism (adapted from (14)).

## 1.5 Microparticles manufacturing techniques for Controlled Release

In the past few years, the interest in CR has grown as well as the development of drug carrier systems. There are several approaches to drug delivery systems. Microparticles, microspheres, and



microcapsules. These microcarriers offer many advantages based on their structural and functional abilities and can be administered via several routes. These systems are generally constituted by polymer-based carrier systems (8,12,29).

Depending on the formulation, they can be incorporated into different pharmaceutical dosage forms such as 1) solids (capsules, tablets, sachets), 2) semisolids (gels, creams, pastes), or 3) liquids (solutions, suspensions, and parenteral injections) (29).

An advantage of microcarriers over nanoparticles is that they can act locally because their size is bigger than 100 nm so they cannot cross into the interstitium (29).

Microcarriers drug delivery systems offer several advantages (8,12,29):

- extend the delivery of the drug;
- improve bioavailability;
- improve stability of the medical preparations;
- modified and targeted (to a specific local) drug release and delivery;
- greater effectiveness and
- lower toxicity.

Microparticles size range from 1 to 1000  $\mu\text{m}$  and can have many different matrix structures (Figure 1.1). Focusing on microspheres, this carrier can be characterized by the drug being homogeneously dispersed or suspended in a matrix (29).

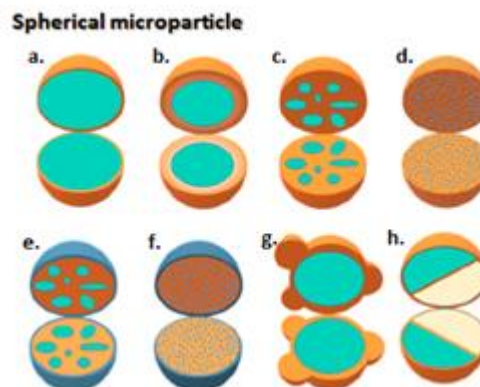


Figure 1.7: Schematic illustration of the different microparticle structures: (a) mononuclear/single core/core-shell, (b) multi-wall, (c) polynuclear/multiple core, (d) matrix, (e) coated polynuclear core, (f) coated matrix particle, (g) patchy microparticle, (h) dual-compartment microcapsule (Adapted from (29)).

Extended release microparticles can be prepared by different methods such as oil-in-water (O/W) single emulsion solvent evaporation and double emulsion techniques, spray drying, microfluid emulsion technology, etc. Table 1.4 presents the production technologies and the main respective advantages/disadvantages (7,18,28,29).

The encapsulation of peptides and proteins presents numerous problems due to their physical and chemical instability. The W/O/W process can encapsulate biodegradable polymeric microspheres with water-soluble compounds (e.g., proteins and peptides). For this purpose, the W/O/W was selected as a microsphere preparation technique (10,28,30).

Table 1.4: Methods for producing biodegradable polymer-based microparticles for sustained CR formulations: advantages and disadvantages.

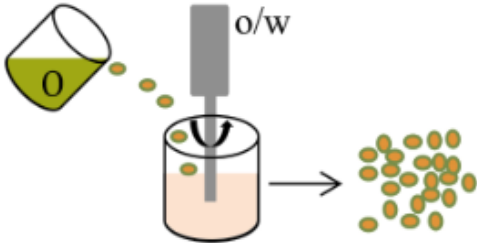
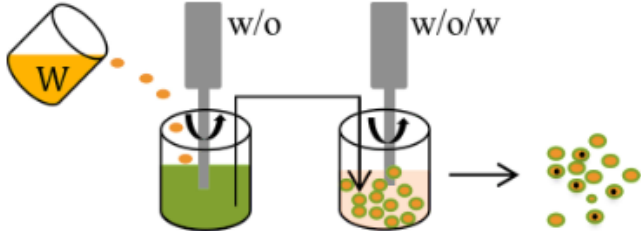
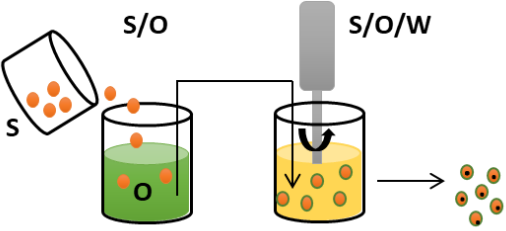
Method	Schematic diagrams	Advantages	Disadvantages	References
<b>Oil-in-water (O/W) emulsion</b>	<p>The oil phase (PLGA + API) is emulsified into the external aqueous phase.</p> 	<ul style="list-style-type: none"> <li>• Simplicity</li> <li>• Suitability for temperature-sensitive compounds</li> <li>• Control of particle size</li> <li>• High throughput (droplets/second)</li> </ul>	<ul style="list-style-type: none"> <li>• Limited ability to encapsulate water-soluble drugs</li> <li>• Residual Solvents</li> <li>• Low yield, and aggregation of the protein</li> <li>• Large coefficient of variation of particle size</li> </ul>	<p><i>Han et al., 2016; Pérez, C. et al., 2002</i></p>
<b>Water-in-oil-in-water (W/O/W) emulsion</b>	<p>The inner aqueous phase (API) is emulsified in the oil phase (PLGA) to form the W/O. Then dispersed in the external aqueous phase (emulsifier).</p> 	<ul style="list-style-type: none"> <li>• Simplicity</li> <li>• Suitability for temperature-sensitive compounds</li> <li>• Efficient encapsulation for water-soluble drugs</li> <li>• High throughput (droplets/second)</li> </ul>	<ul style="list-style-type: none"> <li>• Low drug loading</li> <li>• Residual Solvents</li> <li>• Aggregation of the protein</li> <li>• Large coefficient of variation of particle size</li> </ul>	<p><i>Giri, T.K. et al., 2013; Martín-Sabroso, C. et al., 2015; Han et al., 2016; Chong, D. et al., 2015</i></p>
<b>Solid-in-oil-in-water (S/O/W) emulsion</b>	<p>The solid API is dispersed in the inner oil phase (PLGA) to form the S/O. Then the dispersion is introduced into the external aqueous phase (emulsifier).</p> 	<ul style="list-style-type: none"> <li>• Improves protein stability during encapsulation</li> <li>• Efficiently encapsulation, without loss of activity</li> </ul>	<ul style="list-style-type: none"> <li>• Low drug loading</li> <li>• Solvent residuals</li> </ul>	<p><i>Giri, T.K. et al., 2013; Bilati, U. et al., 2005</i></p>

Table 1.4: Continued 1

Method	Schematic diagrams	Advantages	Disadvantages	References
<b>Membrane emulsification technology</b>	<p>The droplets form and grow at the pore outlet, and eventually detach from the membrane until reaching a certain droplet size and taken away by the continuous fluid.</p>	<ul style="list-style-type: none"> <li>• Low energy consumption</li> <li>• Control the particle size by membrane pore size</li> <li>• Small quantities of surfactant needed</li> <li>• Low coefficient of variation of particle size (4.8-20%)</li> </ul>	<ul style="list-style-type: none"> <li>• High porosity and coalescence</li> <li>• Low throughput (<math>2 \times 10^5</math> droplets/second)</li> <li>• Low efficient encapsulation (55-91%)</li> </ul>	<p><i>Chong, D. et al., 2015;</i> <i>Joscelyne, S. et al., 2000</i></p>
<b>Spray drying</b>	<p>A solid-in-oil dispersion or water-in-oil (W/O) emulsion are sprayed in a stream of heated air.</p>	<ul style="list-style-type: none"> <li>• Can encapsulate a wide range of drugs/peptides/proteins into microparticles without significant loss of activity</li> <li>• Final drying step not required</li> <li>• One-step and reproducible</li> <li>• Atomizers (nozzles) eliminate the need for complicated pre-preparation processes and enable continuous manufacture by utilization of liquid feeds via two separate channels</li> </ul>	<ul style="list-style-type: none"> <li>• Adhesion of microparticles to inner walls of the spray-dryer</li> <li>• Not suitable for temperature-sensitive compounds</li> <li>• Difficult to control particle size</li> <li>• Low yield, agglomeration of sticky particles</li> </ul>	<p><i>Han et al., 2016;</i> <i>Makadia et al., 2011</i></p>

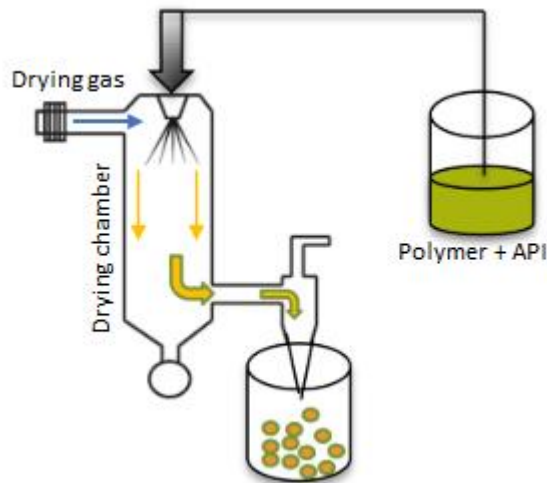
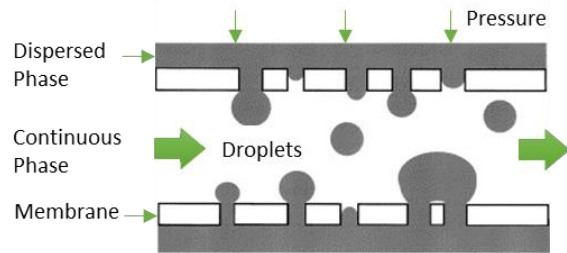


Table 1.4: Continued 2

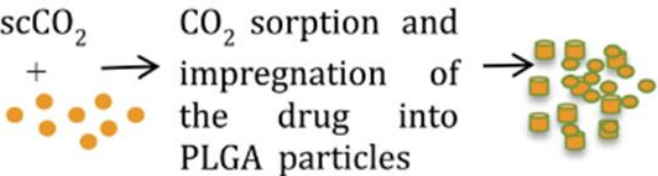
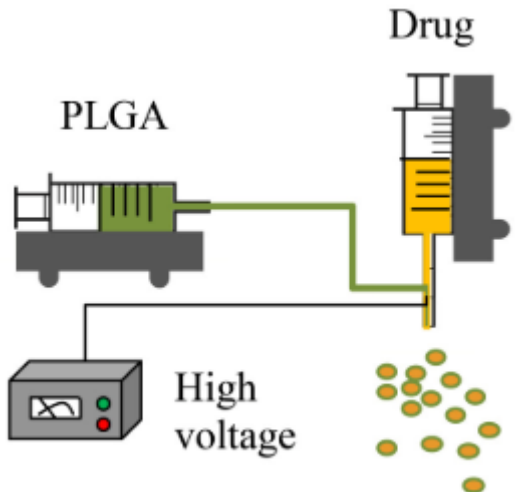
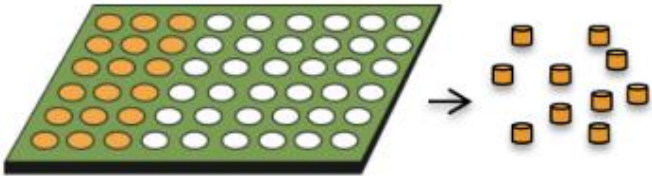
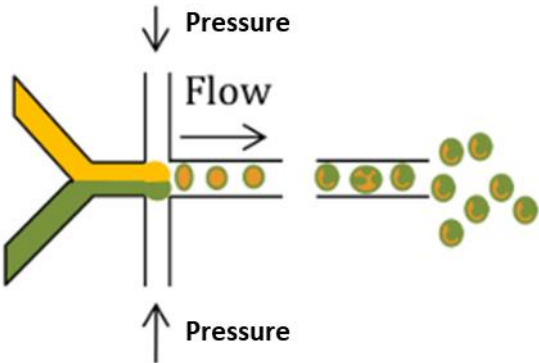
Method	Schematic diagrams	Advantages	Disadvantages	References
<b>Supercritical CO<sub>2</sub></b>	<p>scCO<sub>2</sub> + → CO<sub>2</sub> sorption and impregnation of the drug into PLGA particles →</p> 	<ul style="list-style-type: none"> <li>• The negligible residual organic solvent</li> </ul>	<ul style="list-style-type: none"> <li>• Multiple steps, poor control of particle size, size distribution, and morphology</li> </ul>	<p><i>Han et al., 2016; M. Champeau et al., 2015</i></p>
<b>Coaxial Electro spray (CES)</b>	<p>The outer (PLGA) and the inner (drug loaded) solutions are sprayed simultaneously through two separate feeding channels of a coaxial needle into the one nozzle.</p> 	<ul style="list-style-type: none"> <li>• Nearly 100% encapsulation rate</li> <li>• Useful for encapsulating water-soluble molecules</li> <li>• Protects biologically active payloads from processing-induced damage</li> <li>• Potential to control particle morphology with flexibility and reproducibility for both micro- and nanoparticle size ranges</li> <li>• High throughput (&gt;4.6x10<sup>6</sup> droplets/second)</li> </ul>	<ul style="list-style-type: none"> <li>• Requires more development</li> <li>• Lack of an effective particle collection method; shell hardening, or maintain particle morphology or prevent particle aggregation is needed</li> <li>• Need more productive nozzle design</li> <li>• Large coefficient of variation of particle size (15-44%)</li> <li>• Low efficient encapsulation (51-61%)</li> </ul>	<p><i>Han et al., 2016; Chong, D. et al., 2015</i></p>

Table 1.4: Continued 3

Method	Schematic diagrams	Advantages	Disadvantages	References
<b>Hydrogel template</b>	<p>First, a gelatin hydrogel imprint of the template is formed and then the cavities are filled with a solution or a paste of drug/polymer mixture.</p> 	<ul style="list-style-type: none"> <li>• Higher drug loading (~50%) and sustained release profile</li> <li>• Precise control of the size and shape</li> </ul>	<ul style="list-style-type: none"> <li>• A novel technique not widely used yet</li> </ul>	<p><i>Han et al., 2016; G. Acharya et al., 2010</i></p>
<b>Microfluidic technology</b>	<p>The dispersed phase is pressed into another immiscible continuous phase using specially designed microchannel, and thus monodisperse emulsion is generated.</p> 	<ul style="list-style-type: none"> <li>• Ultra-small quantities of reagents needed</li> <li>• Precise control over drug release rate, drug loading efficiency, particle shell thickness, particle shape and size</li> <li>• Multiple components are easily generated using single-step emulsification</li> <li>• Efficient encapsulation (&gt;91%)</li> <li>• Low coefficient of variation of particle size (2.6-19%)</li> </ul>	<ul style="list-style-type: none"> <li>• A time-consuming method as single drops are generated one at a time</li> <li>• Low throughput (2 500 droplets/second)</li> </ul>	<p><i>Han et al., 2016; Chong, D. et al., 2015</i></p>

## 1.6 Double Emulsion

The single emulsion, oil-in-water (O/W) solvent evaporation method is the most used. Water-insoluble drugs are successfully retained within microspheres prepared by this method. The limitation is its limited ability to encapsulate water-soluble drug for their partition into the aqueous phase of the emulsion. Consequently, the effect of this partition is the accumulation of drug crystals on the surface of microspheres, which produces a burst release of the drug upon administration. In other words, the method is not efficient for the entrapment of hydrophilic drugs because of the rapid dissolution of the compounds into the aqueous continuous phase. The problem of efficient encapsulation of hydrophilic drugs can be overcome by using the double emulsion technique, W/O/W (10,28,30).

The double emulsion method is currently one of the most used for peptide and protein encapsulation because it can encapsulate water-soluble compounds in biodegradable microspheres. This method has been considered one of the best methods because it is relatively simple to control and can be produced with a single instrument, such as a high-shear mixer. Also, it allows to modulate certain parameters such as the type of PLGA or biodegradable polymer used, the addition of surfactants or the mechanical stress or the organic solvent (10,19,28,30). The double emulsion method has efficiently encapsulated highly water-soluble compounds with high throughput (droplets/second). However, typically presents a large coefficient of variation of particle size, this way the particle size can differ inside the same batch and from batch to batch (31,32).

The W/O/W double emulsion solvent evaporation method can be prepared using the two-step emulsification method (Figure 1.8). First, an aqueous solution or suspension of the API (internal aqueous phase,  $W_1$ ) is emulsified in a solution of a polymer in an organic solvent (oil phase, O), resulting in the first emulsion ( $W_1/O$ ). The  $W_1/O$  formed is then dispersed in a second aqueous phase (external aqueous phase,  $W_2$ ) containing a stabilizer(s) to form double emulsion  $W_1/O/W_2$ . Removal of the volatile organic solvent it is a critical step because it leads to the formation of solid microspheres. The solid microspheres are separated by filtration or centrifugation, washed several times in order to eliminate 1) the residual emulsifier; 2) polymeric remains and 3) API present in the surface and dried by freeze-dried (7,11,28,33–36).

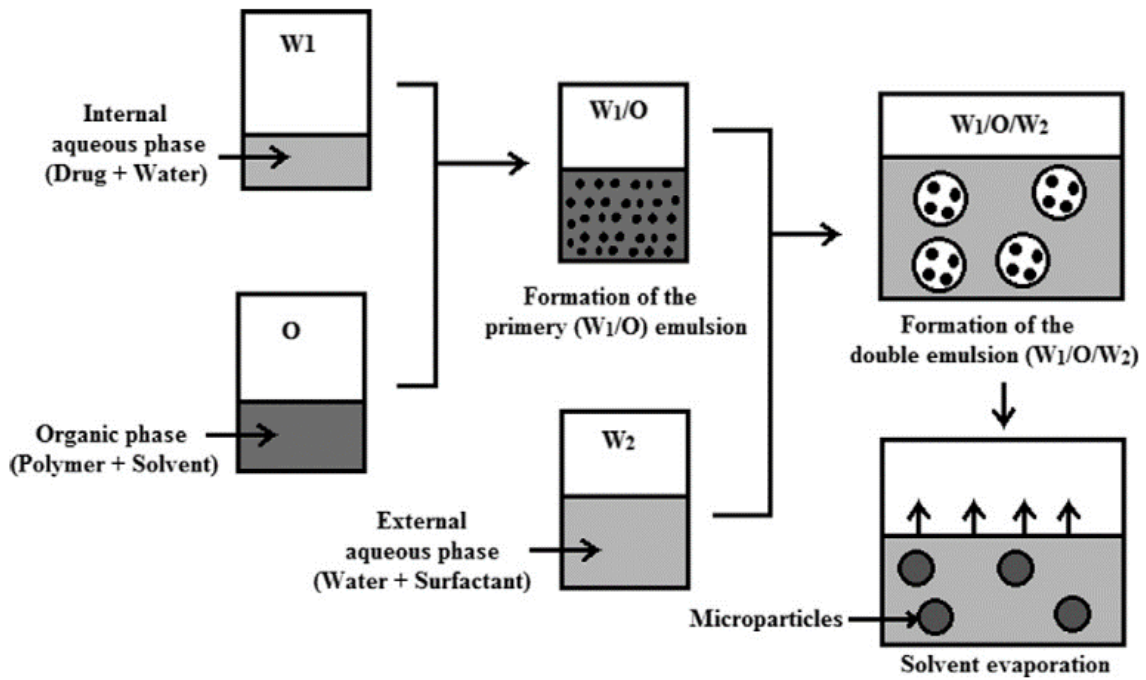


Figure 1.8: Scheme of microparticles preparation by the double emulsion solvent evaporation method (28).

In this chapter of the work, the objective is to use lysozyme as a model protein to form Lysozyme-PLGA loaded microspheres by the W/O/W method. The microspheres produced will be tested in terms of sustained and CR (IVR test), but also for the protein activity. During production, the goal was to maintain protein activity when comparing to the raw material, high encapsulation efficiency (EE), low coefficient of variation of particle size (CV) and high process yield.

Table 1.1 summarizes the main formulation/process conditions of the main literature review papers where W/O/W technique was used. (Table 1.5). The information collected supported the conditions selected for the present work.



Table 1.5: Description of different experimental conditions based on the literature review about W/O/W technique.

Author	Year	Encapsulated Molecule	Inner Phase (W <sub>1</sub> )	Inter Phase (O)	Protein: PLGA (%/mL)	External Phase (W <sub>2</sub> )	Process	Inner phase: Inter phase (v: v) mL	Particle size (µm)	W/O emulsion external phase (v: v) mL	EE (wt%)
A. Ahmed(9)	2012	N/A	0.06g drug in 0.25 mL water (240 mg/mL)	0.30 g of RG755 (75:25) (0.30g) in DCM (4.0 mL) (75 mg/mL) Viscosity ~0.6 dl/g	76.2 : 23.8	800 mL of aqueous phase 0.25% w/v PVA containing 0.25M NaCl	Homogenization (Sonoplus® HD 250) for 30s to form W/O emulsion, propeller stirring (Heidolph Elektro, Kehlheim) for 5 min and magnetic stirrer (IKA Labortechnik, Staufen) for 5 h to form W/O/W emulsion. Wet sieving and water wash (200 mL) to separate the microspheres.	0.25:3.1	50–100	3.35:800	> 85.10
C. Martín-Sabroso(11)	2015	Albumin	1 mL of ALB aqueous solution containing 0.5% PVA or 500 µL PEG 400 (30 mg/mL)	300 mg of RG504 (50:50) in 5 mL of DCM or DCM with 100mg the PEG 4000 (60 mg/mL) Viscosity ~0.52 dl/g	33.3 : 66.6	30 mL aqueous phase 2% w/v PVA and 5% w/v NaCl	Homogenization step 8000 rpm for 2min to form W/O emulsion, mixed at 1000 rpm to form W/O/W emulsion. Magnetic stirred for 18h to removal the DCM. Centrifugation at 2000 rpm for 5 min to separate the microspheres.	1:5	55.9±19.1 <100	6:30 (1:5)	63.03 59.26
T. del Castillo-Santaella(3)	2019	Lysozyme	40 µL of buffered solution (pH 5.5) with 0.8 mg of Lysozyme (20 mg/mL)	100 mg of RG503 H (50:50) in 1 mL ethyl acetate (100 mg/mL)	16.6 : 83.3 Note: 15 : 85 It's the % that I wil use	2 mL of a buffered solution (pH 12.0) of F68 (poloxamer) at 1 mg/mL	Sonicated (Branson Ultrasonics 450) for 1 min with the tube surrounded by ice to form W/O emulsion, sonicated again with same condition to form W/O/W emulsion. The W/O/W emulsion was poured into a glass containing 10 mL of the buffered F68 solution and kept under magnetic stirring for 2 min.	0.04:1	0.57 ± 0.02	1.04:2	98.0
C. Pérez(34)	2002	Lysozyme	15 mg of Lysozyme dissolve in 0.3 mL of phosphate buffer (pH 5.10) (50 mg/mL) 1:37 molar ratio of Lysozyme-additive	900 mg of PLGA (50:50, Mw 10 kDa) dissolve in 7 mL of DCM (128.57mg/ mL)	28 : 72	300 mL of 4% PVA	Homogenization step with a VirTis Tempest homogenizer at approximately 12 000 rpm for 1.5 min to form W/O emulsion, stirring at 470 rpm to obtain W/O/W. (solvent evaporation method)	0.3:7	86±16	7.3:300	65±1



Table 1.5: Continued 1.

Author	Year	Encapsulated Molecule	Inner Phase (W <sub>1</sub> )	Inter Phase (O)	Protein: PLGA (%/mL)	External Phase (W <sub>2</sub> )	Process	Inner phase: Inter phase (v: v) mL	Particle size (µm)	W/O emulsion external phase (v: v) mL	EE (wt%)
J. Wang(30)	2017	trans-Resveratrol	Tween 80 5 wt%	PGPR 10 wt%		N/A	Homogenization step with a Ultra-Turrax (T10, IKA) at 25 000 rpm for 3 min to form W/O emulsion, mixture was homogenized (Nano Homogenize Machine) for 4 passes. Stirring at 10 000 rpm for 2 min followed by homogenization for 3 passes to obtain W/O/W.	20:80 (1:4)	1.60	N/A	94.97

## 1.7 Protein Encapsulation

Proteins are the most versatile macromolecules in living systems and perform crucial functions in essentially all biological processes. They have a variety of function such as 1) catalysts, 2) DNA replication, 3) transport and storage of other molecules (e.g. oxygen), 3) provide immune protection, 4) transmit nerve impulses, and 5) provide structure and support for cells (e.g. Collagen) (37,38).

Proteins are described according to four structural levels and the difference between them is the degree of complexity in the polypeptide chain. The primary structure is a covalent linkage of individual amino acids via peptide bonds in a linear order. The secondary structure is a local conformation of the polypeptide chain or the spatial relationship of amino acids that are close together in the primary structure. The tertiary structure represents the folded polypeptide chain. The folding process corresponds to the linkage of two or more secondary structures, leading to a compact globular molecule stabilized by hydrogen bonds. This structure is the most stable conformation. In case where the protein is formed by more than one polypeptide chain, the interaction between these chains correspond to the quaternary structure (37).

Lysozyme was the chosen protein model for this work due to its high water solubility, well-known characteristics, and ease to quantifying its biological activity. Lysozyme is a globular protein with a molecular size of 14.3 kDa and isoelectric point (pI) around 11. These properties make it an appropriate model for other proteins having potential therapeutic applications, such as bone-growth factors. In the market, the source of lysozyme is the chicken white egg because it has a high content of this protein and its isolation and purification can be done economically (19,33,39).

With an increasing demand for biopharmaceutical products with extended-release, and since proteins are often administered via parenteral due to their short circulation time and instability in plasma, they have to be encapsulated in polymeric carrier systems, such as microparticles (40).

During the encapsulation process, protein stability has been a concern due to 1) contact with the organic solvent, 2) mechanical shear forces, and 3) temperature. All these factors can cause protein degradation, can destroy the hierarchy structure as well as the biologic activity of the protein. Protein denaturation may lead an unwanted immune response since when this happens, a formation of an antibody is triggered. It has been reported that protein aggregates lead to an incomplete release from the microparticles (40,41).

During the W/O/W manufacturing process, the formation of the first W/O emulsion exposes the protein to a water-organic solvent interface which is considered the root-cause for protein inactivation and aggregation. The addition of stabilizers during the preparation of the first emulsion, such as poly(vinyl alcohol) (PVA) surfactants, is a promising way to protect the biomolecule from losing activity during its encapsulation (11,33–36).

Drug delivery of peptides and proteins may require parenteral formulations to avoid degradation in the digestive tract and first-pass metabolism. This route of administration may present some drawbacks for the patient due to the initial burst release of the API caused by the initial release of a large concentration of API. This burst release leads to discomfort for the patient in terms of the dosage regimen and clinical safety as it may reach a toxic concentration of API in the body and also reduces

the effective lifetime of the drug. For a parenteral route of administration, a size range from 25 to 150  $\mu\text{m}$  is suggested (7–11,42).

## 1.7.1 Strategies for protein stabilization

### 1.7.1.1 Effect of the surfactant

The surfactant, when added to the aqueous phase,  $W_1$ , moves the protein from the interface and consequently protect the biomolecule. This can improve the colloidal stability of the microparticles and increase the biological activity of the lysozyme encapsulated. It has been reported that the interaction between surfactant and protein can be determinant in the protection of the protein during the first emulsion step (33,40).

During microparticle production using solvent evaporation methods, a surfactant is needed to ensure droplet stability until the polymer concentration in the organic solvent is high enough to maintain particle conformation (18).

The attractive electrostatic interaction between PLGA negative terminal acid group and lysozyme molecules plays a key role in the protein encapsulation which affects the final protein loading , increasing it (19).

- **Sodium Chloride (NaCl):**

NaCl plays an important role in protein encapsulation into PLGA microparticles. Literature describes that the higher the amount of sodium chloride in the external aqueous phase, the higher both drug loading and encapsulation efficiency (EE) can be obtained. It is possible to keep the protein biological activity and decrease the initial burst effect, due to the higher osmotic pressure that creates very denser and compact microparticle which will retain the protein in the  $W_1$  phase (inner microparticle layer) (11).

- **PVA:**

PVA can be used in  $W_1$  phase to prevent protein inactivation and aggregation onto the water-organic solvent interface. The presence of PVA in  $W_2$  phase has been described to increase the stability of the emulsion, improve the microparticles characteristics and enables a faster removal of the organic solvent, so the microparticles will solidify faster. By increasing the PVA concentration, the interfacial tension between the aqueous and the organic phases droplets decrease. And it can increase the viscosity of the  $W_1$  which increases the EE without modifying the microsphere morphology (11,35).

- **Poloxamer 188:**

Poloxamer is an amphiphilic molecule and presents a hydrophobic centre and two large and hydrophilic tails, which extend in aqueous solution but fold in organic solution. So, this different conformation can originate different behaviour of this molecule at the water-organic interface. With the use of this surfactant in  $W_2$  some advantages have been reported such as 1) reduces the size of the particles, 2) enhances stability, 3) protects the encapsulated protein, and 4) reach the best EE of the protein (19,33).

The poloxamer reduces the non-specific protein-polymer interactions, this way helping the protein loading leading to a more complete and sustained release. It also helps to keep the biological activity of the protein (19). However, the presence of poloxamer in the O/W emulsion leads to a reduction of the EE compared to a formulation without surfactant (33).

#### *1.7.1.2 Effect of the polymer*

It is important to notice that properties of the polymer such as 1) ratio PLA:PGA, 2) molecular weight and 3) viscosity, can influence the microencapsulation process and may control the polymer biodegradation rate. The viscosity of the polymer is an important parameter for the microspheres final product. Some authors describe an increase in the size of the microspheres with the increase in molecular weight, and consequently viscosity (11,26).

An issue related to the molecular weight of the polymer is the presence of pores on the microparticle surface, when 75:25 PLGA (higher molecular weight) is used compared with the smooth and absence of surface pores obtained using 50:50 PLGA. This fact can lead to a faster protein release (11).

The PLA:PGA ratio influences the protein loading into microparticles and thus EE - the higher the polymer hydrophilicity (richer in PGA) the lower the molecular weight and consequently the lower the EE (11).

#### *1.7.1.3 Effect of the organic solvent*

The choice of the organic solvent significantly affects the properties of the final colloidal system, since the organic solvent solubility regulates the inner and surface structure of the particle because it can cause the droplets to agglutinate and coagulate. Besides, the interaction of the solvent with the encapsulated biologic molecule ( $W_1/O$  interface) can change its bioactivity and consequently inactivates the biomolecule (19,43).

The most common solvents used are the dichloromethane (DCM) and ethyl acetate (EA). DCM is used as the organic solvent due to its lower water solubility (13.2 g/l at 25°C (44)) to facilitate the emulsification process and its low boiling point for easy evaporation. EA is used as the organic solvent because it presents a lower denaturation effects on the encapsulated protein and its higher water solubility (80 g/l at 25°C (45)) favours the solvent removal. The solvent removal rate can also be accelerated by the increase in the shear stress during the second emulsion step (11,19).

Some authors described the high porosity of the microparticles obtained with EA. This porosity can facilitate the protein release and may increase the burst release (11).

#### *1.7.1.4 pH*

The protein-polymer interaction can be affected by changing the electric charge of the lysozyme by changing the pH in  $W_1$  phase. This change affects the EE of the protein in the PLGA microparticles. Above the pI of the lysozyme, polymer and protein are negatively charged which leads to an electrostatic

repulsion and consequently to reduction of the EE. Close to the pI, a reduction of the electrical repulsion occurs which improves the EE (33).

#### *1.7.1.5 Inner aqueous phase constitution*

Double emulsions generated with deionized water (pH 5.5-6.0) as the inner phase turns out to be unstable. And when a phosphate-buffered saline (PBS) solution is used as the inner phase, the inner droplets remain stable inside the oil phase, and the PLGA microspheres can be generated by the solvent evaporation technique. This indicates that either the ionic strength and/or the pH of the inner phase plays an important role in controlling the stability of PLGA-containing double emulsions (31).

## 1.8 Quality by Design approach

Pharmaceutical Quality by Design (QbD) is defined in the International Council for Harmonisation (ICH) Q8 guideline as a systematic approach to development that begins with predefined objectives, a emphasizes product, a process understanding and process control, based on sound science and quality risk management (46). Regulatory agencies encourage risk-based approaches and the adoption of QbD principles in drug product development, manufacturing, and regulation to focus on creating robust processes capable to assure that the final product always meets the quality requirement. Quality cannot be tested into products, it should be built-in or should be by design (47,48).

To create a QbD approach to product development, it is essential to identify the quality target product profile (QTPP) and the critical quality attributes (CQAs) of the product. During the QbD process, product design and understanding include the identification of the critical material attributes (CMAs), which are different from CQAs. CQAs are for the medicine while CMAs are for input materials (e.g., API). For process design and understanding is necessary the identification of the critical process parameters (CPPs) and a full understanding of scale-up principles, linking CMAs and CPPs to CQAs. To understand the impact of these parameters on the QTPP the creation and execution of a design of experiments (DoE) is often required. During the product development, a control strategy well defined is mandatory that includes specifications for the drug substance(s), excipient(s), and drug product as well as controls for each step of the manufacturing process, to continuously monitor and improve the manufacturing process to assure consistent product quality (47,49).

A Design of Experiments is a tool for determining the relationship between factors affecting the final product properties and the input of that process. First, it is necessary to use prior knowledge and risk assessment to identify key input and output variables and process parameters to be investigated (49,50).

Table 1.6: Applications of Quality by Design in double emulsion process (11,49).

Pharmaceutical unit operations	Dosage form	Model drug	DoE	CMAs	CPPs	CQAs
<b>W/O/W emulsion</b>	Microspheres	Lysozyme	Ful factorial design	Interfacial tension between aqueous-organic phases; Drug concentration; Polymer type: Mw, viscosity, monomers ratio; Surfactant type; The viscosity of the W <sub>1</sub> phase; O/W ratio	Stirring rate; Stirrer design; Surfactant concentration; Tempering duration	Protein activity; Burst release EE; CV;

## 1.9 *In Vitro* Release – state of the art

The study of *in vitro* drug release is an important way to 1) understand the *in vivo* performance of drugs and develop a method for *in-vitro-in-vivo* correlation (IVIC), 2) can help in the development of the formulation for sustained and prolonged release, and 3) is critical for quality control purposes (25,51,52).

There are several *in vitro* test methods available for measuring the drug release such as 1) rotating basket (U.S. Pharmacopeia (USP) type I apparatus), 2) paddle- type (USP type II apparatus), and 3) reciprocating cylinder (USP type III apparatus). However, these methods were developed specifically for the oral dosage form. Unlike the solid oral dosage form, the extended-release parental dosage forms have a wide range of physicochemical and release characteristics. For parental dosage forms there is no standard compendial method for *in vitro* drug release testing. But, there are literature reports on methods like sample-and-separate, USP type II apparatus and USP type IV apparatus (flow-through method) for extended-release parental dosage forms (25,51,53).

RT-IVR has standard conditions such as 1) temperature at 37°C, 2) release medium with pH neutral (e.g. PBS, pH 7.4), without enzymes and 3) the agitation can be different depending on the method used (e.g., USP apparatus) (25,51,53).

### 1.9.1 Accelerated *In Vitro* Release

The RT-IVR studies for extended-release dosage forms require long experimental periods, which would impact the batch release and this way reduce the effective product shelf-life. In order to solve this problem, aIVR methods started to be considered as a method for shortening the time required to study drug release (25,52).

Temperature, pH, surfactants, and agitation rate are parameters that can be used to achieve accelerated release. It is important to notice that some accelerated conditions may not only accelerate the rate of drug release but also change the mechanism of drug release (25,52).

To identify the ideal conditions for aIVR, the drug release from real-time and accelerated IVR's must follow the same release mechanism and show a good correlation between the release profiles. If during the formulation process any change in the formulation occurs, the correlation between real-time and accelerated IVR must be proved (25,52).

### 1.9.2 Impact of IVR Conditions

In an *in vitro* release study, it is important to understand the impact of the testing conditions since they can influence the test result such as 1) temperature, 2) pH, 3) agitation and even 4) the size or shape of the vessels (25,51,53).

Higher temperature has been widely used for accelerated drug release testing of extended-release parental dosage forms because it can improve hydration and degradation of polymers. This accelerates erosion-controlled drug release. Also, high temperature can increase polymer mobility, resulting in increased drug release via diffusion. The increased polymer mobility can cause microsphere surface morphology changes (e.g., pore closure), which in turn may decrease drug release (25).

pH is another important parameter that can affect the hydrolysis of biodegradable polyesters such as PLGA. Both acidic and basic conditions affect the degradation of this polymer but with different mechanisms. Under acidic conditions, PLGA erosion follows a bulk erosion profile, like the degradation

characteristics obtained at pH 7.4. While under basic conditions ( $\text{pH} > 13$ ), degradation appears to occur by surface erosion (25).

The agitation of the system can modify the drug release profile. When the agitation speed is high enough to totally prevent particle aggregation, the drug release rate is higher than when a lower agitation rate is used. When the degradation rate of PLGA is faster than the diffusion rate of the generated acids, these acids start to accumulate inside the particle consequently reducing the pH of the release medium.. A reduced drug release rate is expected when agitation is minimal, due to particle aggregation. However, it should be noted that when aggregation occurs, not only drug diffusion slows down but also the diffusion of generated acidic degradants (51).

It has been reported that the IVR profile changes according to the diameter of the release vessel. Vessels with a narrow diameter (e.g., centrifuge tube or glass tube) had a lower burst release and a slower rate of release throughout the test than vessels with a larger diameter because aggregation was observed in the vessels with a narrow diameter. This way the microparticles could not achieve the complete drug release in IVR studies (51).

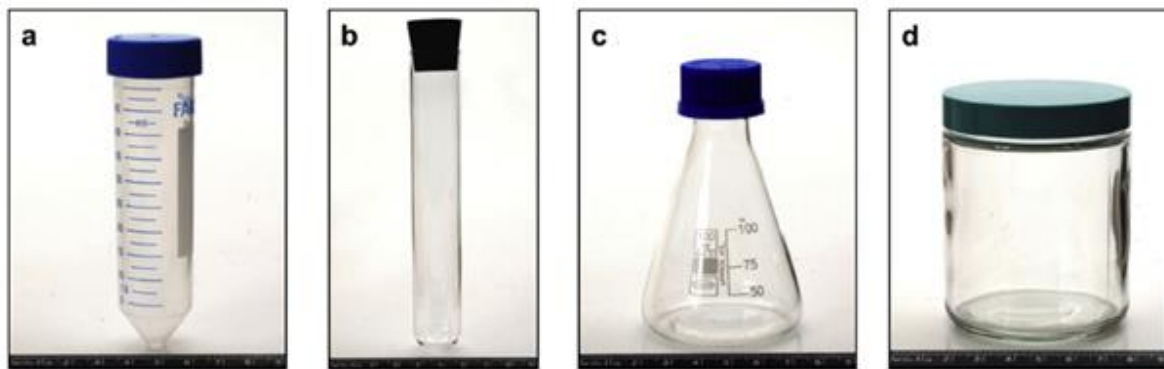


Figure 1.9: Examples of vessels for microparticle release testing: centrifuge tube (a), glass tube (b), glass flask (c) and glass jar (d) (51).



## 1.10 Controlled Release Models

In the past years, the research in the field of CR systems has been focused on injectable administration of sustained controlled release dosage forms of biologic API with narrow therapeutic window and low bioavailability when administered through conventional routes (e.g. oral route). The injectable route has focused the research in biodegradable polymeric carrier systems because they degrade over time in our body (24).

Since RT-IVR testing may require an extended period of time, it was attempted to predict the drug release from biodegradable polymer matrices using modelling techniques. Over the years, the development of many mathematical models for drug release from bulk-degrading systems has been reported. These models intend 1) to elucidate the underlying release mechanisms; 2) to provide a predictive power on the release behavior of the formulation, and 3) to minimize IVR studies (24,54).

The mathematical models can be divided into empirical/semi-empirical models (Table 1.7) and mechanistic models (Table 1.8). Empirical/semi-empirical models are mathematical descriptions and are not based on any chemical, physical or biologic phenomenon. These models do not provide any information on the mechanisms that controls the drug release and has a lower predictive power. But can be helpful to get information on the release behavior in product development. On the other hand, mechanistic models are based on real phenomena such as diffusion, degradation and erosion. These models are useful tools for understanding the drug release process mechanism. In general however, confirmation tests are require to validate model adequacy (27).

Table 1.7: List of some relevant empirical/semi-empirical models to simulate drug controlled release.

Model Name and Variables	Equation
<b>Zero-order release rate</b> (14) (mass released at time t, $Q_t$ ; initial mass, $Q_0$ ; rate constant, $k_0$ )	$Q_t = Q_0 + k_0 t$
<b>First order release rate</b> (14) (mass released at time t, $Q_t$ ; initial mass, $Q_0$ ; rate constant, $k_1$ )	$Q_t = Q_0 \times e^{-k_1 t}$
<b>Weibull Equation</b> (25,27) (percentage of drug release at time t, $X$ ; drug release is complete, $X_{Inf}$ ; scale factor corresponding to the apparent rate constant, $\alpha$ ; shape factor $\beta$ )	$\frac{X}{X_{Inf}} = 1 - e^{-\alpha t^\beta}$
<b>Exponential model</b> (14,27) (amount of drug release at time t, $M_t$ ; mass released at infinite time, $M_\infty$ ; rate constant, $k$ ; release exponent, $n$ )	$\frac{M_t}{M_\infty} = kt^n$
<b>Exponential model with lag time</b> (14) (amount of drug release at time t after lag phase, $M_{t-tlag}$ ; mass released at infinite time, $M_\infty$ ; rate constant, $k$ ; release exponent, $n$ ; lag time, $t_{lag}$ )	$\frac{M_{t-tlag}}{M_\infty} = k(t - t_{lag})^n$
<b>Exponential model</b> (14) (amount of drug release at time t, $M_t$ ; mass released at infinite time, $M_\infty$ ; rate constant, $k$ ; release exponent, $n$ ; mass fraction release as burst, $b$ )	$\frac{M_t}{M_\infty} = kt^n + b$

Table 1.8: List of some important mechanistic mathematical models for simulating drug controlled release.

Model Name and Variables	Equation
<b>Fickian film diffusion model</b> (14) (mass released at time t, $M_t$ ; mass released at infinite time, $M_\infty$ ; diffusivity, $D$ ; thickness, $L$ )	$\frac{M_t}{M_\infty} = 1 - \frac{8}{\pi^2} \sum_{n=0}^{\infty} \left[ \frac{1}{(2n+1)^2} \cdot \exp\left(\frac{-D(2n+1)^2 \pi^2 t}{L^2}\right) \right]$
<b>Higuchi model</b> (14) (mass released at time t per unit area, $Q$ ; diffusivity, $D$ ; initial drug concentration, $C_0$ ; drug solubility, $C_s$ )	$Q = \sqrt{D(2C_0 - C_s)C_s t}$
<b>Hixon-Crowell model</b> (14) (mass fraction dissolved into solution at time t, $f_t$ ; release constant, $K_\beta$ )	$(1 - f_t)^{1/3} = 1 - K_\beta t$
<b>Hopfenberg model based on Monte-Carlo simulation</b> (14) (mass released at time t, $M_t$ ; mass released at infinite time, $M_\infty$ ; erosion rate constant, $k_0$ ; initial drug concentration, $C_0$ ; characteristic length, $a_0$ ; shape factor, $n$ )	$\frac{M_t}{M_\infty} = 1 - \left[ 1 - \frac{k_0 t}{C_0 a_0} \right]^n$

## 1.11 Sustained Release Models

The development of a new formulation for controlled delivery of a new therapeutic requires months of research and spending a lot of time and high costs IVR studies to target an appropriate drug release profile. Focusing on the literature about bulk eroding polymer matrices shows that the release profile can range from single to four-phase release. These four phases are described as 1) an initial burst release, 2) a lag phase, 3) a second burst and 4) a terminal release phase (54,55).

Using modelling techniques to predict CR of drug from biodegradable polymers matrices should satisfy the following requirements (54,55):

- the model must be described according to the available parameters;
- must include all the release mechanisms and
- must apply to a wide range of drugs.

Based on the physical properties of the matrix, the implanted drug, and the employed polymer many studies have been attempted (54,55).

In this chapter of the work, real-time and accelerated IVR data produced in Hovione until early of the year and three different papers (risperidone, naltrexone and vivitrol®) were collected (56–58). With these data, a database was built to compile the information about each IVR study, the drug used, the PLGA type, the technology used to produce the particle. This database was used to analyze the IVR behavior of the release if the polymeric matrix release is in one phase or four phases. The main goal is to find a way to predict release profiles with minimal experimental time.

The mathematical models can be divided into empirical/semi-empirical models and mechanistic models. So, a model was chosen for each. The Weibull equation was the empirical model chose. For the mechanistic model, a model for prediction of controlled release from bulk biodegrading polymer was selected (14,27).

## 1.11.1 Models

### 1.11.1.1 Empirical

The Weibull equation is used in modelling drug release from extended-release dosage forms. This equation is also used to evaluate whether accelerated test data are predictive of real-time release profile. The disadvantage is that experimental data are necessary (25).

The Weibull function is considered to be one of the most powerful mathematical models but it is an empirical model that is not deduced based on kinetics and therefore cannot deduce the drug release kinetics adequately (25,27).

This model considers that 1) drug release is controlled by polymer erosion, 2) minimal burst release and 3) minimal diffuse release. The following equation is used to model the drug release from PLGA microspheres under real-time or accelerated conditions (25).

$$X/X_{Inf} = 1 - e^{-at^\beta}$$

Where  $X$  is the percentage of drug released at time,  $t$  and the drug release is complete when  $X_{Inf}$  is close to 100%,  $\alpha$  is the scale factor corresponding to the apparent rate constant and  $\beta$  is the shape factor. The shape of the simulated curve can be divided in 1) exponential,  $\beta = 1$ ; 2) sigmoid or S-shaped,  $\beta > 1$ ; 3) parabolic with high initial slope and after that exponential,  $\beta < 1$  (25).

Analyze the goodness of fit ( $R^2$ ) of the model parameters  $\alpha$  and  $\beta$  at real-time and accelerated conditions is possible to know if the accelerated condition correlates with real-time release (25).

For this model, the database will be used to see if the real-time and accelerated conditions correlate for different APIs.

### 1.11.1.2 Mechanistic

The mechanistic model selected is an analytical framework model for the prediction of CR from bulk biodegrading polymer microspheres. This method describes the release of several water-soluble agents, such as insulin, encapsulated in bulk biodegrading polymer matrix. In this model, PLGA has been used not only due to the fact of it is monomers formed during the decomposition are not harmful to the human body but also PLGA is a time-dependent water-soluble polymer (54,55).

This model has two correlation functions that enable prediction without knowledge of five parameters. These parameters are microsphere radius  $R_p$ , occlusion radius  $R_{occ}$ , polymer degradation rate constant  $kC_w$ , the initial molecular weight of the polymer  $MW_0$ , and molecular weight of the releasing agent  $MW_A$ . Also, the model considers the drug release profile can follow a four-phase release and particles had to have a uniform PLGA matrix with randomly distributed of the entrapped agent. This agent can be encapsulated as a solution in occlusion such as double emulsion technique (54,55).

When the polymeric matrix enters in contact with the aqueous solution, at time zero, the matrix begins to hydrate, eroding occurs, and the agent present in the surface release rapidly, occurring a burst release, phase 1 of Figure 1.10. As the burst release starts, the polymer degradation begins and the chain mobility increases lead to the formation of pores in the polymeric matrix, phase 2 Figure 1.10. When a pore is formed allows the release of the agent encapsulated. This release is a gradual diffusion and continues while increasing the number and diameter of the pores, phase 3 of Figure 1.10. In the

end, with pore growth and their coalescence leads to the diffusion of API toward the surface of the polymer matrix, phase 4 of Figure 1.10 (54,55).

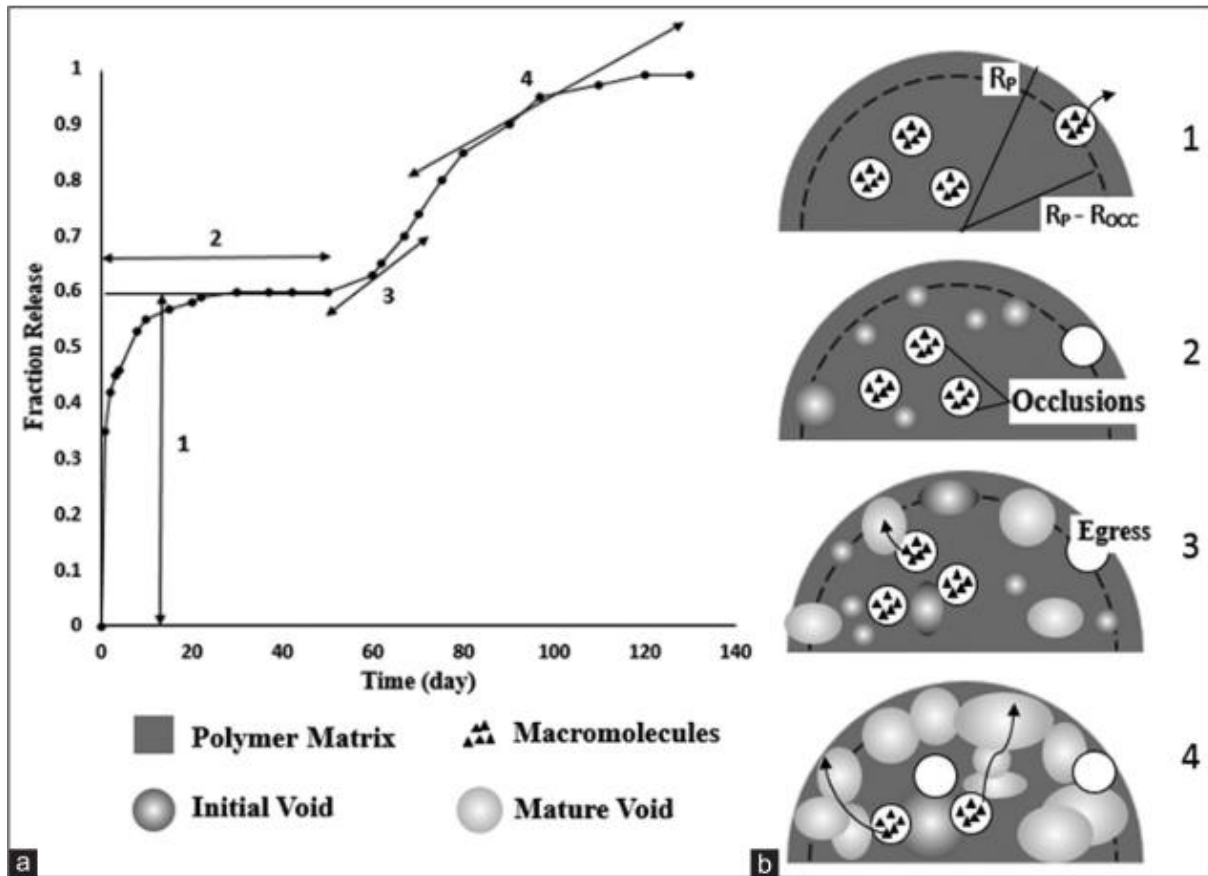


Figure 1.10: Schematic representation of the four-phase release considered in the model. a) Cross-section diagram of the four-phase release for double emulsion microparticles with an encapsulated agent in its occlusions. b) Release profile for a macromolecular drug in a PLGA matrix with four-phase release. The number in the cross-section diagram is associated with the phase of release. These phases are 1) the initial burst, 2) the lag phase, 3) the secondary burst, and 4) the final release (Retired from (54,55)).

For the implementation of this model, the values used were the values used in the paper, Farzane Sivandzade, 2018 (54).



## 2 MATERIALS AND METHODS

---

### 2.1 Materials

Poly(lactic-co-glycolic acid) RESOMER® RG 502 (Lot #D140800507) and RG 504 H (Lot #D160400525) were purchased from Evonik Industries AG. Chicken egg-white lysozyme, Lysozyme Activity Kit, Kolliphor® P 188, Sodium Chloride and Phosphate buffer saline were obtained from Sigma-Aldrich. Poly(vinyl alcohol) GOHSENOL™ was purchased from Mitsubishi Chemical. Milli-Q water (Q-POD and Millipak 0.22 µm), Dichloromethane, Sodium Hydroxide and Hydrochloric acid were provided by Hovione.

### 2.2 Methods

#### 2.2.1 Design of Experiments

In order to assess the optimal microspheres formulation and process parameters, a screening stage was initially conducted. Three parameters were selected based on the literature review: 1) the surfactant type in  $W_2$ , 2) the PLGA viscosity (PLGA grade) and 3) the mixing speed in both emulsion step. The first two parameters are described as CMAs of this technique and the third to assess the influence of the mixing speed in the emulsion step on the particle size (11).

According to the literature and as abovementioned, the main root-cause for protein aggregation and inactivation is the first emulsion step due to the proteins contact with the organic solvent at the  $W_1/O$  interface and as well to the shear stress. One possible solution to overcome this issue is the addition of a stabilizer to the  $W_1$  phase where the protein is solubilized during the formation of the first emulsion step. Therefore, in the current work a surfactant was used in the  $W_1$  phase in all trials. In order to assess the influence of the stabilizer in the second emulsion step, different water solutions were proposed (11,33–36). The Lysozyme:PLGA ratio (5:95) was maintained constant throughout all the work.

##### 2.2.1.1 Stage 1 – Screening

Stage 1 was the first experience made and had the purpose to understand and gain confidence in the process/formulation selected and in the equipment used: high-shear mixer. According to the literature, PVA is a common surfactant used for stabilizing the emulsion and therefore it was used in the current formulation. The concentrations of PVA used in both aqueous phase as well as the mixing speed of the first and second emulsion was based on *C. Martín-Sabroso et al.* work (11,28,35,36,59).

The primary emulsion was obtained by adding 33 ml of an aqueous solution containing 735 mg of Lysozyme and 0.5% (w/v) PVA to 167 ml of DCM containing 14,70 g of dissolved PLGA RG502. Then a mixing step was performed using the high-shear mixer at 8 000 rpm for 2 min. The resulting  $W_1/O$  emulsion was mixed at 1 000 rpm for 3 min with 1 000 ml of the external aqueous phase containing 2% (w/v) PVA. Microspheres were later separated by centrifugation, 2 000 rpm for 5 min, and resuspended in distilled water to remove the PVA. This process was repeated two times. In the end, the microspheres were frozen for 12 h at  $-80^{\circ}\text{C}$  and then were freeze-dried (Figure 2.1). First, the chamber was cooled with both freeze and condenser until it reaches  $-40^{\circ}\text{C}$  and then the vacuum was turned on and the

product freeze-dried for 18h. During the two mixing steps the contained was kept in an ice bath to minimize the temperature increase and the protein degradation. The ice bath was maintained at 0°C.

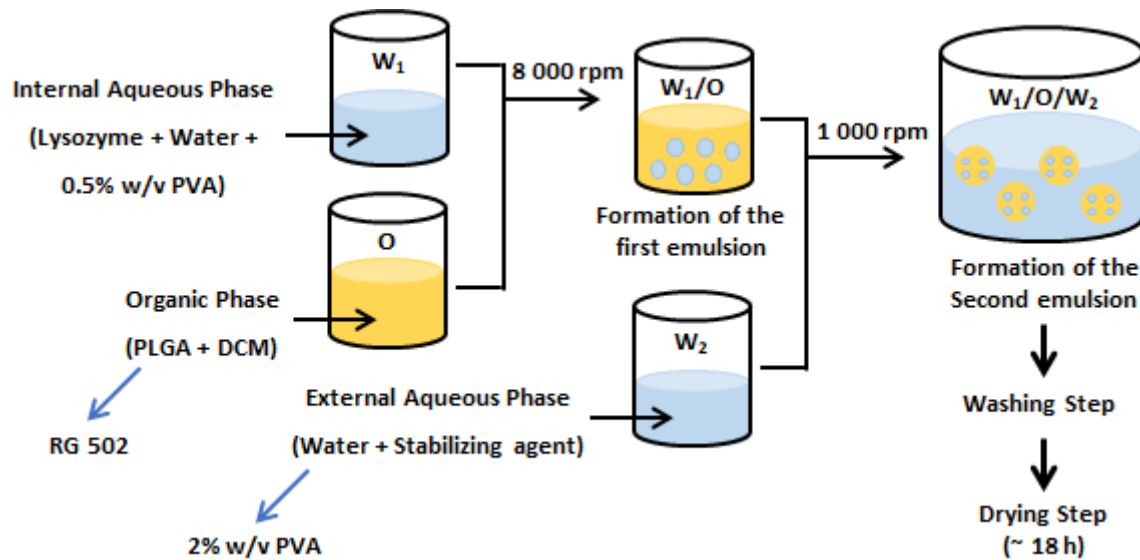


Figure 2.1: Scheme of production of the microspheres in stage 1 by double emulsion.

### 2.2.1.2 Stage 2 – Optimization

The microspheres obtained in stage 1 test were broken and present particles in the surface, this particle appears to be PVA in the surface (visual assessment). In order to improve the characteristics of the microspheres and the process parameters changes were made in this stage, such as (Figure 2.2):

- a three-washing step to remove the PVA from the surface with the following composition: solutions 1) 0.05% (w/v) Polysorbate 20, 2) 0.01% (w/v) Polysorbate 20 and 3) water with a centrifugation step between each solution;
- PVA was combined with NaCl in  $W_2$  phase, to harden the microspheres structure (11);
- poloxamer 188 in  $W_2$  phase, to compare the influence of different surfactants on the second emulsion step, in the characteristics of the microspheres and the EE (33);
- a tempering step prior to the lyophilization step, magnetic stirring, for an easier evaporation of the DCM and the hardening of the microspheres (11,19).

In this stage, the test was performed without the protein (a placebo test) because the focus was to assess the formation of harder microspheres and to challenge the rotation speed in  $W_2$ .



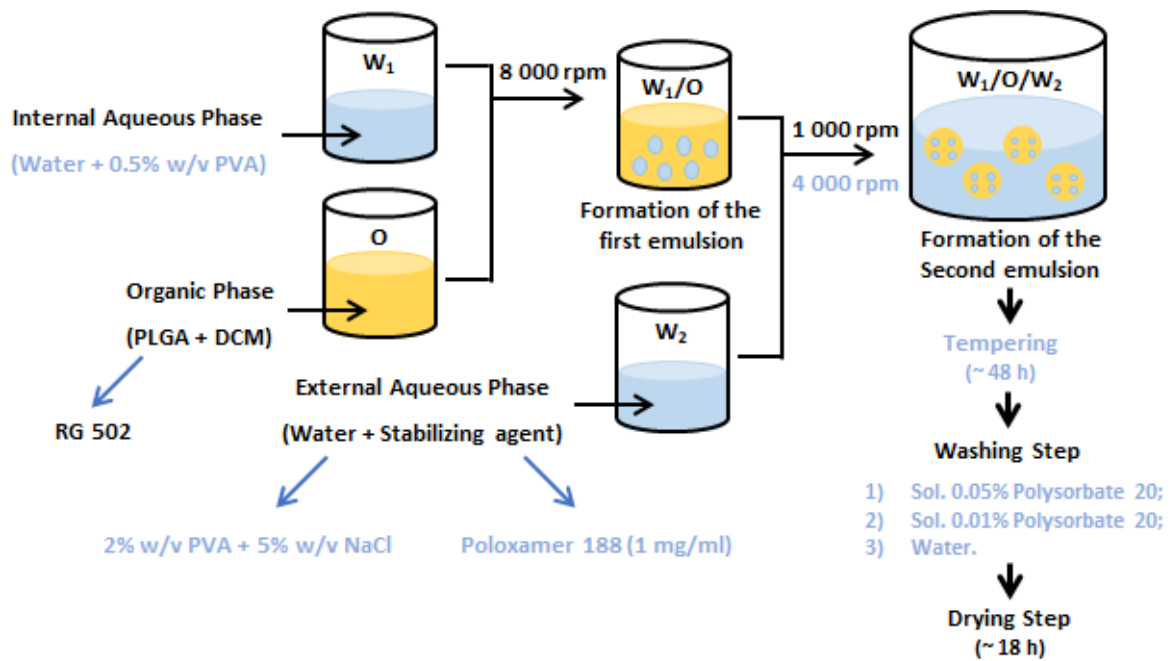


Figure 2.2: Optimized scheme of microsphere production based on stage 1 (the alterations in the scheme are in light blue).

### 2.2.1.3 Test 1 – Impact of the mixing speed

Test 1 was made to understand the impact in the first emulsion step when it is stirred twice. The time between the formation of the first emulsion and the second emulsion proved to be an important parameter. For this test, the use of an optical microscope was essential because this equipment allows the visualization of the droplets formed in the  $W_1/O$  and if their coalescence occurs.

Briefly, the  $W_1$  was mixing with the O at 8 000 rpm for 2 min, a sample was taken and analyzed in the optical microscope only after was performed the second mixing step at 8 900 rpm for 2 min and again a sample was taken and analyzed.

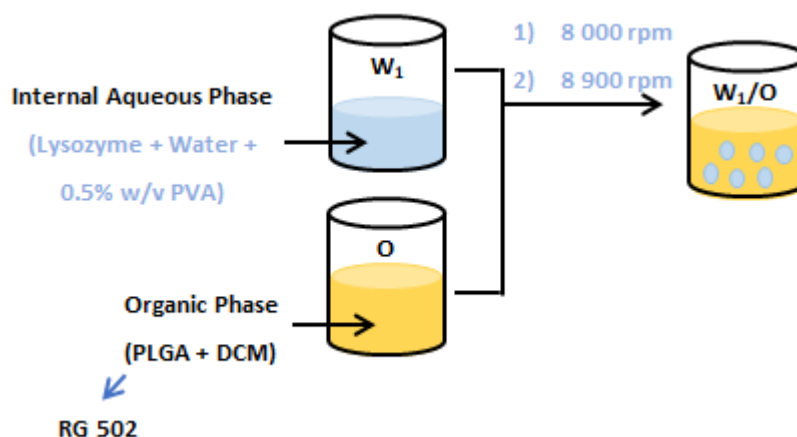


Figure 2.3: Scheme of production of the first emulsion,  $W_1/O$ , with two mixing steps.

### 2.2.1.4 Stage 3 – Optimization

Despite changes made to the washing process in stage 2, the microspheres continued to present particles on the surface. To continue the improvement of the process parameters and microspheres characteristic changes were made in this stage, such as (Figure 2.4):

- a vortex sept was added before the centrifuge step, to promote the contact of the formed microspheres with the washing solutions;
- the 4 000 rpm, 2<sup>nd</sup> mixing step, was removed because the particles obtained were below the desired particle size, 25 to 150 micrometers;
- the impact of a mixing speed in the 1<sup>st</sup> emulsion was tested with 8 000 and 9 000 rpm, to see the impact in the particle size and
- the pH of the aqueous solutions, to improve the EE (33).

According to *T. del Castillo-Santaella et al.* work, the electric charge of the lysozyme changes with pH consequently affects the protein-polymer interactions and EE. When the pH is below the pI of the lysozyme, the attractive electrostatic interaction between negative terminal acid of the PLGA and positive protein molecules improve the protein encapsulation process. Based on this work the pH chosen for the  $W_1$  was 5.5 and the buffered solution was di-sodium phosphate ( $\text{Na}_2\text{HPO}_4$ ) (33).

For the  $W_2$  the pH chosen was 12 because with this pH value, polymer and protein are negatively charged and consequently, electrostatic repulsion occurs. PVA degrades for both higher and lower pH values than 7-9. This way the pH of the  $W_2$  was only changed for the poloxamer solution (32).

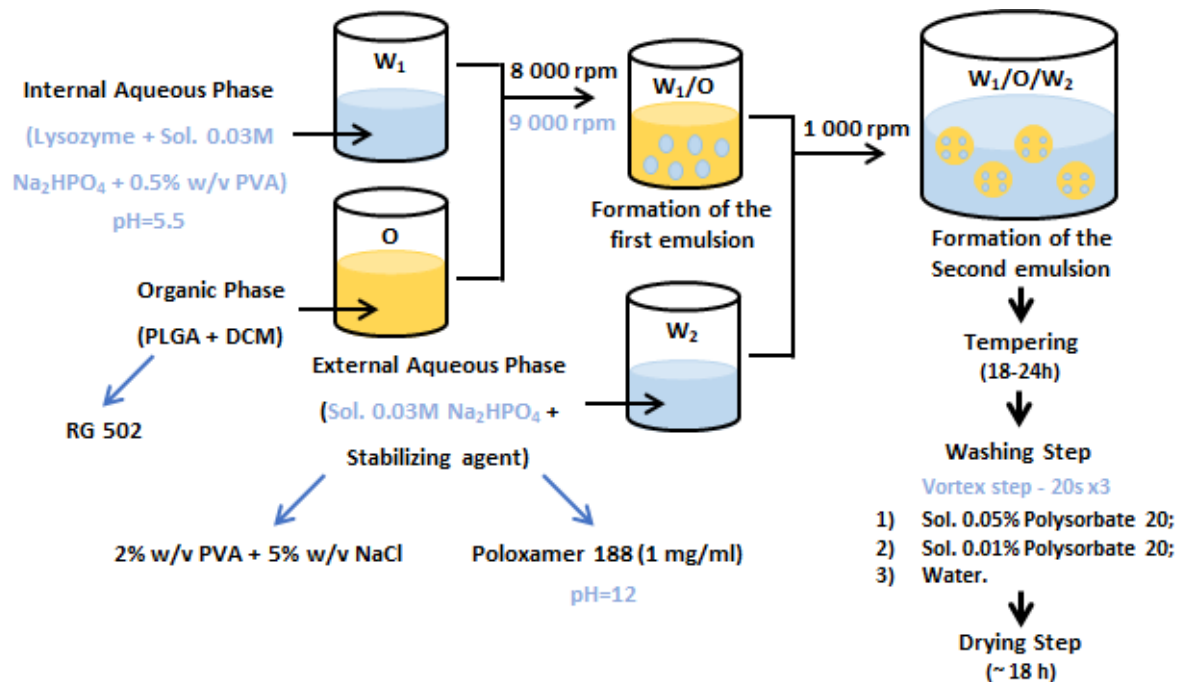


Figure 2.4: Optimized scheme of microspheres production based on stage 2 and test 1 (the alterations in the scheme are in light blue).

In this stage, a design of experiments (DoE) was planned, a full-factorial design without the center point. DoE design (Figure 2.5) focused on the three parameters of the process that were considered important: 1) the surfactant type in the second water solution, 2) the PLGA viscosity and 3) the mixing speed of the first emulsion step. The main strategy was thought to maintain the activity of the protein this way 1) the surfactant was to protect the protein and stabilize the emulsion, 2) the rotation speed can denature the

protein and influence the particle size and 3) the PLGA viscosity can influence the particle size and the EE.

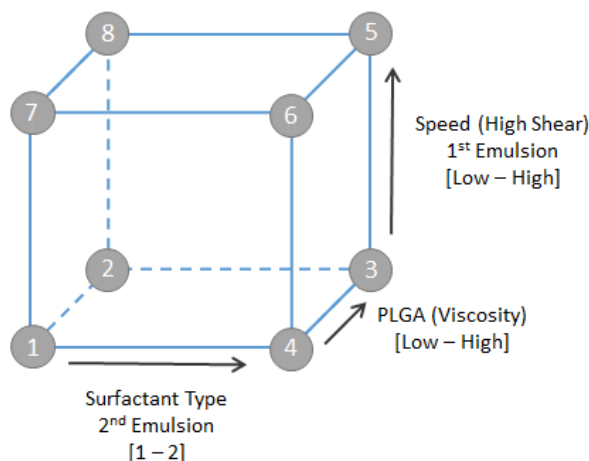


Figure 2.5: Design of experience.

The description of the DoE in term of the constitution of the 1) inner and external aqueous phases and the oil phase, 2) PLGA type and 3) speed rotation is presented in Table 2.1.

Table 2.1: Proposal for the experiences and formulations.

Experiment	Water (W <sub>1</sub> )	Oil	Water (W <sub>2</sub> )	PLGA	Speed (1 <sup>o</sup> Emulsion)
1	Lysozyme + 0.5%PVA	PLGA + DCM	Aqueous solution 2%PVA + 5%NaCl	RG 502	8 000 rpm
2	Lysozyme + 0.5%PVA	PLGA + DCM	Aqueous solution 2%PVA + 5%NaCl	RG 502	9 000 rpm
3	Lysozyme + 0.5%PVA	PLGA + DCM	Aqueous solution 2%PVA + 5%NaCl	RG 504	8 000 rpm
4	Lysozyme + 0.5%PVA	PLGA + DCM	Aqueous solution 2%PVA + 5%NaCl	RG 504	9 000 rpm
5	Lysozyme + 0.5%PVA	PLGA + DCM	Aqueous solution (1 mg/ml) Poloxamer 188	RG 502	8 000 rpm
6	Lysozyme + 0.5%PVA	PLGA + DCM	Aqueous solution (1 mg/ml) Poloxamer 188	RG 502	9 000 rpm
7	Lysozyme + 0.5%PVA	PLGA + DCM	Aqueous solution (1 mg/ml) Poloxamer 188	R G504	8 000 rpm
8	Lysozyme + 0.5%PVA	PLGA + DCM	Aqueous solution (1 mg/ml) Poloxamer 188	RG 504	9 000 rpm

Afterwards, the best formulation will be selected (e.g., PLGA grade and second water solution content). In terms of the process parameters the optimal rotation speed will be selected.

Four more tests were performed afterwards:

- One test to see the robustness of the formulation – replicate a previous trial but with increased batch size to enable a comparison between the spray drying and the lyophilization step;
- Three tests to see the feasibility of the formulation, so on which test one parameter will be changed 1) increase the amount of API, 2) change the solvent for EA and 3) change the PLGA for one more viscous.

The first DoE included four additional experiments  $W_2$  only with aqueous solution of 2%PVA. These experiments were removed because the time was not enough to complete the DoE and the literature mentioned the benefit of combine the PVA with NaCl.

The DoE presented, Figure 2.5, was complete but the analytical analyses of the last bath produced was not complete. The additional four test were not performed.

#### 2.2.1.5 Test 2 - Impact of tempering time

In stage 3, the microspheres exhibited some destruction and a higher presence of polymer at the surface when compared to those obtained in stage 2 – possibly due to the reduced tempering time ~24h . To solidify the microspheres, the removal of the DCM is needed. In this way to understand the time required for DCM evaporation test 2 was performed where the DCM evaporation was monitored over time to establish the time required for its full evaporation, weight loss monitorization.

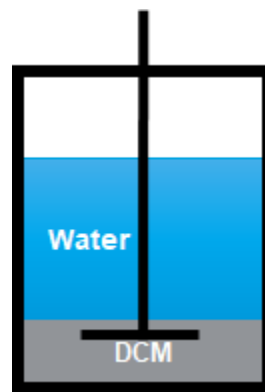


Figure 2.6: Scheme of the test for solvents evaporation, DCM, in water.

#### 2.2.1.6 Stage 4 – Optimization

In test 2, the time required to eliminate the DCM was determined .

In stage 3, during the washing step a white mass formed. So, to eliminate this mass a wet sieving was added to the process.

Was been reported in the literature that the viscosity of the inner phase can influence the EE thereby, the PLGA RG 504 H was used in this stage. This grade of PLGA is more viscous than the PLGA 502, used before (11,26).

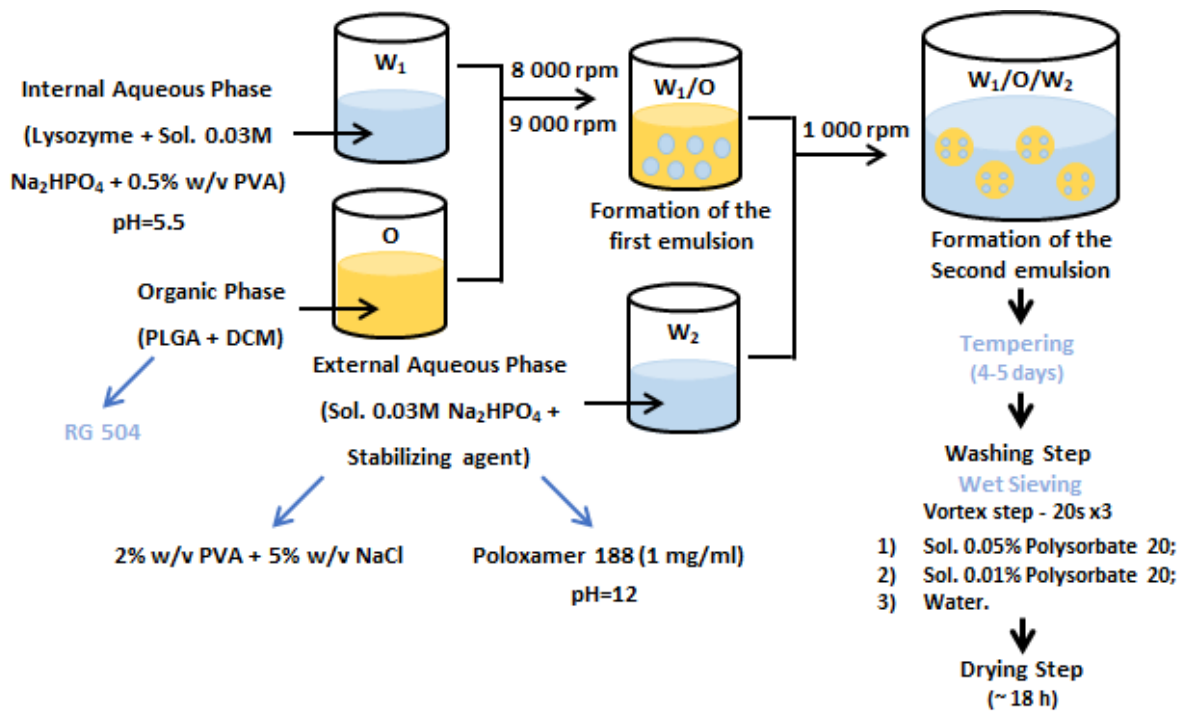


Figure 2.7: Optimized scheme of microsphere production based on stage 3 and test 2 (the alterations in the scheme are in light blue).

## 2.2.2 Solution preparation

- **Solution 0.03M Na<sub>2</sub>HPO<sub>4</sub>:**

For the preparation of 2 L of the buffered solution, 7.3 g of Na<sub>2</sub>HPO<sub>4</sub> were weighted in a Mettler Toledo XPE205 analytical balance and mixed until total dissolution with 2 L of distilled water. In the end, the pH=9.33 was measured using a 780 pH Mettler Toledo and 801 Stirrer Metrohm.

- **First aqueous solution, W<sub>1</sub>:**

To prepared 25 ml of the W<sub>1</sub>, 125 mg of PVA were weighted in a Mettler Toledo XPE205 analytical balance and mixed until total dissolution with 25 ml of solution 0.03M Na<sub>2</sub>HPO<sub>4</sub>. To help the dissolution of the PVA in the buffer solutions the heating of the solution to 80°C was necessary and to maintain the temperature, the flask was covered with aluminium foil. For heating and mixing the solution, a stirring plate VWR Advanced VMS-C4 was used. The solution remained under stirring overnight. Only after the PVA was completely dissolved 550 mg of lysozyme were weighted in a Mettler Toledo XPE205 analytical balance was added and mixed until total dissolution. In the end, the pH of the solution was adjusted to 5.5 using HCl 50% solution and measured with a 780 pH Mettler Toledo and 801 Stirrer Metrohm.

- **Oil phase, O:**

To prepare this solution, 11 g of PLGA (502 or 504) were weighted in a Sartorius ED3202S-CW analytical balance and mixed until total dissolution with 125 ml of DCM.

- **Second aqueous solution, W<sub>2</sub>:**

To prepared 350 ml of the W<sub>2</sub>, 7 g of PVA and 17.5 g of NaCl were weighted in a Mettler Toledo XPE205 analytical balance and mixed until total dissolution with 350 ml of solution 0.03M Na<sub>2</sub>HPO<sub>4</sub>. To achieved the total dissolution heating of the solution to 80°C was necessary and to maintain the temperature, the flask was covered with aluminium foil. For heating and mixing the solution, a stirring plate VWR Advanced VMS-C4 was used. The solution remained under stirring overnight. In the end, the pH of the solution was adjusted to 12 using sodium hydroxide (NaOH) 50% solution and measured with a Mettler 780 pH Mettler Toledo and 801 Stirrer Metrohm.

### 2.2.3 High Shear Mixer

The encapsulation of the protein in PLGA by double emulsion was performed with a high shear equipment. A L4RT-A Silverson homogenizer was the high shear equipment used.

The high-shear mixing uses the high rotational speed of the rotor blades within the precision work head to exert powerful suction by pushing liquid materials up toward the center of the work head. The work head was an emulsifying screen (60).



Figure 2.8: Work head of the L4RT-A used for forming the microspheres (taken from the equipment manual (61)).

### 2.2.4 Washing

In the washing step, 150 ml of the washing solutions were added to the solution that contains the microspheres and then a 30s of a vortex step was performed before the centrifuged step at 3 000 rpm for 5 minutes and the supernatant filtration was done. This process was repeated three times with different washing solutions by the following order 1) 0.05% of polysorbate 20, 2) 0.01% of polysorbate 20 and 3) water. The equipment used was a VWR® Fixed Speed Vortex Mixer and a Beckman Coulter Avanti J-15R centrifuge.

In the end, the microspheres were resuspended with 50 ml of water and then frozen at -80°C on Lab Care ULF40086 deep freezing cabinet.

### 2.2.5 Freeze Drying

To perform the drying step, a Virtis Advantage EL freeze dryer was used. Before the frozen sample be placed inside of the freeze dryer, the chamber was cold down to -40°C. Only after the vacuum pump was turned on and the vacuum inside the chamber goes down to near 200 µbar. The duration of this stage was not constant because the time necessary to dry the water of each sample is dependent on the area of sample inside of the glass bottle. The smaller the amount of sample, up to 10 cm in height, the faster the lyophilization will take place. In some stage, the samples needed only one cycle of 18h but in other stages was needed two cycles of 18h.

### 2.2.6 Lysozyme loading and encapsulation efficiency

The amount of lysozyme entrapped in the microparticles was determined by dissolving 20 mg of microparticles, in duplicate, in 4 mL of 0.1 M NaOH solution. After incubation at 37°C for 48 hours, the solution was centrifuged at 13 400 rpm for 5 min. Protein content in the supernatant was analyzed by UV-photometrically at 280 nm. Then, EE and the final drug loading (DL) was calculated as follow: (19)

$$\%EE = \frac{\%M_F}{\%M_I} \times 100 \quad (1)$$

$$\%DL = \frac{M_F}{M_I} \times 100 \quad (2)$$

Where  $M_I$  is the initial mass of lysozyme, the  $\%M_I$  is the percentage of lysozyme in the formulation, the  $M_F$  is the mass of lysozyme and  $\%M_F$  is the percentage of lysozyme in the microspheres obtained.

### 2.2.7 Morphology

In order to analyze the formation of the first emulsion, the Malvern Instruments Morphologi G2 was used. A droplet of the first emulsion was placed in the microscope slides and covered with a cover glass. After that, the prepared sample was observed to assess the W/O emulsion.droplet size.

### 2.2.8 Scanning Electron Microscopy

The morphology of the lysozyme-PLGA microparticles were analyzed by a Scanning Electron Microscope (SEM) Phenom Pro-X equipment. A small amount of sample was spread on a double-sided carbon adhesive tape. The material that did not stick to the carbon tape was vacuumed. The samples were imaged using SEM with an accelerating voltage of 10 kV.

### 2.2.9 Laser diffraction

The particle size distribution (PSD) was measured using a Helos laser diffraction instrument in combination with the Rodos dry dispersing unit and the Aspiros module (Sympatec GmbH, Germany). Different pressures were tested for each stage in order to assure that for the higher pressure the microspheres were not being broken inside the dispersing unit.

For the microspheres a R4 lens (1.8–350  $\mu\text{m}$ ), with a focal length of 200 mm and a R5 lens (4.5–875  $\mu\text{m}$ ), with a focal length of 500 mm was used, depending on the particle size obtained. A pressure of 0.1 bar was used to disperse the particles with a feeding rate of 25 mm/s.

### 2.2.10 Differential Scanning Calorimetry

Differential Scanning Calorimetry (DSC) studies were performed in a TA Instruments DSC 250 to determine the glass transition temperature of raw lysozyme, PLGA RG 502, and lysozyme-PLGA microspheres. Aluminum pinhole pans loaded with 3 to 5 mg of the sample material were used. The sample material was accurately weighed in a Mettler Toledo XPE26 analytical balance.

The samples were equilibrated at 0 °C, the temperature was modulated at 1 °C every 60 s and then it was maintained constant for 1 min. Finally, the samples were heated 3 °C per minute until the temperature reached 250 °C. The instrument was calibrated daily with indium.

### 2.2.11 Thermal Gravimetric Analysis

Thermal Gravimetric Analysis (TGA) was executed in a TGA 550 from TA Instruments (USA) to determine the degradation temperature and to quantify the water content in the samples. Aluminum pans loaded with 5 mg of the sample material were used. The samples were heated at 10 °C/min until 350 °C.

### 2.2.12 Lysozyme activity kit

The activity of lysozyme was quantified with a lysozyme activity kit (Sigma Aldrich, Cat. no. LY0100) by using freeze-dried cells of *Micrococcus lysodeikticus* as substrate. 200 mL of substrate cell suspension in a PBS (pH 7.4) was prepared and its absorbance at 450 nm ( $A_{450}$ ) was adjusted to be between 0.6 and 0.7, compared to the blank (PBS).

The absorbance was measured for the blank (potassium phosphate buffer), the certified sample that was part of the activity kit, the raw lysozyme and for the samples.

Lysozyme powders were dissolved in the phosphate buffer to achieve a concentration of 1 mg/ml, followed by dilution of 1:10. The samples of lysozyme released from microparticles, were diluted with dilution factors depending on each concentration (previously assessed with HPLC) to achieve a concentration of 0.1 mg/mL. In both cases, each run started by adding 15 µL of lysozyme solution to 185 µL of the substrate cell suspension at 25 °C.

The rate at which the absorbance at 450 nm decreased over 3 min was determined with a Synergy HTX Multi-Mode Microplate Reader from Biotek.

The bioactivity of a protein is usually expressed in Units per mg of protein, where 1 Unit is the amount of enzyme that catalyzes the reaction of 1 µmol of substrate per minute.

The activity was calculated by the follow equation:

$$Activity (Units/mg) = \frac{\Delta A_{450}/min_{Test} - \Delta A_{450}/min_{Blank}}{U \times m_{enzyme}} \quad (3)$$

In this equation *Activity* is the bioactivity of Lysozyme in Units/mg of enzyme, *m<sub>protein</sub>* is the mass of Lysozyme, *U* is the decrease in the  $A_{450}$  per the Unit definition and has the value of 0.001, the  $\Delta A_{450}/min_{Test}$  and  $\Delta A_{450}/min_{Blank}$  is the linear rate in which the absorbance decreases per minute in the sample and in the blank, respectively. All the samples were analyzed with a n=5.

### 2.2.13 In Vitro Release

To study the IVR profiles, 300 mg of microspheres were weighted in a Mettler Toledo XPE205 analytical balance and suspended in 17 mL PBS (pH 7.4). The testing vessels were placed in an orbital shaker-incubator ES-20/60 from Biosan at 37 °C and agitated at 50 rpm. At pre-determined time intervals, 2 mL samples were withdrawn and centrifuged at 13 400 rpm for 5 min in a MiniSpin® centrifuge. The protein content in the supernatants (1 mL) was analyzed by UV-photometrically at 280 nm with a specord® 200 plus from Analytik Jena.

Fresh media (1 mL) were mixed with pellets (if any) and transferred back to the testing vessels. The dilution effect of the medium reposition was considered in the calculations.



## 2.2.14 Implementation of the Weibull equation

To determine and implement the model, Excel was used.

$$X/X_{Inf} = 1 - e^{-\alpha t^\beta} \quad (4)$$

### 1<sup>st</sup> step:

Using the IVR experimental data, time and cumulative release, of both real and accelerated time was determined the percentage of API release,  $X/X_{Inf}$ . With the Excel solver function, the  $\alpha$  and  $\beta$  values were found.

### 2<sup>nd</sup> step:

Using the  $\alpha$  and  $\beta$  values predicted in 1<sup>st</sup> step, the time value for a given percentage of drug release for both real and accelerated release was determined. For this calculation, the solver function was used. With the predicted time a correlation between the real and accelerated was established and the  $R^2$  obtained will indicate the model fitting.

### 3<sup>rd</sup> step:

With the model fitting equation, the time of release was predicted and compared with the IVR experimental data.

## 2.2.15 Implementation of the mechanistic model (54,55)

To determine and implement the model, MATLAB R2018 was used.

Before starting the implementation, the knowledge of the values of six parameters is required, without them it is not possible to implement the model. These parameters are  $Rp$ ,  $Rocc$ ,  $D$ ,  $kC_w$ ,  $MW_0$ , and  $MW_A$ .

### Part 1: Initial burst

In this part, the particles enter in contact with an aqueous solution, at time zero.

$$\frac{m_{t_1}}{m_{\infty 1}} = 1 - \sum_{n=1}^{\infty} \frac{6}{n^2 \pi^2} \exp\left(-\frac{Dt}{Rp^2} n^2 \pi^2\right) \quad (5)$$

Where,  $m_{t_1}$  is the magnitude of the available agent at any instant of time during the initial burst,  $m_{\infty 1}$  is the magnitude of the available agent during the initial burst phase,  $D$  is the diffusivity of the agent through the porous matrix,  $t$  is the time and  $Rp$  is the microspheres radius.

### Part 2: Lag phase

The agent present in the surface has been release and the pores are forming in the matrix of the microparticle.

### Part 3: Secondary burst

In this part, the encapsulated agent molecules pass through the formed pores. These pores will become bigger gradually and coalesce so the diffusion will increase.

$$\frac{m_{t_2}}{m_{\infty 2}} = 1 - \sum_{n=1}^{\infty} \frac{6}{n^2 \pi^2} \exp\left(-\frac{T}{Rp^2} n^2 \pi^2\right) \quad (6)$$

Where,  $m_{t_2}$  is the magnitude of the available agent at any instant of time during the secondary burst phase,  $m_{\infty 2}$  is the magnitude of the available agent during the secondary burst and  $Rp$  the microsphere radius. The following equations are necessary to determinate the other parameters required in this equation.

$$T = \frac{1}{2} D \left( \frac{b \exp\left(-\left(\frac{t-\tau}{b}\right)^2\right)}{\sqrt{\pi}} + (t+\tau) \operatorname{erf}\left(\frac{t-\tau}{b}\right) + t \right) \quad (7)$$

$$b = \sqrt{2\delta^2} \quad (8)$$

Where,  $\tau$  is the time for pore formation and  $\delta^2$  is the variance of time required form pores. This parameter can be calculated with the following equation.

$$(\delta)^2 = \frac{1}{n-1} \sum_{i=0}^n (\tau - \bar{\tau})^2 \quad (9)$$

Where,  $\bar{\tau}$  is the meantime for pore formation.

$$\bar{\tau} = \frac{-1}{kC_W} \ln\left(\frac{MW_r}{MW_0}\right) \quad (10)$$

Where,  $kC_W$  is the polymer degradation rate constant,  $MW_r$  is the average polymer molecular weight and  $MW_0$  the initial molecular weight of the polymer.

The total diffusion is determined with the following equation:

$$\frac{m_t}{m_{\infty}} = \varphi \frac{m_{t1}}{m_{\infty 1}} + (1 - \varphi) \frac{m_{t2}}{m_{\infty 2}} \quad (11)$$

Where,  $m_t$  is the total magnitude of the agent at any instant of time,  $m_{\infty}$  is the total magnitude of the agent and  $\varphi$  is the ratio of the first layer of matrix volume to the total volume of the matrix.

$$\varphi = 1 - \frac{(Rp - R_{occ})^3}{R_p^3} \quad (12)$$

## 3 RESULTS AND DISCUSSION

---

### 3.1 Double emulsion

The analytical results of each stage are presented in a summary table (Table 3.1). This table also contains a summary of the process parameters and formulation. For an easy way to legend all the results, each stage has an alphabetic letter associated which is explained in Table 3.1. For example, stage 1 is batch A. After this table, a compilation of the SEM and morphology images is presented.

Table 3.1: Experimental conditions, process parameters and analytical results of the different batch of lysozyme polymeric microparticles.

Batch	Process					Powder Properties					Performance			Yield (%)	
	Process Parameters					SEM		PSD (µm)			DL (mg)	EE (%)	Activity (%)		
	W1	O	Protein: PLGA (%)	W2		Shape	Obs.	Dv10	Dv50	Dv90					
Stage 1	A	Lysozyme + 0.5%w/v PVA	RG502 + DCM	5 : 95	2%w/v PVA	W <sub>1</sub> /O 8 000 rpm for 2 min; W <sub>1</sub> /O/W <sub>2</sub> 1 000 rpm for 3 min	Spherical but broken	Polymer remains in the surface	23	168	333	1.45	21.89	-	0.61
	B	Lysozyme + 0.5%w/v PVA	RG502 + DCM	5 : 95	2%w/v PVA + 5%w/v NaCl	W <sub>1</sub> /O 8 000 rpm for 2 min; W <sub>1</sub> /O/W <sub>2</sub> 1 000 rpm for 3 min	Spherical	Polymer remains in surface	41	95	262	-	-	-	-
Stage 2	C	Lysozyme + 0.5%w/v PVA	RG502 + DCM	5 : 95	2%w/v PVA + 5%w/v NaCl	W <sub>1</sub> /O 8 000 rpm for 2 min; W <sub>1</sub> /O/W <sub>2</sub> 4 000 rpm for 3 min	Spherical	Very small and all connected	-	-	-	-	-	-	-
	D	Lysozyme + 0.5%w/v PVA	RG502 + DCM	5 : 95	1 mg/ml Poloxamer 188	W <sub>1</sub> /O 8 000 rpm for 2 min; W <sub>1</sub> /O/W <sub>2</sub> 1 000 rpm for 3 min	-	Not obtained	-	-	-	-	-	-	-
	E	Lysozyme + 0.5%w/v PVA	RG502 + DCM	5 : 95	1 mg/ml Poloxamer 188	W <sub>1</sub> /O 8 000 rpm for 2 min; W <sub>1</sub> /O/W <sub>2</sub> 4 000 rpm for 3 min	Spherical	Very small and all connected	-	-	-	-	-	-	-
Stage 3	F	Lysozyme + 0.5%w/v PVA	RG502 + DCM	5 : 95	2%w/v PVA + 5%w/v NaCl	W <sub>1</sub> /O 8 000 rpm for 2 min; W <sub>1</sub> /O/W <sub>2</sub> 1 000 rpm for 3 min	Few microspheres and many polymeric remains around it		-	-	-	19.34	59.68	-	12.49
	G	Lysozyme + 0.5%w/v PVA	RG502 + DCM	5 : 95	2%w/v PVA + 5%w/v NaCl	W <sub>1</sub> /O 9 000 rpm for 2 min; W <sub>1</sub> /O/W <sub>2</sub> 1 000 rpm for 3 min	Few microspheres and many polymeric remains around it		-	-	-	2.57	3.50	-	2.14
	H	Lysozyme + 0.5%w/v PVA	RG502 + DCM	5 : 95	1 mg/ml Poloxamer 188	W <sub>1</sub> /O 8 000 rpm for 2 min; W <sub>1</sub> /O/W <sub>2</sub> 1 000 rpm for 3 min	-	Not obtained	-	-	-	0.18	43.24	-	1.97
	I	Lysozyme + 0.5%w/v PVA	RG502 + DCM	5 : 95	1 mg/ml Poloxamer 188	W <sub>1</sub> /O 9 000 rpm for 2 min; W <sub>1</sub> /O/W <sub>2</sub> 1 000 rpm for 3 min	-	Not obtained	-	-	-	3.84	13.10	-	10.54

Table 3.1: Continued 1.

Batch	Process					Process Parameters	Powder Properties					Performance			Yield (%)
	W <sub>1</sub>	O	Protein: PLGA (%)	W <sub>2</sub>			SEM		PSD (µm)			DL (mg)	EE (%)	Activity (%)	
							Shape	Obs.	DV <sub>10</sub>	DV <sub>50</sub>	DV <sub>90</sub>				
Stage 4	J	Lysozyme + 0.5%w/v PVA	RG504 + DCM	5 : 95	2%w/v PVA + 5%w/v NaCl	W <sub>1</sub> /O 8 000 rpm for 2 min; W <sub>1</sub> /O/W <sub>2</sub> 1 000 rpm for 3 min	Spherical	Without polymeric remains in the surface	11	34	72	251.66	104.76	100	89.74
	K	Lysozyme + 0.5%w/v PVA	RG504 + DCM	5 : 95	2%w/v PVA + 5%w/v NaCl	W <sub>1</sub> /O 9 000 rpm for 2 min; W <sub>1</sub> /O/W <sub>2</sub> 1 000 rpm for 3 min	Spherical	Without polymeric remains in the surface	-	-	-	244.64	100.27	-	95.06
	L	Lysozyme + 0.5%w/v PVA	RG504 + DCM	5 : 95	1 mg/ml Poloxamer 188	W <sub>1</sub> /O 8 000 rpm for 2 min; W <sub>1</sub> /O/W <sub>2</sub> 1 000 rpm for 3 min	-	No obtained	-	-	-	-	-	-	-
	M	Lysozyme + 0.5%w/v PVA	RG504 + DCM	5 : 95	1 mg/ml Poloxamer 188	W <sub>1</sub> /O 9 000 rpm for 2 min; W <sub>1</sub> /O/W <sub>2</sub> 1 000 rpm for 3 min	-	No obtained	-	-	-	-	-	-	-

Legend:      Optimal conditions tests

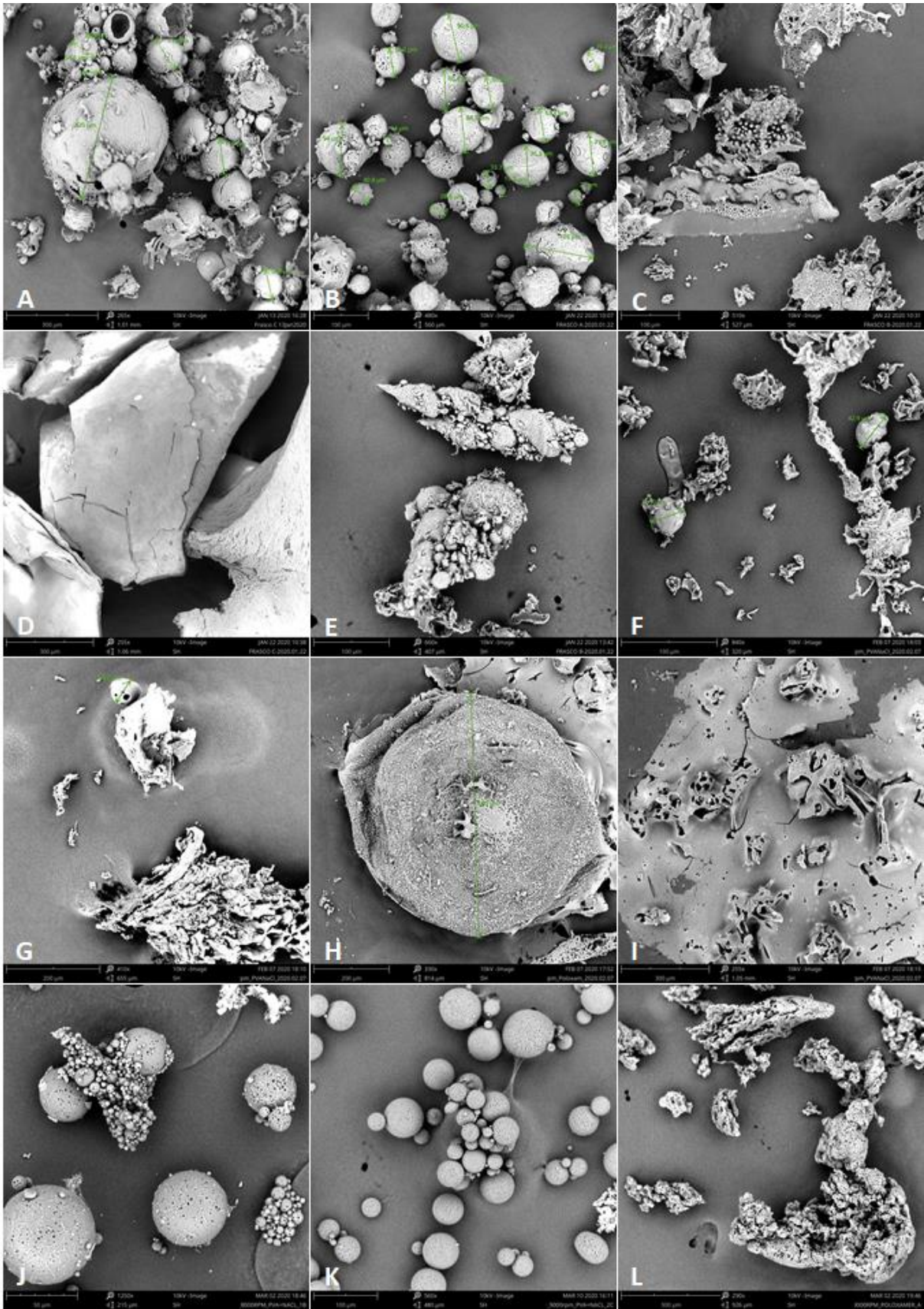


Figure 3.1: SEM images of microspheres obtained in the different batches. Batch A magnification of 265 times, batch B magnification 480 times, batch C magnification of 510 times, batch D magnification of 255 times, batch E magnification of 660 times, batch F magnification of 840 times, batch G magnification of 330 times, batch I magnification of 255 times, batch J magnification of 1250 times, batch K magnification of 560 times and batch L magnification of 290 times.



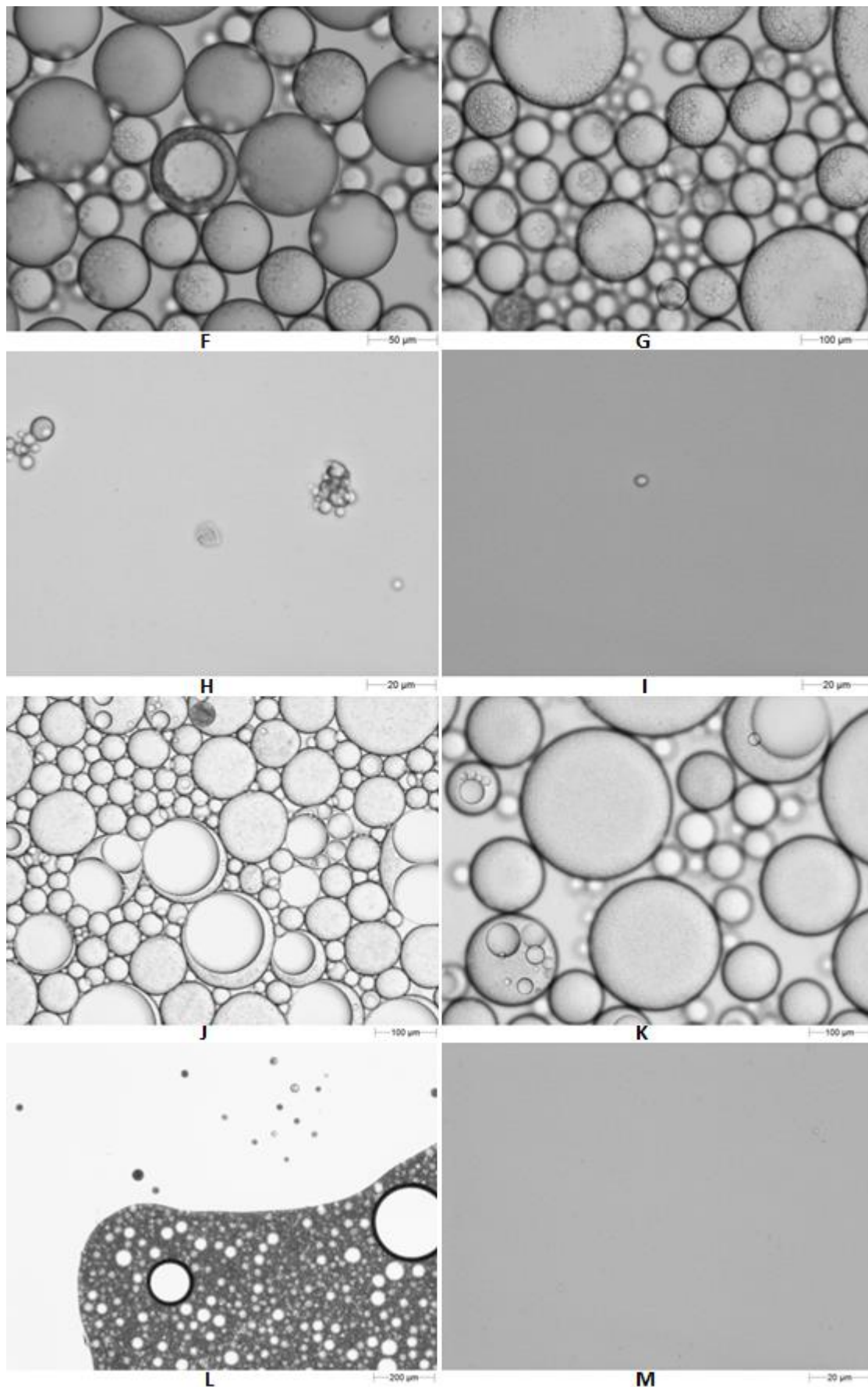


Figure 3.2: Morphologi images of the sample taken at the end of each batch starting in stage 3. Batch F scale bar of 50  $\mu\text{m}$ , batch G scale bar of 100  $\mu\text{m}$ , batches H and I scale bar of 20  $\mu\text{m}$ , batches J and K scale bar of 20  $\mu\text{m}$ , batch L scale bar of 200  $\mu\text{m}$  and batch M scale bar of 20  $\mu\text{m}$ .

Until stage 4, changes were made in the process and formulation in order to achieve a final product with the desired proprieties.

Stage 1 was the starting point of the experimental work and understanding of the process. In this stage the PLGA used was RG 502, the least viscous. The first analyze performed was SEM and the mains observations were (Figure 3.1 A):

- a spherical shape was obtained but the microspheres present particles on the surface;
- the microspheres obtained were mostly broken, when performed the DL and EE assed by UV the results were expected a minimal presence of lysozyme, 1.45 mg and 22% respectively.

In stage 2, batch B to E, was performed without lysozyme and other changes were made such as 1) optimization of the washing step, 2) the addition of NaCl to PVA in W<sub>2</sub>, 3) the addition of poloxamer as a surfactant in W<sub>2</sub>, 4) other rotation speed in W<sub>2</sub>, 4 000 rpm, and 5) the addition the tempering step of 48h. The main observations from this stage were (Figure 3.1 B to E):

- besides the optimization in the washing step the microspheres continue to present particles on the surface;
- in batch C and E, the microspheres obtained using 4 000 rpm in the 2<sup>nd</sup> mixing step were smaller than the desired particle size (25 to 150 μm) and the remains of the polymers appear to form a network around the microspheres. Thus, this rotation speed was eliminated from the process;
- in batch B, the microspheres obtained showed to be denser than before (stage 1). The combination of PVA and NaCl in W<sub>2</sub> proves to work for the hardening of the particles.

In test 1 the first emulsion was mixed twice with different speeds, 8 000 and 8 900 rpm respectively. The samples taken in this test were analyzed in the morphology microscope (Figure 3.3).

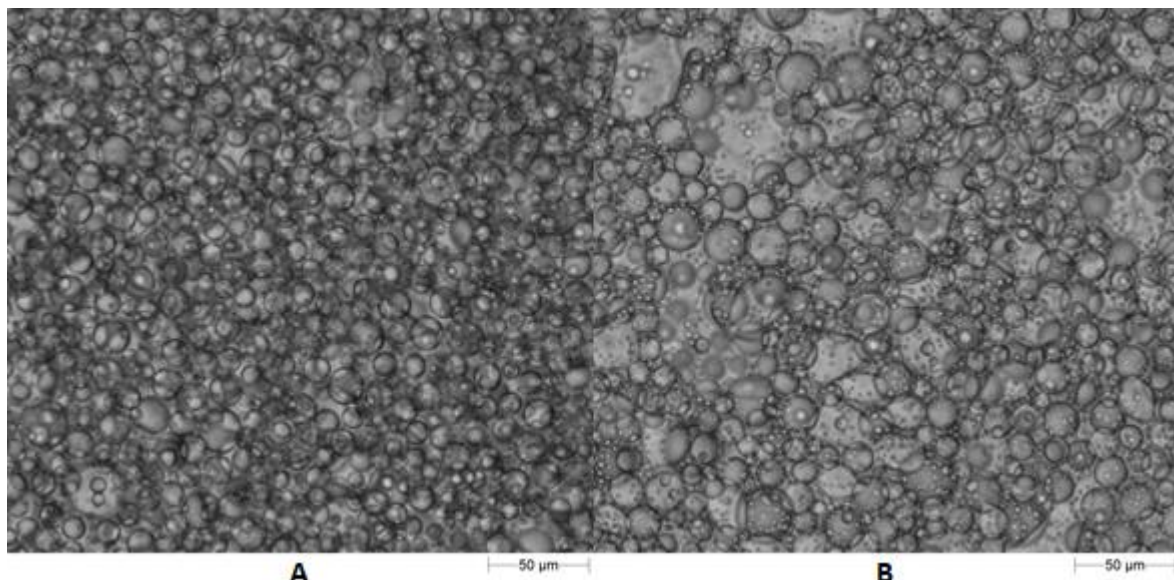


Figure 3.3: Morphologi images of the sample taken after mixing at 8 900 rpm: A) moments after the sample was taken and B) a few minutes after the first image was taken.

The droplets obtained present to be unstable because they coalesced to form a bigger one through the time and with the 2<sup>nd</sup> mixing the droplets coalescence faster because they are smaller. With this test concludes, the time factor is a critical parameter during the formation of the double emulsion.



And the smaller the droplets obtain in the first emulsion more unstable is the emulsion and the droplets coalescences faster.

In stage 3, batch F to I, some optimizations were made such as 1) adding another speed rotation in  $W_1$ , 9 000 rpm, 2) the pH change in both aqueous solution and 3) a vortex step between each washing solution. In this stage, the main conclusions were (Figure 3.1 F to I):

- the tempering step was shorter than stage 2, less than 24h;
- batches H and I, that used poloxamer as surfactant not obtained microspheres;
- batches F and G, got some microspheres and others broken. The lysozyme was successfully encapsulated, Figure 3.2 F and G, and for batch F the EE was ~60%.

The double emulsion solvent evaporation method requires that all DCM used need to be evaporated to allow the solidification of the microspheres. In this stage, compared to stage 2, the particles were more destroyed so, the tempering step was not enough to eliminate all the solvent present in the emulsion.

Test 2 was performed to understand the necessary time to remove the DCM of the emulsion. A solution with the same amount of water and DCM used in the process was mixed with a constant speed, 243 rpm. It was needed 90 h to eliminate all the solvent of the solution. During this time, the loss of DMC was monitored test through mass losses.

In stage 4, batch J to M, the PLGA used was the RG 504, more viscous than RG 502. The tempering time not only was increased but also the loss of DMC was monitored in this stage. This way, it is possible to guarantee that the solvent was evaporated and continue the process without damage the produced microspheres. For the emulsion who used Poloxamer in  $W_2$ , batch L and M, the conclusions were:

- a visual confirmation of the  $W_1/O/W_2$  formation only for batch L, Figure 3.2 L;
- a rigid white mass was formed for both batch during the tempering step, Figure 3.4.

A SEM analysis was performed to this rigid mass and the image do not show any presence of microspheres, Figure 3.1 L. The image only presents what appears to be polymeric remains and a possible justification can be the precipitation of them.

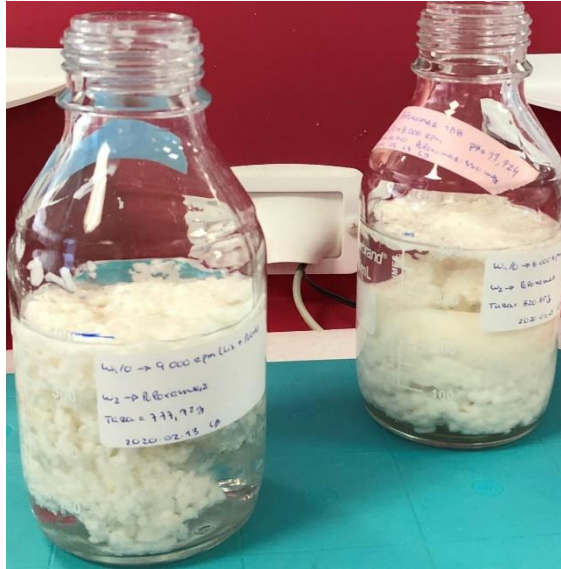


Figure 3.4: White mass formed during the tempering step for batches L and M.

### 3.1.1 Optical conditions tests

For the emulsion who used PVA and NaCl in  $W_2$ , batch J and K, the formation of  $W_1/O/W_2$  was confirmed, Figure 3.2 J and K. In Figure 3.1 J and K, can be observed that microspheres were obtained with a cleaner surface than in previous stages. These microspheres do not appear broken, but the small ones presented agglomerated. The yield of the process was 90% and 95%, respectively for batch J and L.

For batch J, the following analyzes were performed: a PSD, EE and DL, with an  $n=2$ . The particle size distribution of the two samples proved to be similar and the average value is near the intended values (25 to 150  $\mu\text{m}$ ) except the  $Dv_{10}$ , Figure 3.5. At the end of the process, it is possible to do sieving to the final powder and guarantee the desired PSD.

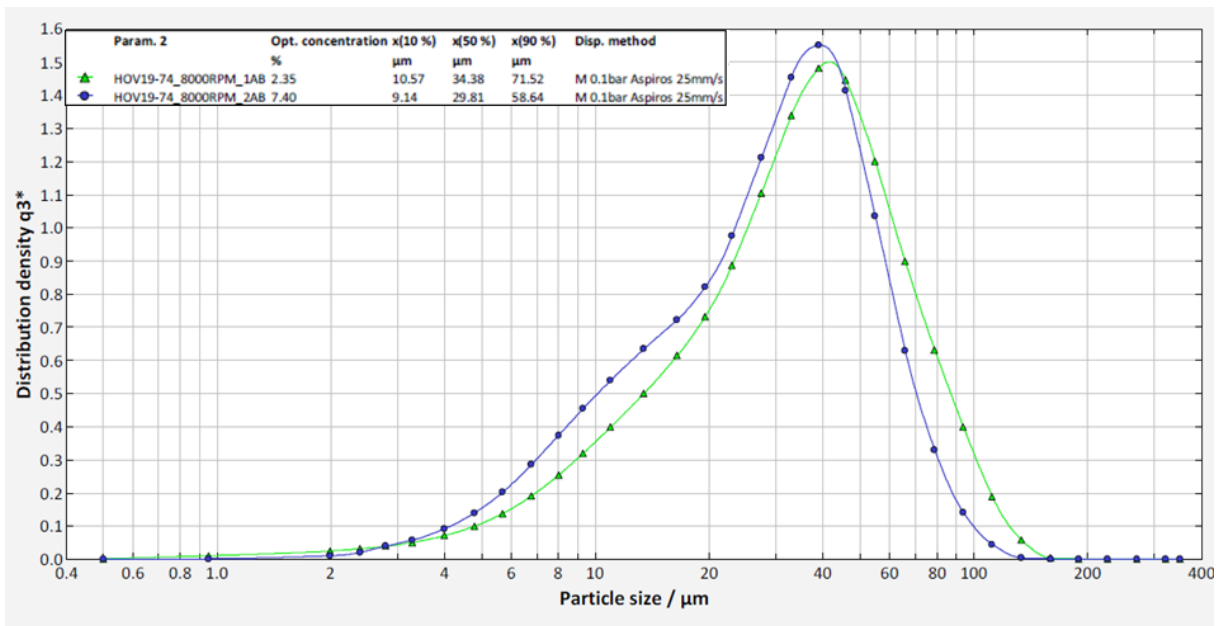


Figure 3.5: Particle size distribution for the batch J,  $n=1$  (green) and  $n=2$  (blue).

The results of EE and DL was 105% and 252 mg. The 5% more in EE can be justified by an analytical error, default in the UV machine in terms of the baseline, because the expected was less than 100% in EE. During the formation of the microspheres, the loss of Lysozyme was minimal that indicates the process can encapsulate efficiently the protein. The next analysis was an IVR study, the relative concentration of lysozyme released from microspheres, assessed by UV, is described in Figure 3.6.

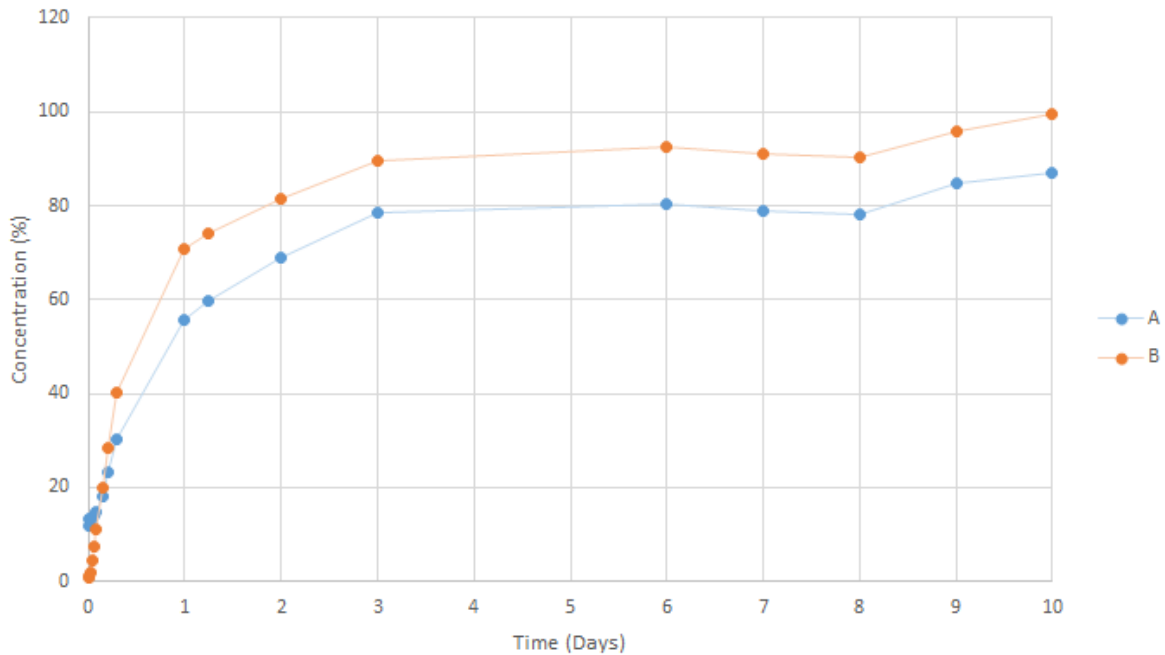


Figure 3.6: IVR data for batch J, A is  $n=1$  (blue) and B is  $n=2$  (orange).

Figure 3.6 shows a different release behavior of the two samples, in the beginning of the study, besides the same testing conditions with an average standard deviation ( $\bar{\sigma}$ ) of 8%. Sample A shows a burst release in contrast with sample B that has near to a zero-order release. After the first day, the behavior of the two samples seems to be the same despite the 20% difference in protein released. This difference can be due to 1) sampling and storage of the sample, 2) analytical error, 3) an UV error in the baseline, that has to be discounted from the sample reading.

After this analysis, samples were taken and Lysozyme activity kit was performed, activity over time (Figure 3.7).

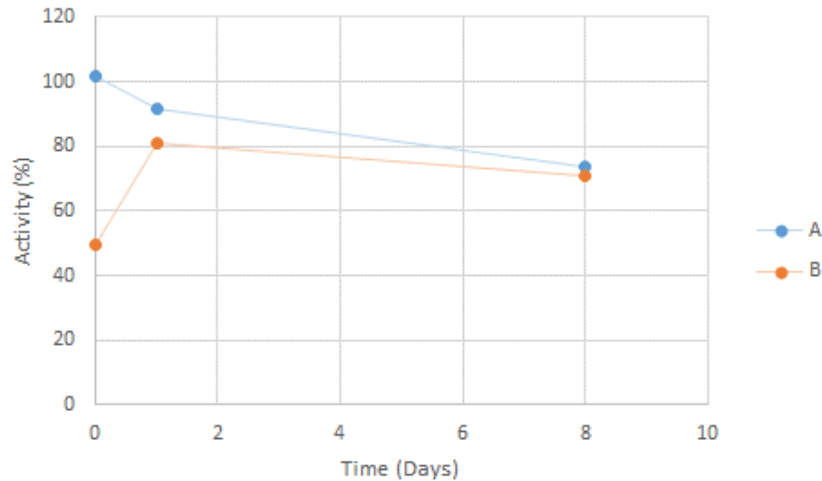


Figure 3.7: Activity data of the Lysozyme for batch J, A is n=1 (blue) and B is n=2 (orange).

Figure 3.7 presents the results of the lysozyme activity, assessed by microplate reader, during the IVR study. For both samples, the same activity results were expected. The apparent activity loss in sample B at T0 could be due to an experimental error. A dilution of the IVR sample is needed and a different amount than desired due to a simple bubble in the tip of the micropipette can influence the result of the test. And it is not possible to have 30% more activity in the day 1 than day 0, the  $\bar{\sigma}$  was 15%. The B sample is the n=2 of the sample A, so should be the same value. It can be concluded that the activity of lysozyme was successfully maintained during the formation process of  $W_1/O/W_2$ .

For batch K, the results of EE and DL was 100% and 245 mg, a loss of ~5%. For 9 000 rpm, lysozyme was successfully encapsulated as well. The EE and DL can be justified with the loss of PLGA.

The IVR study and activity test for batches J and K was not performed due to the onset of the Covid-19 pandemic crisis.

## 3.2 Sustain Release Models

In the first part of this chapter a database was created. This database consists of IVR data from five different API's, some data was obtained in Hovione (lysozyme, diclofenac and minocycline) and other from literature review (risperidone and naltrexone).(56–58) For an easier understanding, the database table was divided into two parts, input and output. The input described the parameters of the formulation: API type, the grade of PLGA and its characteristics, and drug loading value. And also the process condition: type of production technology and it's set of parameters. The output is the analytical information of the product obtained in terms of particle size and IVR conditions (e.g., temperature) and data. The burst release value and percentage of drug release at the end of the study were indicated in the database table.

The slopes of the IVR curve were calculated with the goal to understand the release behavior of each formulation. In Figure 3.8 is presented the four different curves obtained and the behavior are:

- Curve A - release of a big amount of API in the first two days and followed by a lag-phase, a constant release of API;
- Curve B – starts with a burst release followed by a lag-phase;
- Curve C - a constant slow release of the API followed by a lag-phase;
- Curve D – 3 phase release, first a release of a minimum amount of API in a long period followed by a secondary burst release and final release.

For curve A and B, the release profile can be described as API presence in the surface of the particle, burst release, and its diffusion through water-filled pores. The release profile of curve C it is possible to be an API diffusion through water-filled pores and increased release is due to the increase of the pore diameter. The release profile of curve D can start with the formation of the pores in the polymeric matrix and follow by its growth. So, the release started with a minimum API release and increase with the increasing of the pores size.

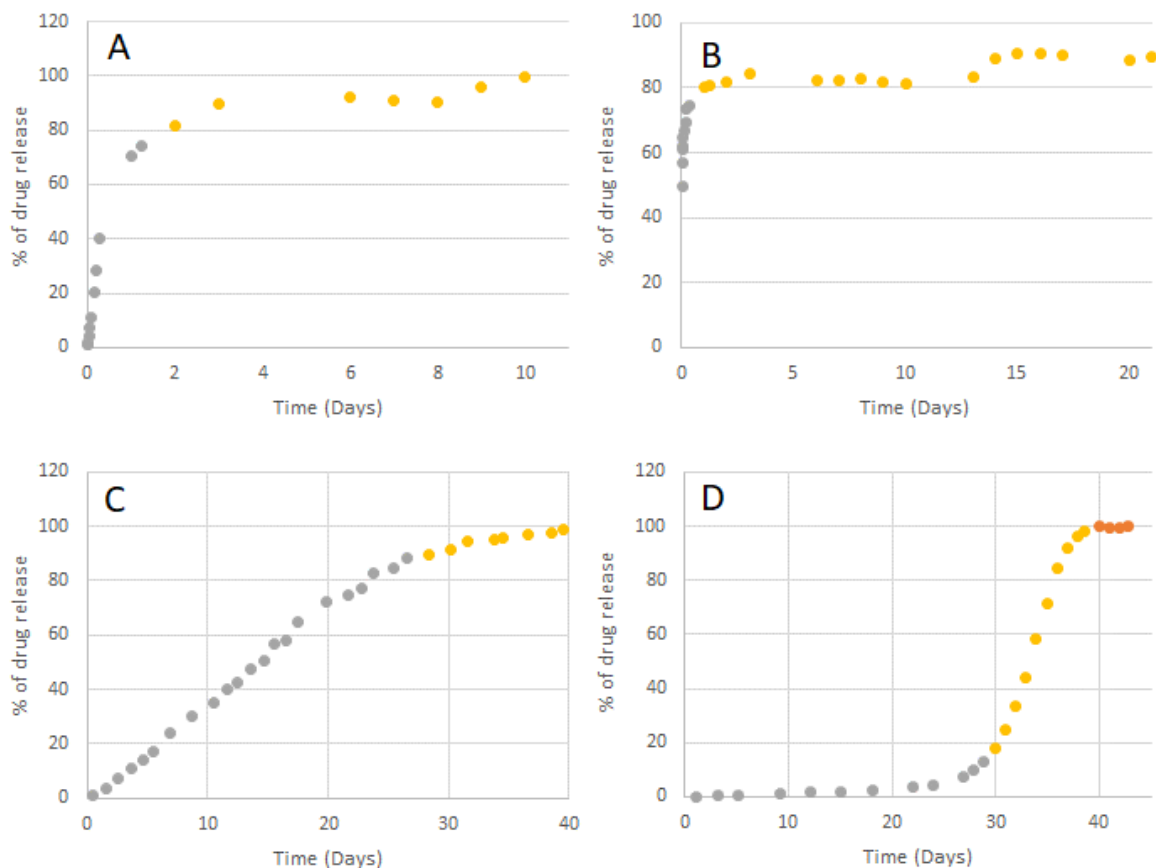


Figure 3.8: Representation of four different formulations. A and B lysozyme, C) vivitrol® and D) Risperdal. The different colors in the graphic representation indicates the different parts of the IVR curve.

### 3.2.1 Weibull equation

The second part was the implementation of the Weibull equation in five different formulations (iclofenac, risperdal, naltrexone and vivitrol®). The results will be present by formulation and each will have an image with the compiled results.

- **Diclofenac:**

Diclofenac was a chemical API used in some tests done at Hovione, which was combined with high viscosity PLGA. It is a formulation for CR that uses the hot melt extrusion as a production technique. The results obtained in each step are presented in Figure 3.9.

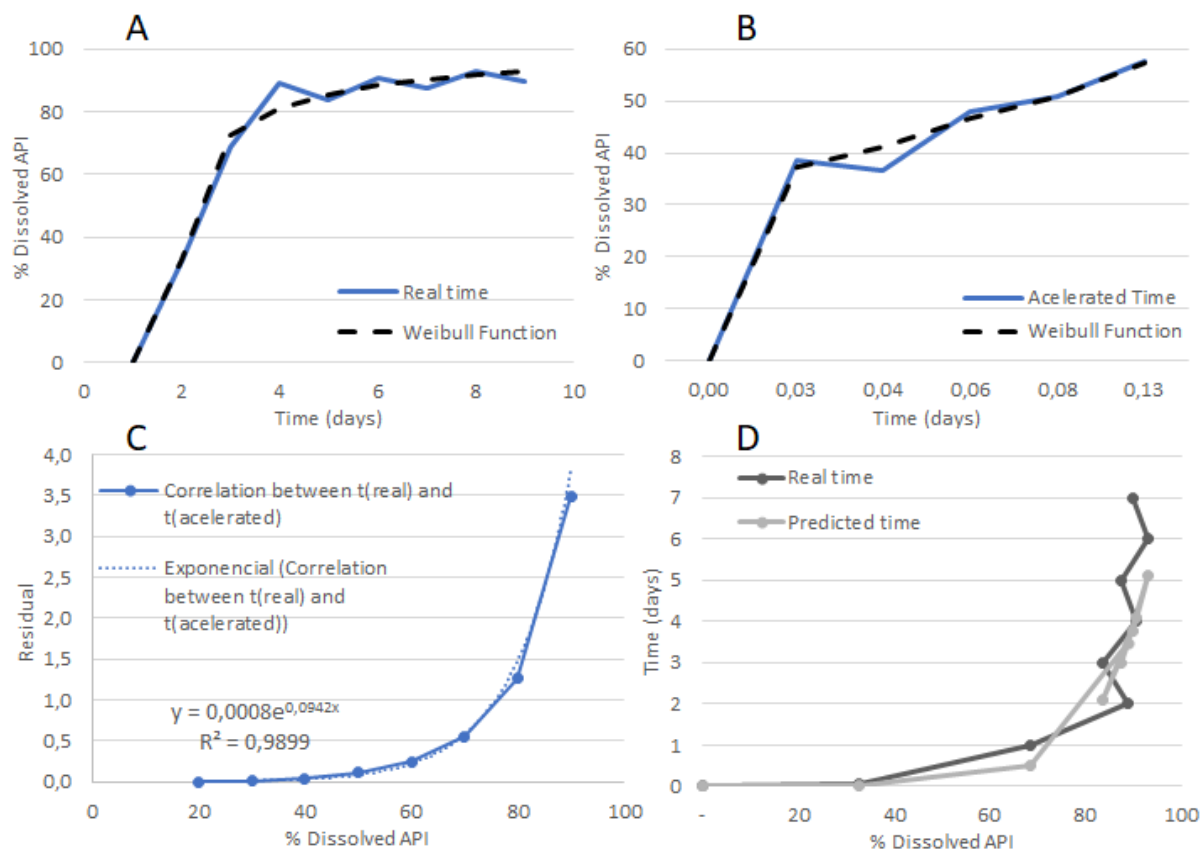


Figure 3.9: IVR data and values of API release obtain by Weibull Equation for diclofenac: (A) IVR experimental data of real-time release and Weibull values for real-time; (B) IVR experimental data of accelerated time release and Weibull values for accelerated time; (C) Correlation between predicted real and accelerated time data; (D) IVR data of real-time and predicted data with the equation:  $y = 0.0008e^{0.0942x}$ .

In Figure 3.9 A and B, it is possible to observe that the experimental values present analytical error, increase and decrease of the percentage of the dissolved API. Comparing these values with those obtained by the Weibull equation it is possible to observe some deviation in the curve profile. The correlation between the predicted percentage of the dissolved API values for real and accelerated time presents a good fitting of the model,  $R^2=0.989$ , in Figure 3.9 C. But when the equation obtained in C was used to predict the time of release and compared with the experimental IVR data it is possible to say that the system is described in an acceptable way, Figure 3.9 D. Due to the analytical error in the data, it's possible to observe a different profile of the two curves starting at 70% API dissolved.

- **Risperdal:**

Risperdal is a chemical API that was combined with PLGA 75:25 to form the Risperdal Consta®. This medicine is an injectable powder for reconstitution for the treatment psychoses. The IVR data was retired from the paper, *Comparison of in vitro-in vivo release of Risperdal® Consta® microspheres*, *Int. J. Pharm.* **434**, 2012. The results obtained in each step are presented in Figure 3.10 (56).

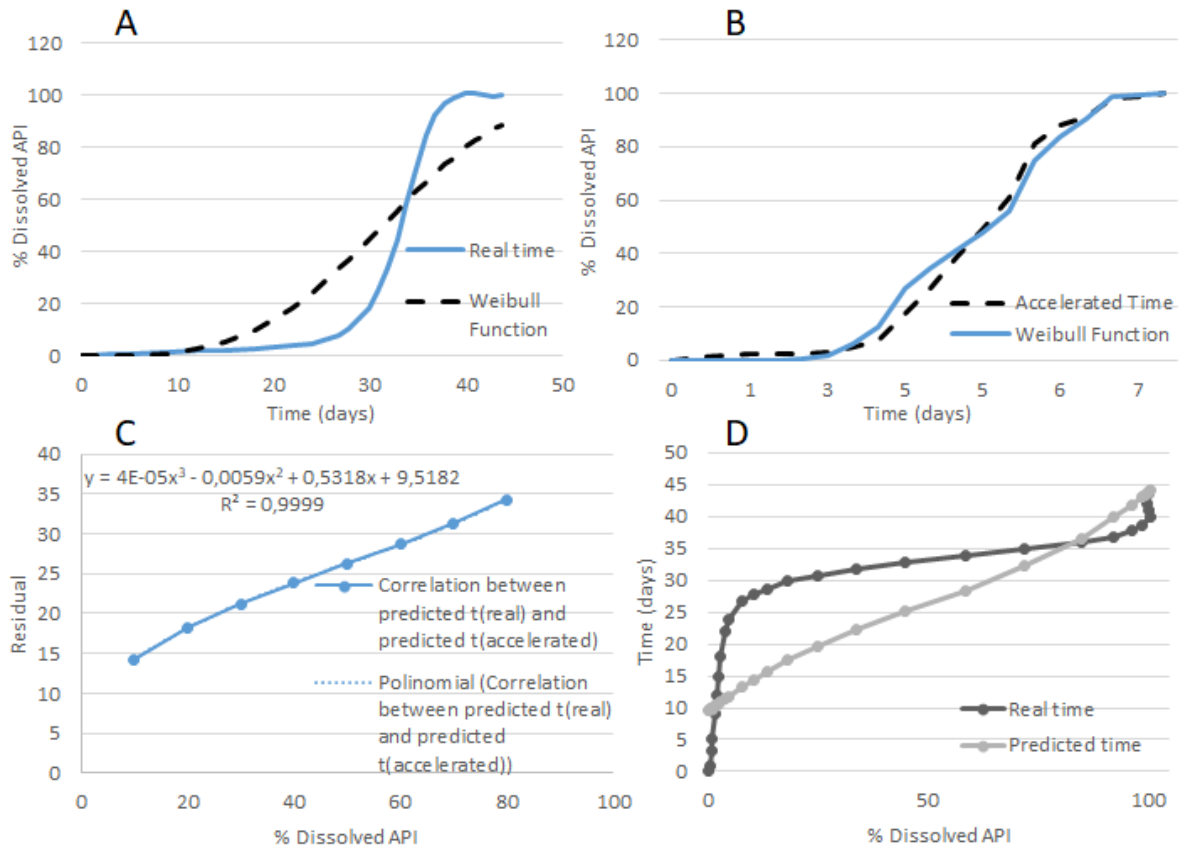


Figure 3.10: IVR data and values of API release obtain by Weibull Equation for risperdal: (A) IVR experimental data of real-time release and Weibull values for real-time; (B) IVR experimental data of accelerated time release and Weibull values for accelerated time; (C) Correlation between predicted real and accelerated time data; (D) IVR data of real-time and predicted data with the equation:  $y = 4E-05x^3 - 0.0059x^2 + 0.5318x + 9.5182$ .

In Figure 3.10 A, it is possible to observe that the experimental values present a different release profile of the values obtained with the Weibull equation, so the Weibull equation does not fit this release profile. In Figure 3.10 B, the values obtain showed to be similar to the experimental data. The correlation between the predicted percentage of the dissolved API values for real and accelerated time presents a good fitting of the model,  $R^2=0,999$ , in Figure 3.10 C. Besides the good fitting of the model when the equation obtained in C was used to predict the release and compared with the experimental IVR data two different curves were presented, Figure 3.10 D. Although good fitting achieved, the Weibull equation doesn't describe well this system. A possible justification: the formulation is governed by a different release mechanism and therefore is not properly described by the Weibull equation.

- **Naltrexone:**

Naltrexone is a chemical API used for the treatment of alcohol dependence. The IVR data of this API was retired from the paper: *Accelerated in vitro release testing method for naltrexone loaded PLGA microspheres*, *Int. J. Pharm.* **520**, 2017. In this paper, the naltrexone was combined with PLGA 75:25 to produce microparticles using the single emulsion technique. The results obtained in each step are presented in Figure 3.11.



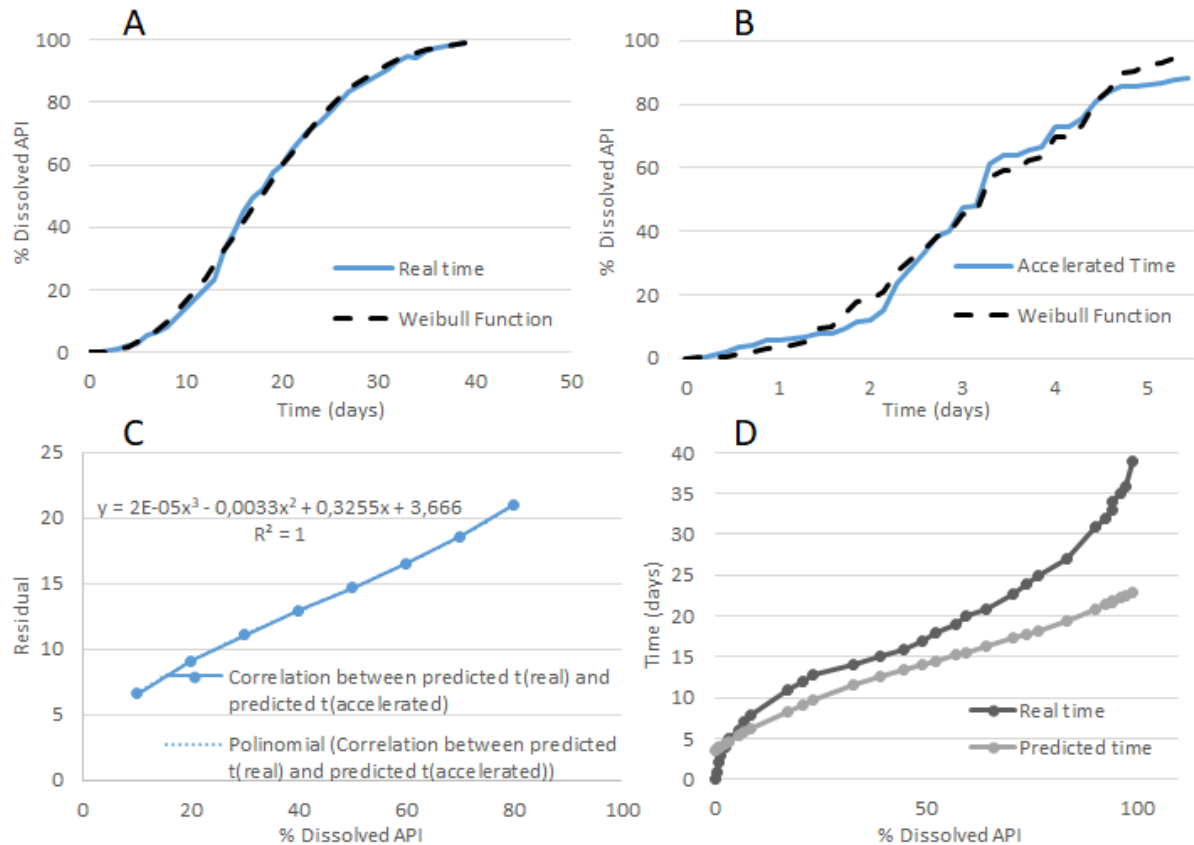


Figure 3.11: IVR data and values of API release obtain by Weibull Equation for naltrexone: (A) IVR experimental data of real-time release and Weibull values for real-time; (B) IVR experimental data of accelerated time release and Weibull values for accelerated time; (C) Correlation between predicted real and accelerated time data; (D) IVR data of real-time and predicted data with the equation:  $y = 2E-05x^3 - 0.0033x^2 + 0.3255x + 3.666$ .

In Figure 3.11 A the values obtained by Weibull equation follows the same behaviour as the experimental real time data. But when observing the values obtained for accelerated time it is possible to see a deviation to the experimental data, Figure 3.11 B. The correlation between the predicted percentage of the dissolved API values for real and accelerated time presents a good fitting of the model,  $R^2=1$ , when adjusted the trendline to a third order polynomial, Figure 3.11 C. When the polynomial equation obtained was used to predict the time of release and compared with the experimental IVR data completely different release behavior was got, Figure 3.11D. A good fitting was achieved, but the Weibull equation doesn't describe well this system. The  $\beta$  value was above 1, the shape factor is a sigmoid or S-shaped. So, polynomial isn't the best trendline to describe this model. In this case, it is possible that the release profile is controlled by a different release mechanisms and the Weibull equation only considers a minimal diffusion (25,27).

- **Vivitrol®:**

Vivitrol® is an injectable medicine for extended-release compose by naltrexone as API and PLGA 75:25 as matrix polymer. The IVR data was retired in the same paper as naltrexone, API presented before. The results obtained in each step are presented in Figure 3.12.

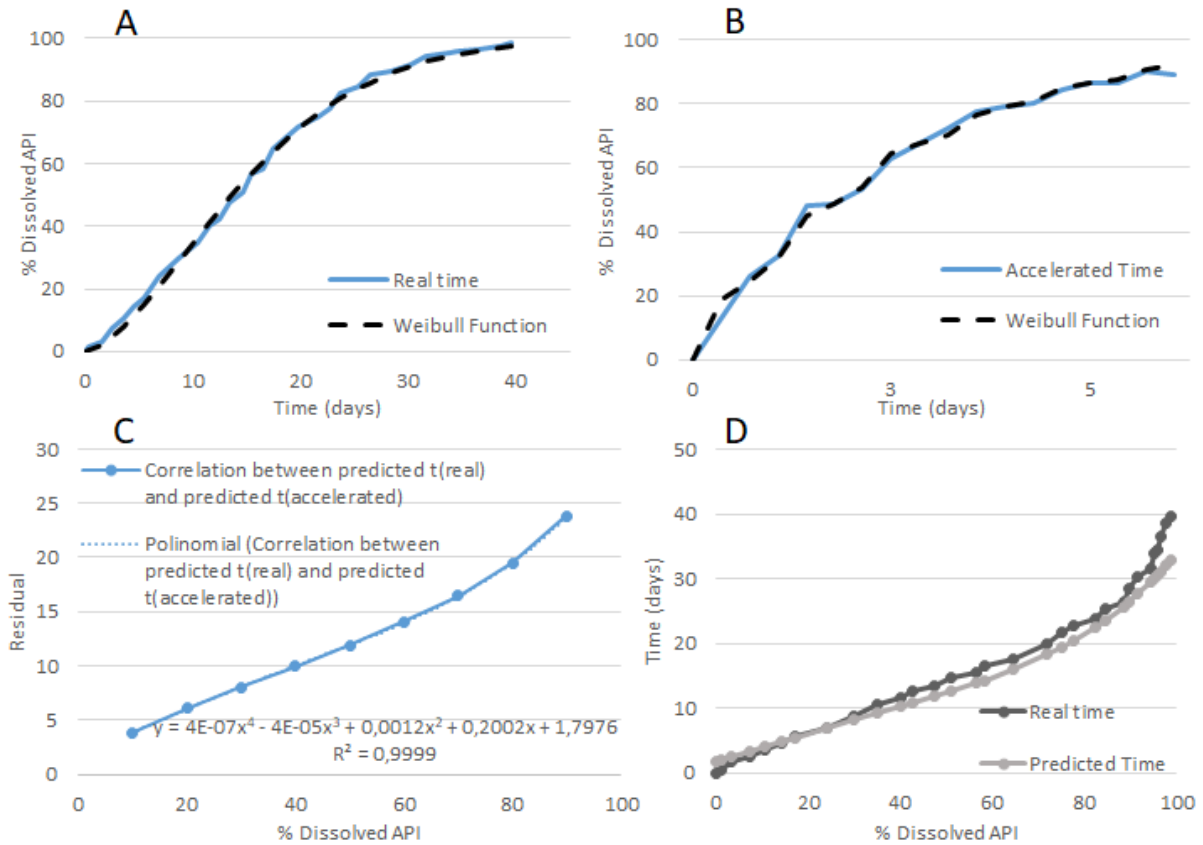


Figure 3.12: IVR data and values of API release obtain by Weibull Equation for vivitrol®: (A) IVR experimental data of real-time release and Weibull values for real-time; (B) IVR experimental data of accelerated time release and Weibull values for accelerated time; (C) Correlation between predicted real and accelerated time data; (D) IVR data of real-time and predicted data with the equation:  $y = 4E-07x^4 - 4E-05x^3 + 0.0012x^2 + 0.2002x + 1.7976$ .

In Figure 3.12 A and B the values obtained by Weibull equation follows the same behavior as the experimental data for both real and accelerated time. The correlation between the predicted percentage of the dissolved API values for real and accelerated time presents a good fitting of the model,  $R^2=0.999$ , when adjusted the trendline to a fourth order polynomial, Figure 3.12 C. When the equation obtained before was used to predict the time of release and compared with the experimental IVR data a similar release behavior was achieved with some differences at the end of the curve, Figure 3.12 D. The Weibull equation does not describe well this system at the end of the release. A possible justification is in the end of the release the profile is controlled by a different release mechanism.

### 3.2.2 Mechanistic model

The 3<sup>rd</sup> part was the implementation and simulation of the mechanistic model considering the data published in the article, "An analytical model for prediction of controlled release from bulk biodegrading polymer microspheres".

Before starting the implementation, the values of the followed parameters of the raw-materials and final product have to be known:  $R_p$ ,  $R_{occ}$ ,  $D$ ,  $kC_w$ ,  $MW_0$ , and  $MW_A$ . In the article (54), all parameters values were indicated except  $kC_w$ . This parameter is the polymer degradation rate constant and it is specific to the grade of the polymer and molecular weight used. Without this value it is not possible to continue the implementation of the model. So, following the references of the article a value was found for of the PLGA 50:50,  $kC_w = 0.011$  for particles size with 1  $\mu\text{m}$  (62), but the simulation will not have

the same reliability. The PLGA used in the simulation was a 75:25, richer in PLA, this way will absorb less water and then degrade more slowly. So, its  $kC_W$  will be lower. In Figure 3.13 is presented the release profile obtained and the parameters used in the paper.

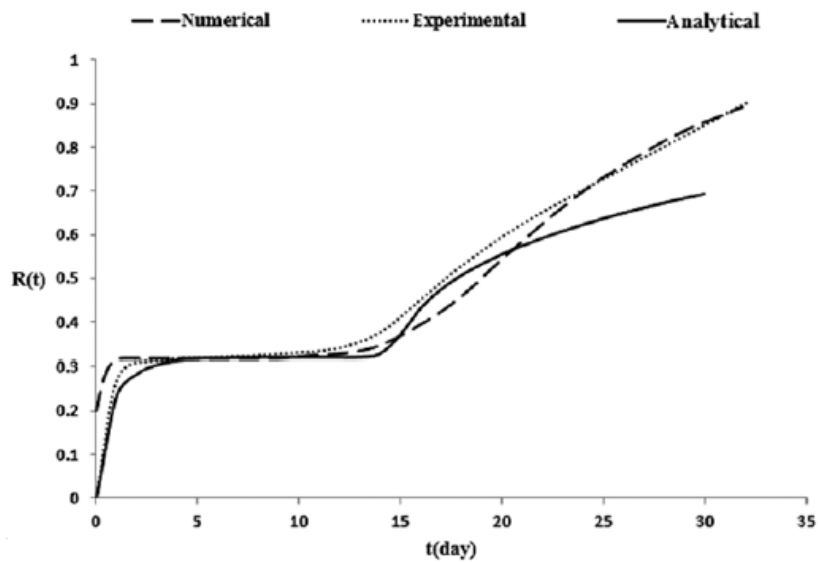


Figure 3.13: Release profile of a peptide, melittin  $MW_A = 2.86 \text{ kDa}$ , from poly lactic-co-glycolic acid (PLGA) microspheres, PLGA 75:25  $MW_0 = 9.3 \text{ kDa}$ . The  $MW_r = 4.68 \text{ kDa}$ ,  $D = 6.34 \times 10^{-18}$ ,  $R_p = 4.5 \mu\text{m}$  and  $R_{occ} = 0.54 \mu\text{m}$ . (Adapted from (54)).

When implemented these parameters values in MATLAB and the  $kC_W$  multiple with the particle size,  $kC_W = 0.0495$ , the melittin release profile obtained, Figure 3.14, was completely different from the one obtained in the paper, Figure 3.13.

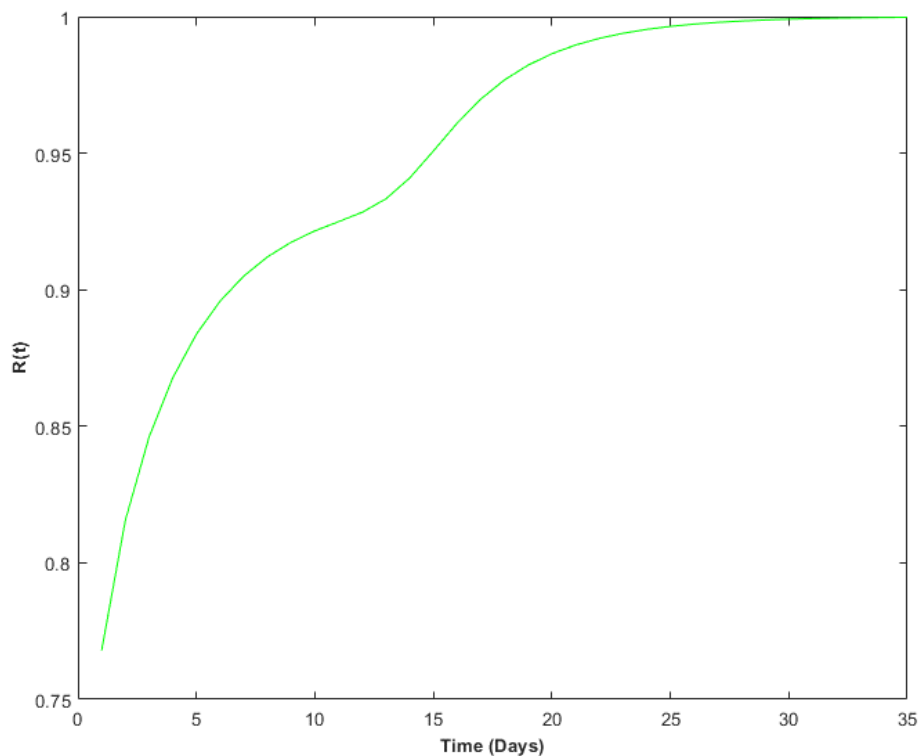


Figure 3.14: Melittin release profile obtained in the simulation in Matlab, using the same parameters values of Figure 3.13.

In Figure 3.13, the release curve present a four-phase release and in Figure 3.14 presents a different release curve, not only in terms of time but also the release fraction. Some of the differences in the release profile can be explained by the different values of the  $kC_W$ , because this value was not indicated in the paper and for a better understanding of the different profile obtained the author was contacted but without any success. It is possible to conclude that with a change of one parameter the release curve change.

It was not possible to implement the model to the IVR data used before because 1) the implementation of the presented case was not possible to replicate the same release profile and 2) to implement other IVR data to this model analytical testing will be needed or used an analytical method to solve the fundamental equations used by Rothstein *et al.*(55) to determine some parameters values of the raw material (PLGA, e.g:  $kC_W$ ) and the final product (e.g:  $Rocc$  and  $\tau$ ). It is important to notice that some parameters values can be difficult to calculate. Despite there are a few studies about this model, it is still not robust enough. This way more studies are needed to complement the model structure.

## 4 CONCLUSIONS

---

The first part of this thesis work, a formulation of PLGA microparticles encapsulated with lysozyme was successfully obtained. The high shear mixer proves to be adequate for this work because the lysozyme activity was maintained and the size of the particles was near to the desired.

The parameters that allowed the process optimization were 1) tempering step; 2) washing step; 3) speed rotation.

In the case of the speed rotation, 4 000 rpm in the 2<sup>nd</sup> emulsion step produced microspheres smaller than the desired sized, so this speed rotation was eliminated. In the 1<sup>st</sup> emulsion step, the microspheres obtained with 8 000 and 9 000 rpm showed to be similar.

A process parameter that proves to be crucial in the hardening of the microspheres was the tempering step and only when the DCM is residual, the particles are ready to move on to the next step of the process. The optimal time for tempering is 4-5 days, stage 4.

Only in stage 4 was achieved the optimal washing conditions for removal all the particles on the surface of the microspheres produced.

The formulation that used poloxamer formed a rigid white mass during the tempering step and a possible explanation can be the degradation of the double emulsion.

The formulation that used PVA combine with NaCl, for both speed rotation, proved to be a better option because 1) a stable emulsion was obtained; 2) the drug loading was near the 98%; 3) the activity of the protein was maintained and 4) the yield of the was between 89 and 95%.

The IVR study done to the particles obtained in stage 4 can be considered as a preliminary test because the test has not been completed or repeated. But the result obtained was good, minimal or none burst release.

The second part of this work was using an empirical and mathematical model to predict IVR data but for the models selected it was not possible to predict data.

The Weibull equation cannot predict well the IVR data, can fit the model in some case where the main release is governed by polymer erosion and minimal diffuse release. In the case of the mathematical model, it was not possible to implement the model with the values of the articles.

As future work, further testing of formulations that used the combination PVA and NaCl as a stabilizer in terms of IVR, activity test and stability test. It is important to understand the mechanism of release of the PLGA not only for the formation of new formulations but also to help with the creation of an IVR predict model. The Raman imaging technique should be used to understand the PLGA mechanism of the degradation and the release of the API. And before, during and after the washing step in order to evaluate if the PLGA matrix has any API or polymeric remains in the surface.

Although there is a lot of information about mathematical models but these models are not robust enough, It is necessary to complement the model structure as well as to estimate better the parameters for the specific particles that were produced.



## REFERENCES

---

1. Lalor F, Fitzpatrick J, Sage C, Byrne E. Sustainability in the biopharmaceutical industry: Seeking a holistic perspective. *Biotechnol Adv.* 2019;37(5):698–707.
2. Deloitte. 2020 Global life sciences sector outlook | Deloitte. Deloitte. 2020;1–81.
3. Deloitte. Global life sciences outlook Moving forward with cautious optimism. Deloitte. 2016;1–28. [Care/gx-lshc-2016-life-sciences-outlook.pdf](#)
4. Deloitte. 2019 Global life sciences outlook | Focus and transform | Accelerating change in life sciences. 2019;
5. Purple Book: Database [Internet]. [cited 2020 Jun 25]. Available from: <https://purplebooksearch.fda.gov/advanced-search>
6. Škalko-Basnet N. Biologics: Targets and Therapy Dovepress Biologics: the role of delivery systems in improved therapy. *Biol Targets Ther.* 2014;8:107–14.
7. Makadia HK, Siegel SJ. Poly Lactic-co-Glycolic Acid (PLGA) as biodegradable controlled drug delivery carrier. *Polymers (Basel).* 2011;3(3):1377–97.
8. Huang X, Brazel CS. On the importance and mechanisms of burst release in matrix-controlled drug delivery systems. *J Control Release.* 2001;73(2–3):121–36.
9. Ahmed AR, Elkharraz K, Irfan M, Bodmeier R. Reduction in burst release after coating poly(D,L-lactide-co-glycolide) (PLGA) microparticles with a drug-free PLGA layer. *Pharm Dev Technol.* 2012;17(1):66–72.
10. Wischke C, Schwendeman SP. Principles of encapsulating hydrophobic drugs in PLA/PLGA microparticles. *Int J Pharm.* 2008;364(2):298–327.
11. Martín-Sabroso C, Fraguas-Sánchez AI, Aparicio-Blanco J, Cano-Abad MF, Torres-Suárez AI. Critical attributes of formulation and of elaboration process of PLGA-protein microparticles. *Int J Pharm.* 2015;480(1–2):27–36.
12. Mansour HM, Sohn MJ, Al-Ghananeem A, DeLuca PP. Materials for pharmaceutical dosage forms: Molecular pharmaceuticals and controlled release drug delivery aspects. *Int J Mol Sci.* 2010;11(9):3298–322.
13. Pandit NK, Soltis RP. *Introduction to the pharmaceutical sciences : an integrated approach.* 2nd ed. Lippincott Williams and Wilkins ; 2011. 480 p.
14. Hines DJ, Kaplan DL. Poly(lactic-co-glycolic) acid-controlled-release systems: Experimental and modeling insights. *Crit Rev Ther Drug Carrier Syst.* 2013;30(3):257–76.
15. Huynh CT, Lee DS. Controlled Release. In: *Encyclopedia of Polymeric Nanomaterials.* Springer Berlin Heidelberg; 2015. p. 439–49.
16. Csaba N, González L, Sánchez A, Alonso MJ. Design and characterisation of new nanoparticulate polymer blends for drug delivery. *J Biomater Sci Polym Ed.* 2004;15(9):1137–51.
17. Dhaliwal K. Biodegradable Polymers and their Role in Drug Delivery Systems. *Biomed J Sci Tech Res.* 2018 Nov 16;11(1).
18. Han FY, Thurecht KJ, Whittaker AK, Smith MT. Bioerodable PLGA-based microparticles for producing sustained-release drug formulations and strategies for improving drug loading. *Front*

- Pharmacol. 2016;7(JUN):1–11.
19. Ortega-Oller I, del Castillo-Santaella T, Padial-Molina M, Galindo-Moreno P, Jódar-Reyes AB, Peula-García JM. Dual delivery nanosystem for biomolecules. Formulation, characterization, and in vitro release. *Colloids Surfaces B Biointerfaces*. 2017;159:586–95.
  20. Gentile P, Chiono V, Carmagnola I, Hatton P V. An overview of poly(lactic-co-glycolic) Acid (PLGA)-based biomaterials for bone tissue engineering. *Int J Mol Sci*. 2014 Feb 28;15(3):3640–59.
  21. Biodegradable polymers for controlled release - Evonik Health Care [Internet]. [cited 2020 Jun 15]. Available from: <https://healthcare.evonik.com/product/health-care/en/products/biomaterials/resomer/pages/controlled-release.aspx>
  22. FDA's Regulatory Science Program for Generic PLA/ PLGA-Based Drug Products | American Pharmaceutical Review - The Review of American Pharmaceutical Business & Technology [Internet]. [cited 2020 Jun 16]. Available from: <https://www.americanpharmaceuticalreview.com/Featured-Articles/188841-FDA-s-Regulatory-Science-Program-for-Generic-PLA-PLGA-Based-Drug-Products/>
  23. Alexis F. Factors affecting the degradation and drug-release mechanism of poly(lactic acid) and poly[(lactic acid)-co-(glycolic acid)]. *Polym Int*. 2005;54(1):36–46.
  24. Lao LL, Peppas NA, Boey FYC, Venkatraman SS. Modeling of drug release from bulk-degrading polymers. *Int J Pharm*. 2011;418(1):28–41.
  25. Shen J, Burgess DJ. Accelerated in-vitro release testing methods for extended-release parenteral dosage forms. *J Pharm Pharmacol*. 2012;64(7):986–96.
  26. Jain RA. The manufacturing techniques of various drug loaded biodegradable poly(lactide-co-glycolide) (PLGA) devices. *Biomaterials*. 2000;21(23):2475–90.
  27. Fredenberg S, Wahlgren M, Reslow M, Axelsson A. The mechanisms of drug release in poly(lactic-co-glycolic acid)-based drug delivery systems - A review. *Int J Pharm*. 2011;415(1–2):34–52.
  28. Giri TK, Choudhary C, Ajazuddin, Alexander A, Badwaik H, Tripathi DK. Prospects of pharmaceuticals and biopharmaceuticals loaded microparticles prepared by double emulsion technique for controlled delivery. *Saudi Pharm J*. 2013;21(2):125–41.
  29. Nikolett K, Antal V, Lengyel M, Kállai-Szabó N, Antal V, Laki AJ, et al. Microparticles , Microspheres , and Microcapsules for Advanced Drug Delivery. *Sci Pharm*. 2019;87(3):20.
  30. Wang J, Shi A, Agyei D, Wang Q. Formulation of water-in-oil-in-water (W/O/W) emulsions containing trans-resveratrol. *RSC Adv*. 2017;7(57):35917–27.
  31. Tu F, Lee D. Controlling the stability and size of double-emulsion-templated poly(lactic- co - glycolic) acid microcapsules. *Langmuir*. 2012;28(26):9944–52.
  32. Vijayalakshmi SP, Madras G. Effects of the pH, concentration, and solvents on the ultrasonic degradation of poly(vinyl alcohol). *J Appl Polym Sci*. 2006;100(6):4888–92.
  33. del Castillo-Santaella T, Peula-García JM, Maldonado-Valderrama J, Jódar-Reyes AB. Interaction of surfactant and protein at the O/W interface and its effect on colloidal and biological properties of polymeric nanocarriers. *Colloids Surfaces B Biointerfaces*. 2019;173(July 2018):295–302.



34. Pérez C, De Jesús P, Griebenow K. Preservation of lysozyme structure and function upon encapsulation and release from poly(lactic-co-glycolic) acid microspheres prepared by the water-in-oil-in-water method. *Int J Pharm.* 2002;248(1–2):193–206.
35. Van De Weert M, Hoehstetter J, Hennink WE, Crommelin DJA. The effect of a water/organic solvent interface on the structural stability of lysozyme. *J Control Release.* 2000;68(3):351–9.
36. Taluja A, Bae YH. Role of a novel multifunctional excipient poly(ethylene glycol)-block-oligo(vinyl sulfadimethoxine) in controlled release of lysozyme from PLGA microspheres. *Int J Pharm.* 2008;358(1–2):50–9.
37. Whitford D. *Proteins: Structure and Function.* John Wiley & Sons, Ltd; 2005. 542 p.
38. Berg JM, Tymoczko JL, Stryer L. *Protein Structure and Function.* 2002.
39. Swaminathan R, Ravi VK, Kumar S, Kumar MVS, Chandra N. Lysozyme: A model protein for amyloid research. In: *Advances in Protein Chemistry and Structural Biology.* Academic Press Inc.; 2011. p. 63–111.
40. Lee ES, Kwon MJ, Lee H, Kim JJ. Stabilization of protein encapsulated in poly(lactide-co-glycolide) microspheres by novel viscous S/W/O/W method. *Int J Pharm.* 2007;331(1):27–37.
41. Kang F, Jiang G, Hinderliter A, Deluca PP, Singh J. Lysozyme stability in primary emulsion for PLGA microsphere preparation: Effect of recovery methods and stabilizing excipients. *Pharm Res.* 2002;19(5):629–33.
42. Pre-Press Copy Industry Perspective on the Medical Risk of Visible Particles in Injectable Drug Products.
43. Meng FT, Ma GH, Qiu W, Su ZG. W/O/W double emulsion technique using ethyl acetate as organic solvent: Effects of its diffusion rate on the characteristics of microparticles. *J Control Release.* 2003;91(3):407–16.
44. Dichloromethane | CH<sub>2</sub>Cl<sub>2</sub> - PubChem [Internet]. [cited 2020 Oct 28]. Available from: <https://pubchem.ncbi.nlm.nih.gov/compound/6344#section=Solubility>
45. Ethyl acetate | CH<sub>3</sub>COOC<sub>2</sub>H<sub>5</sub> - PubChem [Internet]. [cited 2020 Oct 28]. Available from: <https://pubchem.ncbi.nlm.nih.gov/compound/Ethyl-acetate#section=Solubility>
46. INTERNATIONAL CONFERENCE ON HARMONISATION OF TECHNICAL REQUIREMENTS FOR REGISTRATION OF PHARMACEUTICALS FOR HUMAN USE PHARMACEUTICAL DEVELOPMENT Q8(R2). 2009.
47. Yu LX, Amidon G, Khan MA, Hoag SW, Polli J, Raju GK, et al. Understanding Pharmaceutical Quality by Design. *AAPS J.* 2014;16(4):771–83.
48. Fda. Guidance for Industry PAT - A Framework for Innovative Pharmaceutical Development, manufacturing, and Quality Assurance [Internet]. 2004 [cited 2019 Nov 12]. Available from: <http://www.fda.gov/cvm/guidance/published.html>
49. Zhang L, Mao S. Application of quality by design in the current drug development. *Asian J Pharm Sci.* 2017;12(1):1–8.
50. Yu LX. Pharmaceutical quality by design: Product and process development, understanding, and control. *Pharm Res.* 2008;25(4):781–91.
51. Garner J, Skidmore S, Park H, Park K, Choi S, Wang Y. Beyond Q1/Q2: The Impact of Manufacturing Conditions and Test Methods on Drug Release From PLGA-Based Microparticle

- Depot Formulations. *J Pharm Sci.* 2018;107(1):353–61.
52. Xie X, Li Z, Zhang L, Chi Q, Yang Y, Zhang H, et al. A novel accelerated in vitro release method to evaluate the release of thymopentin from PLGA microspheres. *Pharm Dev Technol.* 2015;20(5):633–40.
  53. Shen J, Lee K, Choi S, Qu W, Wang Y, Burgess DJ. A reproducible accelerated in vitro release testing method for PLGA microspheres. *Int J Pharm.* 2016;498(1–2):274–82.
  54. Sivandzade F. An analytical model for prediction of controlled release from bulk biodegrading polymer microspheres. *Asian J Pharm Clin Res.* 2018;11(3):432–7.
  55. Little SR, Rothstein SN, Federspiel WJ. A simple model framework for the prediction of controlled release from bulk eroding polymer matrices. *J Mater Chem.* 2008;18(16):1873–80.
  56. Rawat A, Bhardwaj U, Burgess DJ. Comparison of in vitro-in vivo release of Risperdal® Consta® microspheres. *Int J Pharm.* 2012;434(1–2):115–21.
  57. Shen J, Choi S, Qu W, Wang Y, Burgess DJ. In vitro-in vivo correlation of parenteral risperidone polymeric microspheres. *J Control Release.* 2015;218:2–12.
  58. Andhariya J V., Choi S, Wang Y, Zou Y, Burgess DJ, Shen J. Accelerated in vitro release testing method for naltrexone loaded PLGA microspheres. *Int J Pharm.* 2017;520(1–2):79–85.
  59. Ding S, Serra CA, Vandamme TF, Yu W, Anton N. Double emulsions prepared by two–step emulsification: History, state-of-the-art and perspective. *J Control Release.* 2019;295(September 2018):31–49.
  60. Laboratory Mixers [Internet]. [cited 2019 Oct 25]. Available from: <https://www.silverson.com.br/pt/produtos/misturadores-de-laboratorio/>
  61. Silverson Machines Inc. Silverson L4RT High Shear Mixer. 2008.
  62. Panyam J, Dali MM, Sahoo SK, Ma W. Polymer degradation and in vitro release of a model protein from poly ( D , L -lactide- co -glycolide ) nano- and microparticles. 2003;92:173–87.